STATE OF THE CALIFORNIA CURRENT 2015–16: COMPARISONS WITH THE 1997–98 EL NIÑO

SAM MCCLATCHIE
NOAA Fisheries
Southwest Fisheries Science Center
8901 La Jolla Shores Drive
La Jolla, CA 92037-1509

RALF GOERICKE
Scripps Institution of Oceanography
University of California, San Diego
La Jolla, CA 92024

ANDREW LEISING
Environmental Research Division
National Marine Fisheries Service
99 Pacific St., Suite 255A
Monterey, CA 93940-7200

TOBY D. AUTH
Pacific States Marine Fisheries Commission
Hatfield Marine Science Center
2030 Marine Science Drive
Newport, OR 97365

ERIC BJORKSTEDT[1] AND
ROXANNE R. ROBERTSON[2]
[1]Southwest Fisheries Science Center
National Marine Fisheries Service
NOAA
Santa Cruz, CA 95064
[2]CIMEC
Humboldt State University

RICHARD D. BRODEUR[1],
XIUNING DU[2], ELIZABETH A. DALY[2],
AND CHERYL A. MORGAN[2]
[1]NOAA-Fisheries
Northwest Fisheries Science Center
Hatfield Marine Science Center
Newport, OR 97365
[2]Cooperative Institute for
Marine Resources Studies
Oregon State University
2030 Marine Science Drive
Newport, OR 97365

FRANCISCO P. CHAVEZ
Monterey Bay Aquarium Research Institute
Moss Landing, CA 95039

AMANDA J. DEBICH AND
JOHN HILDEBRAND
Marine Physical Laboratory
Scripps Institution of Oceanography
University of California, San Diego
La Jolla, CA 92024

JOHN FIELD AND KEITH SAKUMA
Southwest Fisheries Science Center
National Marine Fisheries Service
NOAA
Santa Cruz, CA 95064

MICHAEL G. JACOX[1, 2]
Institute of Marine Sciences
University of California, Santa Cruz
Santa Cruz, CA 95064
[2]Southwest Fisheries Science Center
NOAA
Monterey, CA 93940

MATI KAHRU
Scripps Institution of Oceanography
University of California, San Diego
La Jolla, CA 92024

RAPHAEL KUDELA[1] AND
CLARISSA ANDERSON[2, 3]
[1]Ocean Sciences Department
University of California, Santa Cruz
Santa Cruz, CA 95064
[2]Institute of Marine Sciences
University of California, Santa Cruz
Santa Cruz, CA 95064
[3]Southern California Coastal
Ocean Observing System
Scripps Institution of Oceanography
University of California, San Diego
San Diego, CA 92037

JOHN LARGIER
Bodega Marine Laboratory
University of California, Davis
P.O. Box 247
Bodega Bay, CA 94923

BERTHA E. LAVANIEGOS[1],
JOSE GOMEZ-VALDES[1], AND
S. PATRICIA A. JIMÉNEZ-ROSENBERG[2]
[1]Oceanology Division
Centro de Investigación Científica y
Educación Superior de Ensenada
Carretera Ensenada-Tijuana No. 3918
Zona Playitas, C.P. 22860, Ensenada
Baja California, Mexico
[2]Department of Plankton and Marine Ecology
Instituto Politécnico Nacional
CICIMAR
Av. IPN s/n, Col. Playa Palo de Sta. Rita
C.P. 23096, La Paz
BCS, Mexico

RYAN MCCABE
Joint Institute for the Study
of the Atmosphere and Ocean
University of Washington
Seattle, WA 98195

SHARON R. MELIN
National Marine Fisheries Service
Alaska Fisheries Science Center
Marine Mammal Laboratory
NOAA
7600 Sand Point Way N. E.
Seattle, WA 98115

MARK D. OHMAN AND LINSEY M. SALA
Scripps Institution of Oceanography
University of California, San Diego
La Jolla, CA 92093

BILL PETERSON AND JENNIFER FISHER
NOAA-Fisheries
Northwest Fisheries Science Center
Hatfield Marine Science Center
Newport, OR 97365

ISAAC D. SCHROEDER,
STEVEN J. BOGRAD, AND
ELLIOTT L. HAZEN
Environmental Research Division
National Marine Fisheries Service
99 Pacific St., Suite 255A
Monterey, CA 93940-7200

STEPHANIE R. SCHNEIDER AND
RICHARD T. GOLIGHTLY
Department of Wildlife
Humboldt State University
1 Harpst St.
Arcata, CA 95521

ROBERT M. SURYAN[1],
AMANDA J. GLADICS[1],
STEPHANIE LOREDO[1], AND
JESSICA M. PORQUEZ[2]
[1]Department of Fisheries and Wildlife
[2]College of Earth, Ocean, and
Atmospheric Sciences
Oregon State University
Hatfield Marine Science Center
Newport, OR 97365

ANDREW R. THOMPSON,
EDWARD D. WEBER, AND
WILLIAM WATSON
NOAA
Southwest Fisheries Science Center
8901 La Jolla Shores Drive
La Jolla, CA 92037-1509

VERA TRAINER
Northwest Fisheries Science Center
National Marine Fisheries Service
National Oceanic and
Atmospheric Administration
Seattle, WA 98112

PETE WARZYBOK, RUSSELL BRADLEY,
AND JAIME JAHNCKE
Point Blue Conservation Science
3820 Cypress Drive, Suite 11
Petaluma, CA 94954

ABSTRACT

Warm conditions in the North Pacific in 2014–15 were a result of the continuation of the North Pacific marine heat wave, a large area of exceptionally high SST anomalies that originated in the Gulf of Alaska in late 2013. The North Pacific heat wave interacted with an El Niño developing in the equatorial Pacific in 2015. Weekly periods of exceptionally high temperature anomalies (>2°C) occurred until the start of the El Niño (winter of 2015), when SSTs were still high but not as high as those due to the marine heat wave. During the 2015–16 El Niño, the depth of the 26.0 kg m^{-3} isopycnal ($d_{26.0}$) was considerably shallower than during the 1982–83 and 1997–98 events. The area affected by the marine heat wave and the 2015–16 El Niño in the mixed layer was comparable to the 1997–98 El Niño, but lasted longer. Water column stratification in the upper 100 m during 2015–16 was as strong as the most extreme values during the 1997–98 El Niño. This stratification was primarily driven by the warming of the upper 100 m. Despite notable perturbations, the effects of the 2015–16 El Niño on hydrographic properties in the CalCOFI domain were not as strong as those observed during the 1997–98 El Niño.

Warm ocean conditions, stratification, nutrient suppression, and silicic acid stress likely favored initiation of a toxic *Pseudo-nitzschia* bloom in fall 2014. Very low zooplankton displacement volumes were associated with anomalously warm and saline surface waters off Baja California. In contrast, during the 1997–98 El Niño, zooplankton volume was near average. Off California, pelagic red crab (*Pleuroncodes planipes*) adults were abundant in the water column and frequently washed up on beaches of southern California from January 2015 into 2016, and central California by September 2015. Glider measurements of integrated transport up to June 2015 did not detect anomalous northward advection. As expected, HF radar indicated northward surface currents along the central California coast in fall and winter 2015–16. Northward advection appeared to be much stronger during the 1997–98 El Niño. Throughout 2015–16, the zooplankton community on the Oregon shelf was dominated by lipid-poor tropical and sub-tropical copepods and gelatinous zooplankton, indicating poor feeding conditions for small fishes that are prey for juvenile salmon. The presence of rarely encountered species increased copepod species richness during 2015–16 to levels higher than the 1998 El Niño. We infer that the unusual copepod vagrants of 2015–16 originated from an offshore and southwesterly source; an important difference from the southerly origin of vagrants during the 1997–98 El Niño.

The very warm conditions caused sardine spawning to shift from central California to Oregon. Mesopelagic fish assemblage off southern California exhibited higher abundances of species with southern affinities, and lower abundances of species with northern affinities. Forage fish (Pacific herring, northern anchovy, and Pacific sardine) were much less abundant in 2015–16 compared to previous years. In contrast, catches of salmon were close to average off northern California. Catches of young-of-the-year rockfishes were high off central California, but low off both northern and southern California. Seabirds at Southeast Farallon Island in 2015 exhibited reduced breeding populations, reduced breeding success, lower chick growth rates, and lower fledging weights. Common murres were negatively affected in central and northern California, but seabird responses were species-specific. It is clear from the results presented here that the warm anomaly effects on the ecosystem were complicated, regionally specific, and that we do not fully understand them yet.

Online supplementary material: http://calcofi.org/ccpublications/state-of-the-california-current-live-supplement.html

INTRODUCTION

Over the last three years the California Current System (CCS) has been profoundly affected by the North Pacific marine heat wave of 2014–15 (DiLorenzo and Mantua 2016), formerly known as the "blob" (Bond et al. 2015), and the El Niño of 2015–16. A consequence of this forcing has been an unusually long period of strong warm anomalies in the CCS from 2014 until mid 2016. There are many precedents for anomalously warm years in the California Current System. Some of them (for example 1940–41, 1982–83, 1997–98, and 2005) are well studied. In this introduction to the 2015–16 warm year, we draw comparisons not only between the 2015–16 event and the 1997–98 El Niño, but also between the recent conditions and previous warm anomalies in the California Current System. Important questions that will guide us are: What caused the anomalous warming of 2015–16 in the California Current System? To what degree was the warming caused by the 2015–16 El Niño? And did the current El Niño have an effect on the California Current System as large as that of the 1997–98 El Niño?

Atmospheric Teleconnections (Local Forcing) And Oceanic Coastally Trapped Waves (Remote Forcing)

DiLorenzo and Mantua (2016) consider that "there is good evidence that [North Pacific] atmospheric teleconnections of tropical origin played a key role in the winter 2013/14 sea-level pressure anomalies." The patterns in sea surface temperature (SST) anomalies are mirrored in the sea level pressure anomalies. The peak anomalies shifted from the central Gulf of Alaska to the coastal

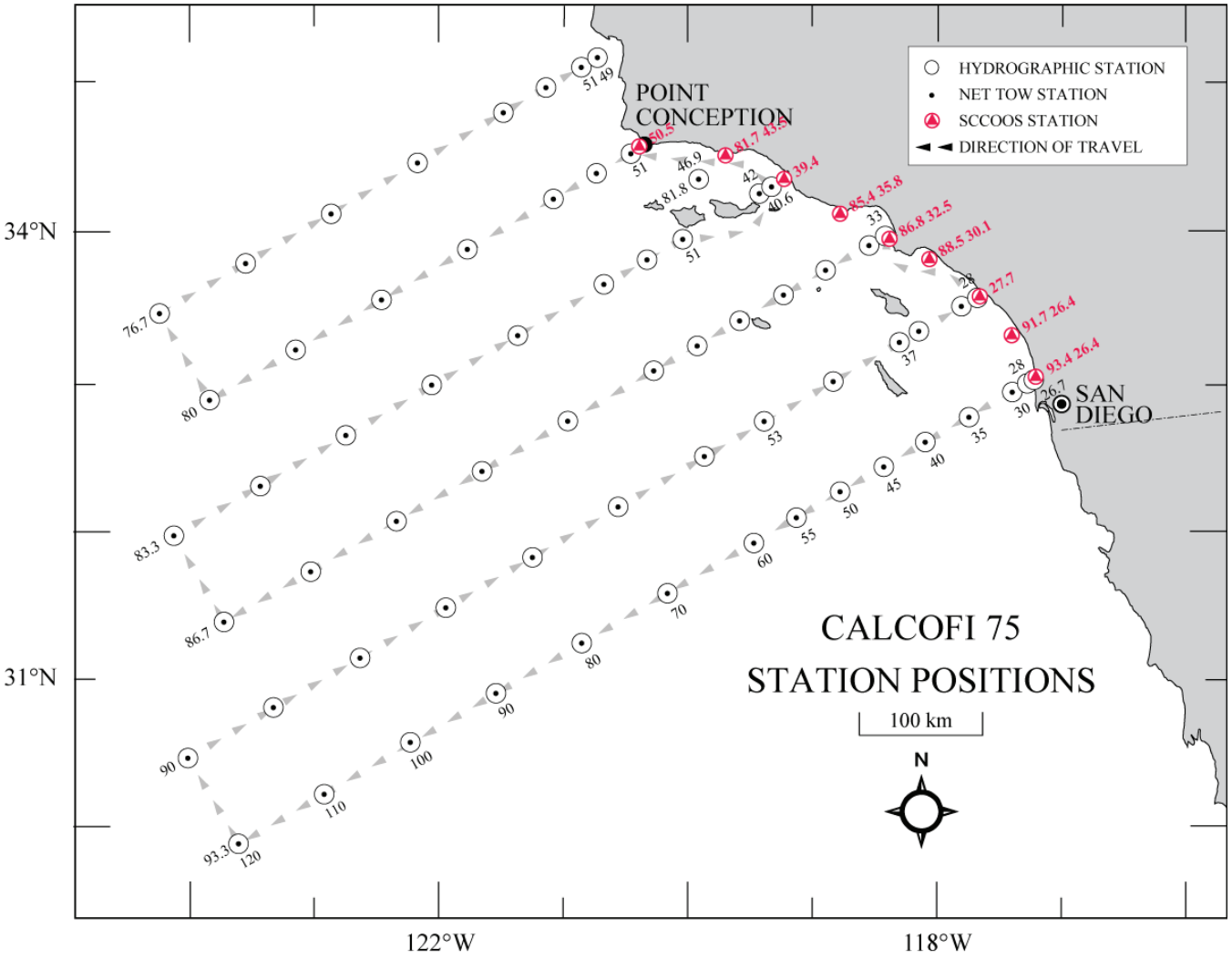

Figure 1. Map of the 75 station CalCOFI station pattern, including 66 core stations and 9 inshore SCCOOS stations.

areas of the Gulf of Alaska and the US West Coast in 2015 (DiLorenzo and Mantua 2016). This shift reflected a transition in the spatial pattern of SST anomalies from an NPGO-like pattern to a PDO-like pattern. Multiyear warm events, depending on the definition of a warm event, occurred in historical times in 1957–58, 1962–63, 1991–92 and 2014–15 (DiLorenzo and Mantua 2016).

As the spatial transition from NPGO to PDO-like patterns was occurring in the North Pacific, an El Niño developed in the tropics (DiLorenzo and Mantua 2016). The subtropical Pacific is connected to the central equatorial Pacific by positive thermodynamic feedback between the oceans and the atmosphere[1], where positive temperature anomalies can reduce the winds, and favor the development of El Niño. Once El Niño feedbacks arise along the equator, "the rearrangement of tropical convection excites atmospheric Rossby waves… which in the case of an eastern Pacific El Niño…injects variance into the Aleutian low in the next boreal fall/winter season" (DiLorenzo and Mantua 2016). In short, the North Pacific warming affected the development of the El Niño, and teleconnections of tropical origin fed back to the variance of the North Pacific, which was manifested in the spatial pattern of sea level pressure anomalies. DiLorenzo and Mantua (2016) estimated that tropical teleconnections accounted for about 50% or ~1.5°C of the peak SST anomalies in the index of their PDO-like pattern in January to March 2015, contributing significantly to making the North Pacific warming an extreme event, which they refer to as a "marine heat wave." Without the tropical teleconnections, the anomalous warming would have fallen within the normal range of variability of SST in the northeast Pacific (DiLorenzo and Mantua 2016).

While the role of atmospheric teleconnections and local forcing on the 2014–16 anomalous warming seems reasonably well understood, the importance of remote

[1]The winds-evaporation-SST (WES) feedback.

forcing remains an open question. There is currently little evidence of coastally trapped waves, connected to remote forcing, along the US West Coast in 2015–16. Downwelling phases of equatorial Kelvin waves were observed propagating eastward across the Pacific in October–November 2015 and January–February 2016 (NOAA Climate Prediction Center/NCEP 29 August, 2016 web page, accessed Sept. 1, 2016). Whether these equatorial waves generated northward propagating coastally trapped waves along the US West Coast, with potential effects on the California Current System, does not appear to have been determined at the time of writing. Until further evidence is accumulated, it is difficult to apportion relative importance of local forcing (via atmospheric pathways) versus remote forcing (propagating along oceanic pathways) on the 2015–16 warm event.

Northward Transport

Among other effects, strong El Niños generally cause changes in the spatial pattern and volume transport of the California Current System. The temporal evolution of volume transport between the surface and 500 m depth across CalCOFI line 90 between nearshore station 30 (11 km of the shelf) and offshore station 120 (683 km from the coast) (fig. 1) reflects the net flow of the equatorward California Current and the poleward flows of the deeper California Undercurrent and shallower Inshore Countercurrent[2,3], (Lynn and Bograd 2002). Anomalous flows can be detected by comparison with the climatological seasonal mean flows (Lynn and Bograd 2002; Zaba and Rudnick 2016).

The 1997–98 El Niño was a case where transport from the south brought unusual fish into the southern California region, probably both by advection of larvae and by adult fish swimming in water masses with favorable conditions (Lea and Rosenblatt 2000). Although occurrences of unusual animals were also a feature of the 2015–16 anomalous warming (see sections below), the observed transport derived from glider data off southern California from 2014 up to June 2015 was not anomalous when averaged over a horizontal distance of 200 km[4] (Zaba and Rudnick 2016).

In contrast to what has so far been reported for the 2015–16 warming, there was clear evidence of anomalous poleward flows during the 1997–98 El Niño. Lynn and Bograd (2002) reported anomalous poleward flows integrated over 0–500 m from November 1997 to February 1998, due to strengthening and broadening of both the Inshore Countercurrent and the California Undercurrent (Lynn and Bograd 2002). Flows between 200–500 m were similar except that there was an earlier poleward flux in July 1997 equaling that observed in November 1997, so there were two poleward transport pulses at depth during the 1997 El Niño (see Lynn and Bograd 2002, their fig. 9). After February 1998 the poleward flows weakened and equatorward flow strengthened. By April 1998 the dominant flow was again toward the equator in a revived California Current that moved progressively offshore at the speed of a propagating Rossby wave (Lynn and Bograd 2002).

The northward extension of animals that are weak swimmers, such as adult red crabs (*Pleuroncodes planipes*) suggests that advective transport from the south occurred in 2015–16, as it did in 1997–98. HF-radar data show that northward-directed surface currents developed off central California in the fall and winter of 2015–16—in addition to the usual poleward surface currents observed in the Southern California Bight during summer (see section below). Beach strandings of red crabs in southern California were reported from January to October 2015. This suggests that the crabs either swam there in water with favorable conditions, or that they were carried there by advection. Further analysis of the glider and HF-radar current velocity data may resolve the issue of how slow swimming red crabs, which are usually found in more tropical southern waters, arrived off southern California.

DESCRIPTIVE PHYSICAL OCEANOGRAPHY

El Niño/Southern Oscillation (ENSO) is a dominant mode of interannual variability in the equatorial Pacific, causing physical and ecological impacts throughout the Pacific basin and California Current System. The Oceanic Niño Index (ONI; http://www.cpc.ncep.noaa.gov/data/indices/), a three-month running mean of sea-surface temperature anomalies averaged over the NINO3.4 region of 5°S–5°N and 120°W–170°W, is used by NOAA as a diagnostic to gauge the state of ENSO. ONI values exceeding the 0.5°C threshold that signifies an El Niño event were observed from April 2015 through May 2016 (Supplement fig. S1). The ONI dropped below the 0.5°C threshold during June 2016. NOAA's Climate Prediction Center (http://www.cpc.ncep.noaa.gov) issued a report in September 2016 stating that El Niño neutral conditions were reached by June 2016 and forecasted a 55%–60% probability of ENSO-neutral conditions by the fall and winter of 2016–17.

Warm conditions in the North Pacific were a result of the continuation of the marine heat wave, a large area of exceptionally high SST anomalies that originated in the Gulf of Alaska in late 2013 (Bond et al. 2015). By the middle of 2014, high SST anomalies were also observed

[2]Other studies (e.g., Zaba and Rudnick 2016) integrate flows over different horizontal intervals.

[3]Note that the Inshore Countercurrent is a surface manifestation of the California Undercurrent and Todd et al. (2011) considered that there is little physical justification for separate names because there is no depth related discontinuity in the transport.

[4]Data of Zaba and Rudnick (2016) only extends to June 2015.

in the CCS and as far south as Baja California (Leising et al. 2015). The Pacific Decadal Oscillation (PDO) index describes the temporal evolution of the dominant spatial pattern of SST anomalies over the North Pacific (Mantua et al. 1997). The PDO values during December 2014 until March 2015 were all higher than 2, which were some of the highest values in the time series (Supplement fig. S1), following a period of consistent negative values from June 2010 through 2013. These high winter PDO values indicate the presence of the marine heat wave since they precede the onset of the 2015 El Niño event, and modulated the regional expression of the El Niño event on the California Current (Jacox et al. 2016). The PDO value of April 2016 was the highest since the 1997–98 El Niño event.

The North Pacific Gyre Oscillation (NPGO) is a low-frequency signal of sea-surface height, indicating variations in the circulation of the North Pacific Subtropical Gyre and Alaskan Gyre, which in turn relate to the source waters for the California Current (Di Lorenzo et al. 2008). Positive values of the NPGO are linked with increased equatorward flow in the California Current, along with increased surface salinities, nutrients, and chlorophyll *a* values. Negative NPGO values are associated with decreases of these variables, inferring less subarctic source waters and generally lower productivity. Negative values of the NPGO occurred from mid-2013 to May 2016, except for a couple of very small positive values in 2014 and at the start of 2016 (Supplement fig. S1).

North Pacific Climate Patterns

A basin-scale examination of sea surface temperatures (SST) and surface wind vectors allows for the interpretation of the spatial evolution of climate patterns and wind forcing over the North Pacific related to trends in the basin-scale and upwelling indices (Supplement fig. S2, S3). Negative SST anomalies in the region of the Subarctic Frontal Zone were evident in the summer of 2015, winter 2016, and spring 2016 (Supplement fig. S3); these negative anomalies first arose in the summer of 2014 (Leising et al. 2015). The SST anomaly pattern during these months with negative SST anomalies in the west and central North Pacific and positive SST anomalies along the west coast of North America and equatorial Pacific resemble the warm phase of the PDO (Mantua et al. 1997). Enhanced westerly wind anomalies, especially in the western Pacific, coincided with these negative SST anomalies. Positive SST anomalies associated with the El Niño were high across the eastern equatorial Pacific from July 2015 to February 2016. During this time, the usual easterly winds along the equator slackened or changed direction as seen by arrows pointing north/south in the region near South America and arrows pointing eastward in the east (fig. S3). The positive SST anomalies first started to subside in the Niño 1+2 region, a coastal region of South America near the equator, in February 2016 and by May 2016 negative SST anomalies extended along the equator from 130° to 80°W and stronger easterly winds extended from 170° to 160°W. Along the coast of North America, high positive SST anomalies due to the marine heat wave started to diminish by December 2015, with values dropping by 1°C from high values experienced in the early part of 2015. Positive SST anomalies remained along the coast in late winter and early spring of 2016, with SST anomalies ranging from 0.5° to 1.5°C. Alongshore winds in the Gulf of Alaska were associated with anomalously cyclonic winds forced by low atmospheric pressure during February 2016. This cyclonic wind pattern switched to an anticyclonic pattern by May 2016 due to a strong North Pacific High (Supplement fig. S3).

Upwelling in the California Current

Monthly means of daily upwelling index (Bakun 1973; Schwing et al. 1996) show the strongest upwelling occurring between 36°–45°N (Supplement fig. S2). Upwelling in these latitudes was unusually strong during the spring and summer of 2014 and for the majority of the year in 2015 (Supplement fig. S2, bottom). El Niño causes the North Pacific atmospheric pressure system to weaken and decrease in size (Schroeder et al. 2013), and as a result, winds that promote upwelling slacken (Schwing et al. 2002). During the winter of 2015–16 downwelling was anomalously strong for latitudes north of 36°N.

The Cumulative Upwelling Index (CUI) is the cumulative sum of the daily UI starting January 1 and ending on December 31, and is used here to compare the 1997–98 El Niño to the current event. Cumulative upwelling during the first two months of 1997 and 2015 was average to slightly greater than average for all latitudes (Supplement fig. S4). By November, downwelling winds associated with El Niño caused the CUI to decline, which is most evident for locations 39° to 48°N. Strong downwelling continued into 1998 and 2016 for all latitudes north of 33°N. The CUI values for 1998 were some of the lowest for all years of the record (since 1967) due to extreme negative upwelling indices, i.e., downwelling in January 1998. In conclusion, upwelling associated with the two El Niño events proceeded similarly, but upwelling during the winter for the 1997–98 event was much weaker than 2015–16.

The date when CUI values increased above their seasonal minimum can be used as an index of the "spring transition." Periods of strong upwelling can occur before the spring transition and these winter upwelling events can precondition the ecosystem for increased production in the spring (Black et al. 2010). The preconditioning index (pCUI) is defined as the cumulative sum of only

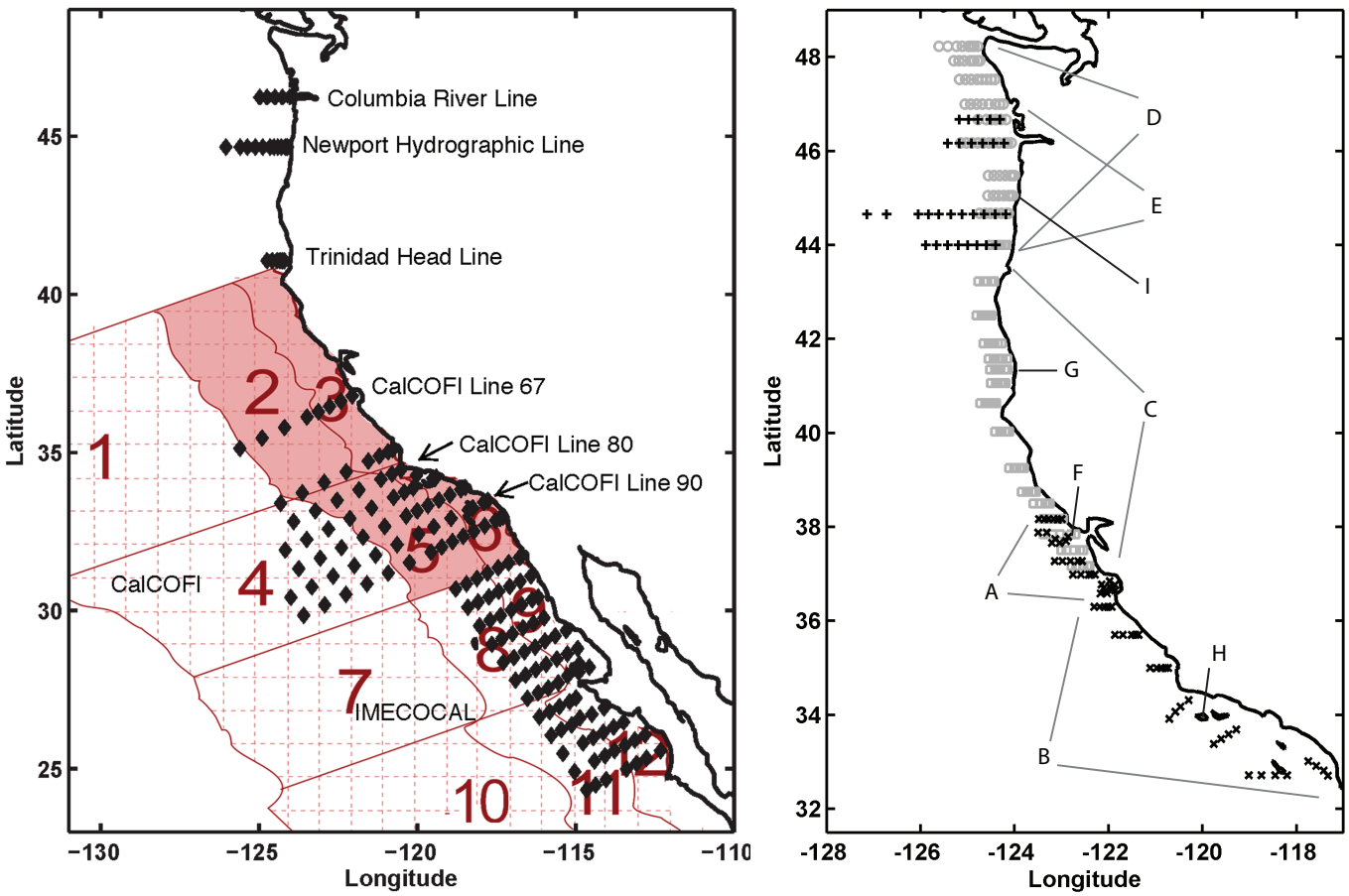

Figure 2. Station maps for surveys that were conducted multiple times per year during different seasons to provide year-round observations in the California Current System. The CalCOFI survey (including CalCOFI Line 67) was occupied quarterly; the winter and spring CalCOFI survey grid usually extends just north of San Francisco. The IMECOCAL survey is conducted quarterly or semiannually. The Newport Hydrographic Line was occupied biweekly. The Trinidad Head Line was occupied at biweekly to monthly intervals. Red overlay and numbers denotes areas for SST and chlorophyll *a* analysis. Right: Location of annual or seasonal surveys, including locations of studies on higher trophic levels, from which data was included in this report. Different symbols are used to help differentiate the extent of overlapping surveys. A. SWFSC Fisheries Ecology Division (FED) midwater trawl survey core region (May–June) B. SWFSC FED midwater trawl survey south region (May–June). C. SWFSC FED salmon survey (June and September) (gray squares). D. NWFSC salmon survey (May, June, and September). E. NOAA/BPA pelagic rope trawl survey (May through September). F. Southeast Farallon Island. G. Castle Rock. H. San Miguel Island. I. Yaquina Head Outstanding Natural Area.

the positive values of the UI from January 1 to the end of February (Schroeder et al. 2013). The pCUI values for 2016 were very low, indicating very few days of upwelling, and the values were very similar to the pCUI values during 1998 (not shown).

Coastal Sea Surface Temperature

Daily SSTs as measured by National Data Buoy Center (NDBC) buoys along the West Coast have mostly been above long-term averages since the summer of 2014 (Supplement fig. S5). Weekly periods of exceptionally high temperature anomalies (greater than 2°C) occurred at all buoy locations from the fall of 2014 to the fall of 2015. By December 2015 SSTs were still high, but not as high as those during the previous year. The meridional winds during the warm SST period were not unusually weak in magnitude or overly downwelling favorable (+ values). The decrease in SST values seen in the central CCS during the spring of 2015 corresponded with an extended period of upwelling favorable winds (– values). Long episodes of downwelling favoring winds occurred during January and March of 2016 at all locations.

Sea Surface Temperature and Chlorophyll Anomalies off California from Remote Sensing

To analyze temporal trends of remotely sensed SST and surface chlorophyll *a*, the southern CCS region has been divided into 10 areas (fig. 2). For this analysis data from areas 2, 3, 5, and 6 were used. Significant SST and chlorophyll *a* anomalies[5] were present before

[5]The effects of the 2015–16 El Niño on the California Current System (CCS) were evaluated using satellite-detected SST and surface chlorophyll *a* concentration, using the same methods that Kahru and Mitchell (2000) applied to the major 1997–98 El Niño. SST data were derived from the version 2.0 daily datasets of optimally interpolated global blended AVHRR temperatures (Reynolds et al. 2007; https://podaac.jpl.nasa.gov/dataset/AVHRR_OI-NCEI-L4-GLOB-v2.0). Chlorophyll *a* data were derived from the merged multisensor regionally optimized dataset for the CCS (Kahru et al. 2012, 2015; http://spg.ucsd.edu/Satellite_Data/CC4km/CC4km.htm). Anomalies were calculated relative to the long-term (1981–2016) mean monthly values.

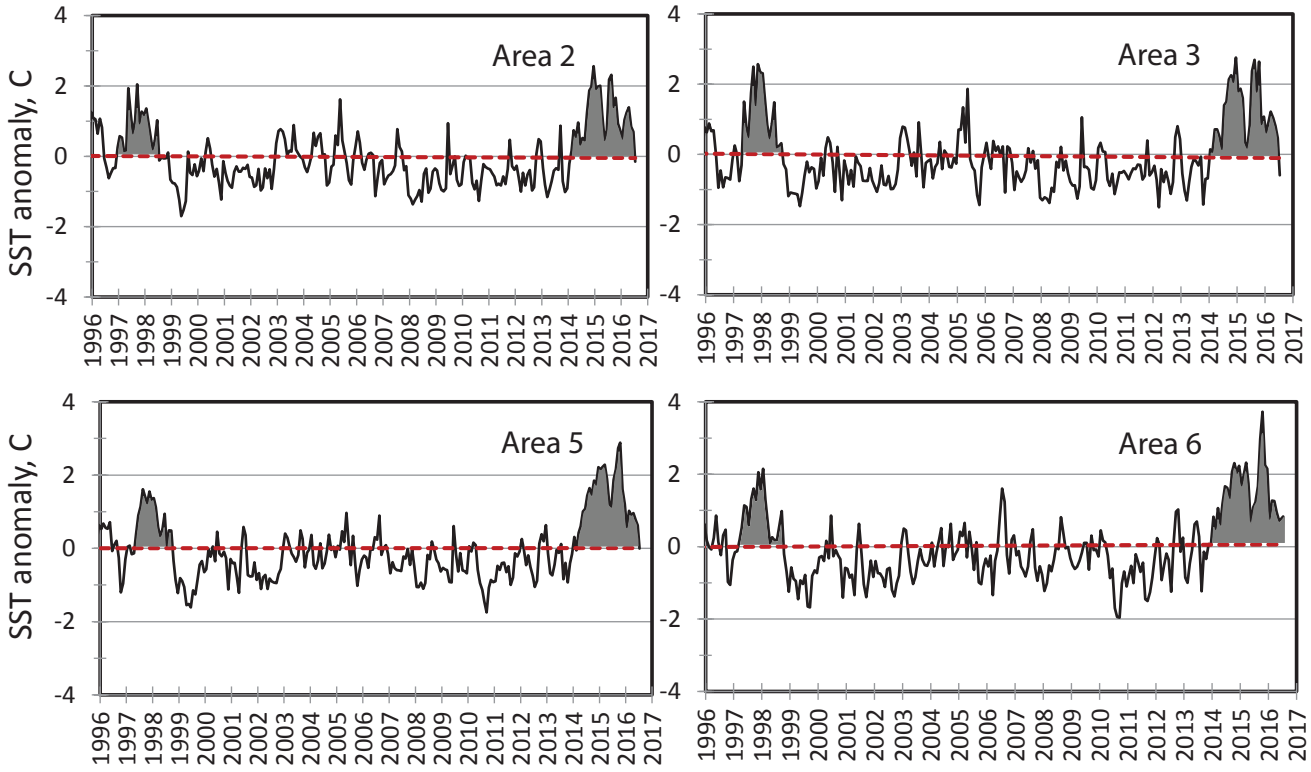

Figure 3. Anomalies of monthly mean sea-surface temperature in coastal and transitional areas of central and southern California (see map in fig. 2). Anomalies were calculated relative to monthly means of Sept. 1981–July 2016. The shaded areas correspond to the anomalies of 1997–98 and 2014–16, respectively. Anomalies were calculated relative to the long-term (1981–2016) mean monthly values.

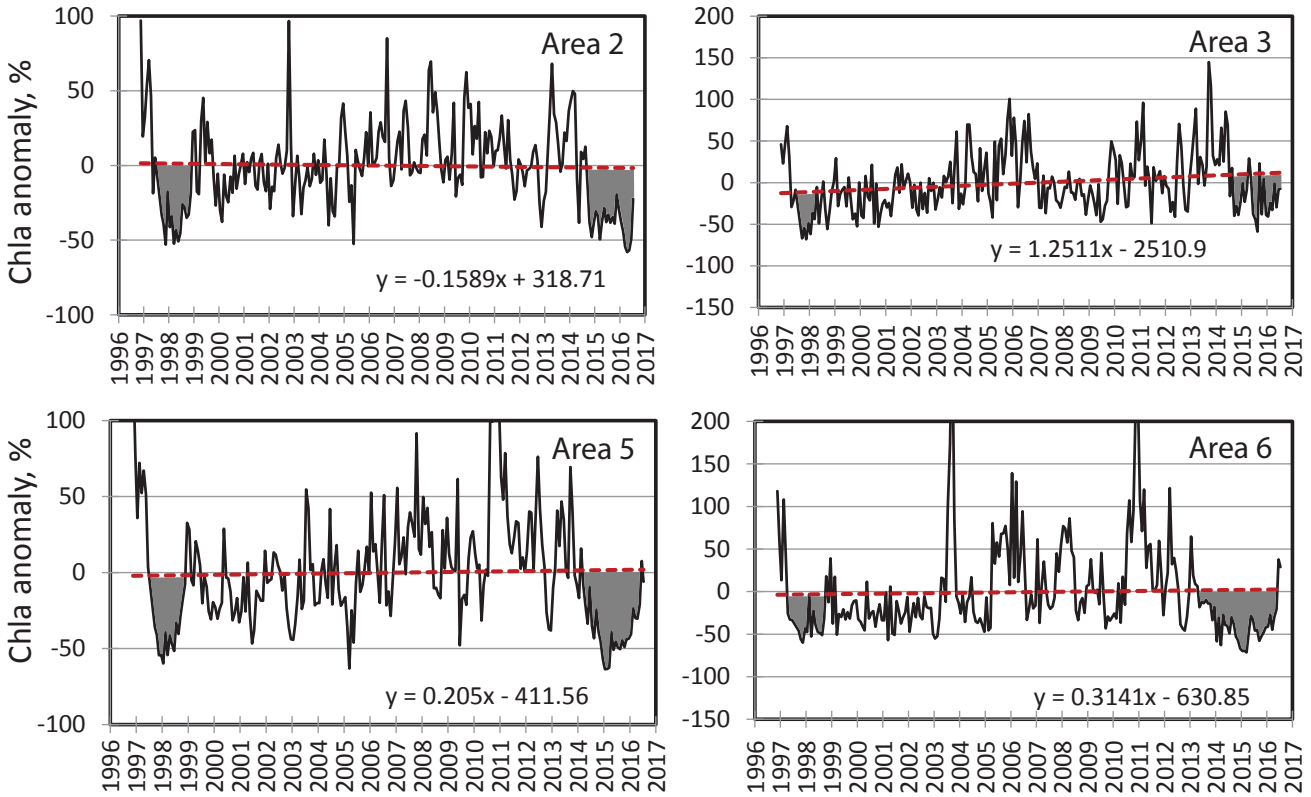

Figure 4. Anomalies in monthly mean surface chlorophyll *a* concentration in coastal and transitional areas of central and southern California (see fig. 2a). Anomalies were calculated relative to monthly means of Nov. 1996–July 2016. The red dashed line and the linear equation shows the mean linear trend. The shaded areas correspond to the anomalies of 1997–98 and 2014–16, respectively.

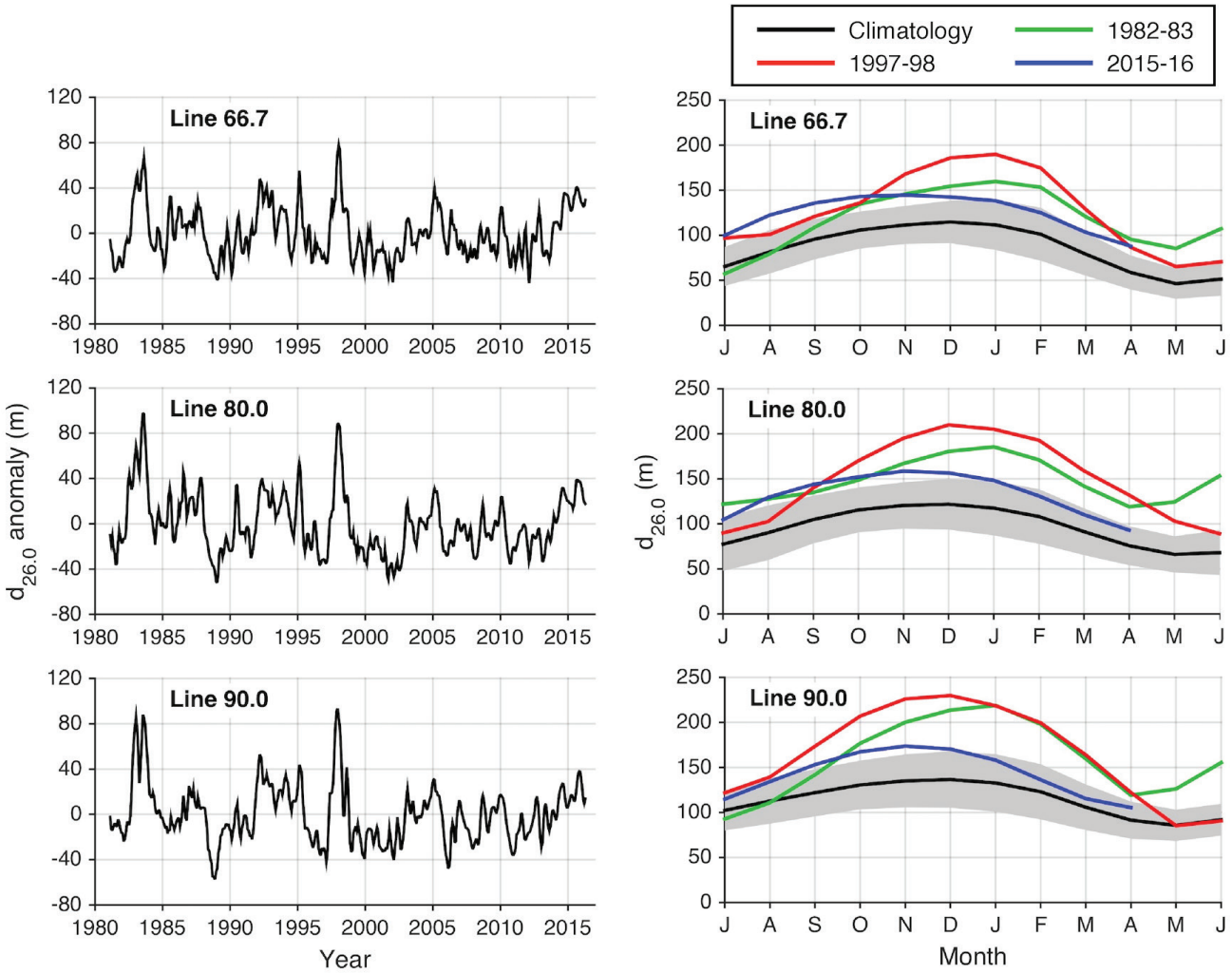

Figure 5. Time series of 26.0 kg m^{-3} isopycnal depth ($d_{26.0}$), averaged within 50 km of shore on CalCOFI lines 66.7, 80, and 90. (Left) $d_{26.0}$ anomalies from 1981 to April 2016, computed relative to a 1981–2015 climatology. (Right) 12-month (July–June) progression of $d_{26.0}$ for the three strongest El Niños of recent decades. Gray shading marks one standard deviation of the interannual variability about the climatology (black line). All time series are smoothed with a three-month running mean. Adapted from Jacox et al. (2016).

as well as during the 2015–16 warming. SST anomalies exceeded 2.5°C, which is comparable to or higher than those observed during the 1997–98 El Niño when SST anomalies reached about 2.0°C (2.5°C off central California coastal region) (fig. 3). Corresponding negative chlorophyll anomalies of about 50% were comparable to those of the 1997–98 El Niño (fig. 4). The strongest SST anomalies during 2014–16 occurred in two events separated by a weakening in the middle of 2015[6]. The anomalies began prior to the El Niño proper and were part of the multiyear North Pacific heat wave. This contrasts with the short-lived 1997–98 anomaly.

The spatial distribution of the chlorophyll *a* anomalies was evaluated using principal component analysis. The first principal component (PC1, not shown) was associated with a negative anomaly along the central California coast where upwelling is common. During El Niño events PC1 is weaker as it is associated with reduced upwelling and lower than normal chlorophyll *a* off central California. According to this measure, the 2015–16 chlorophyll *a* anomaly was weaker than the 1997–98 El Niño.

Vertical Structure of the Marine Heat Wave off California

The impact of recent climate anomalies on the subsurface structure of the CCS is highlighted by temporal variability in the depth of the 26.0 kg m^{-3} isopycnal ($d_{26.0}$). Figure 5 shows time series of $d_{26.0}$ in the nearshore region (<50 km from the coast) of CalCOFI lines 66.7, 80, and 90. These time series were obtained by combining a data assimilative regional ocean model with sustained underwater glider observations (see Jacox et al. 2016). The past year produced positive (deep) $d_{26.0}$

[6]The developing El Niño of early 2014 that was aborted by easterly wind burst in June 2014 is beyond the scope of this manuscript.

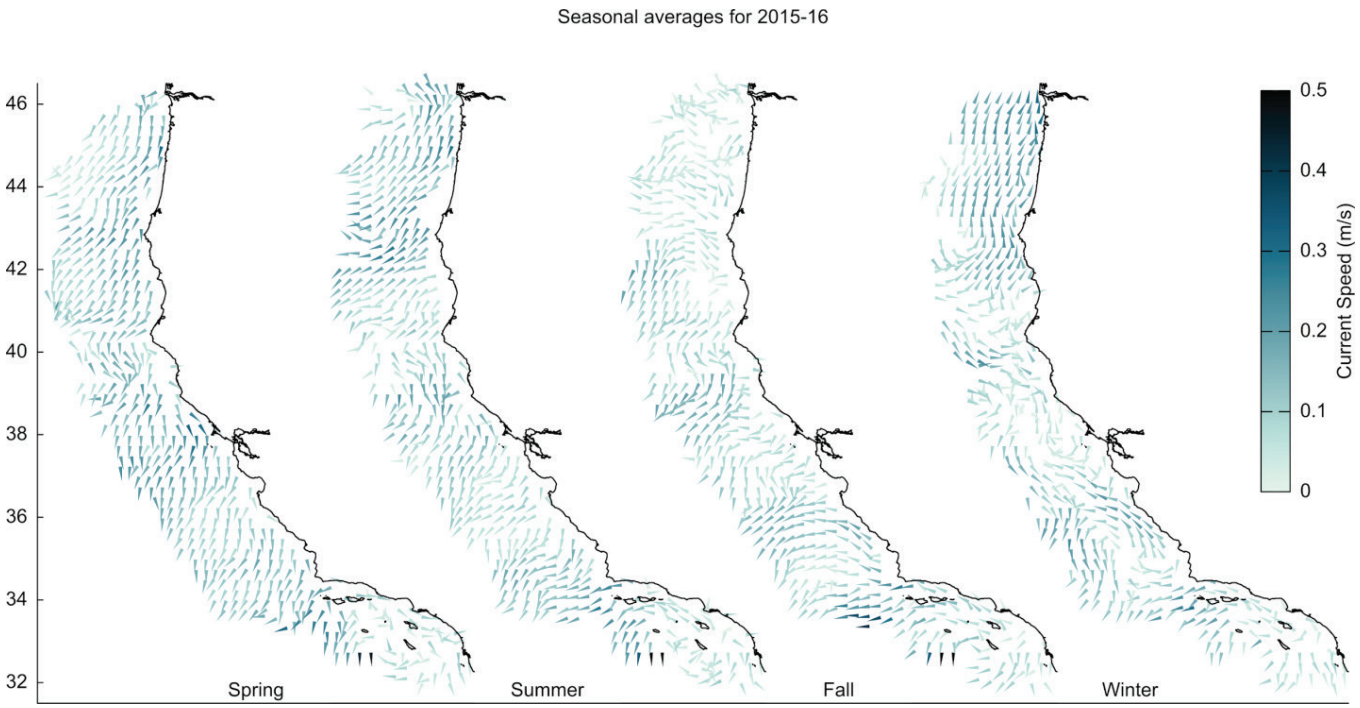

Figure 6. Maps of seasonal mean surface currents observed in the CCS with HF radar. From left to right, the panels present data for spring (March–May 2015), summer (June–August 2015), fall (September–November 2015), and winter (December–February 2016). Current speed is indicated by depth of shading and direction given by orientation of arrow extending from observation location. Currents are displayed with spatial resolution of 0.25°.

anomalies, a condition associated with limited nutrient availability and suppressed productivity. However, during the 2015–16 warming, $d_{26.0}$ was considerably shallower than during the 1982–83 and 1997–98 events, and also showcased a much different temporal evolution. The past strong El Niño events were characterized by $d_{26.0}$ increasing rapidly beginning in summer, reaching peak anomalies in winter (November to February), and then decreasing again into the spring. In contrast, 2015–16 saw $d_{26.0}$ anomalies that were already positive due to anomalous warming that began in 2014 (Zaba and Rudnick 2016), and those anomalies remained nearly constant throughout the latter half of 2015 rather than growing as would be expected during a strong El Niño. These data suggest that observed anomalies in 2015–16 were still associated with warm anomalies present for several years, with El Niño's contribution being relatively minor when compared to past strong El Niños. In the first half of 2016, $d_{26.0}$ has gradually shoaled, approaching climatological values and suggesting the decline of both El Niño and the preexisting warm anomalies.

Surface Coastal Jets Associated with 2015–16 El Niño

During 2015–16, surface currents[7] between Point Conception (34°N) and the Columbia River (46°N) were predominantly southward through spring and summer (fig. 6). During fall, as in most years, a strong mean northward flow was seen between Point Conception (34°N) and Point Sur (36.3°N). In addition, a northward flow associated with El Niño conditions was present in winter (fig. 6). This flow was weaker, farther offshore and less coherent between 37° and 41°N (San Francisco to Trinidad Head). As is usual in the winter, a coherent northward flow was observed north of the Oregon-California border (42°N), but the flow was stronger in 2015–16 than in other years.

In the Southern California Bight, the usual southward flow was observed south of San Diego (33°N) in all seasons. A poleward (westward) flow was observed between Point Vicente and Point Conception (33.8°–34.5°N) in summer, fall, and winter linking to the westward flow jetting offshore from Point Conception. Offshore jets were also observed in spring and summer southwest of major headlands as in past years (Cape Blanco 43°N, Cape Mendocino 40°N and Point Arena 39°N). In the fall, the Mendocino and Arena features appear as one, and the Blanco feature had dissipated. Meanwhile, a well-defined jet was observed off Point Sur (36.3°N) in fall associated with northward flow. In winter the northward flow continued past Point Sur.

[7]These data on surface currents were obtained from high-frequency (HF) radar, with vectors calculated hourly at 6 km resolution using optimal interpolation (Kim et. al. 2008; Terrill et. al. 2006). Real-time displays can be viewed at www.sccoos.org/data/hfrnet/ and www.cencoos.org/sections/conditions/Google_currents/ as well as at websites maintained by the institutions that contributed the data reported here (listed in Acknowledgments).

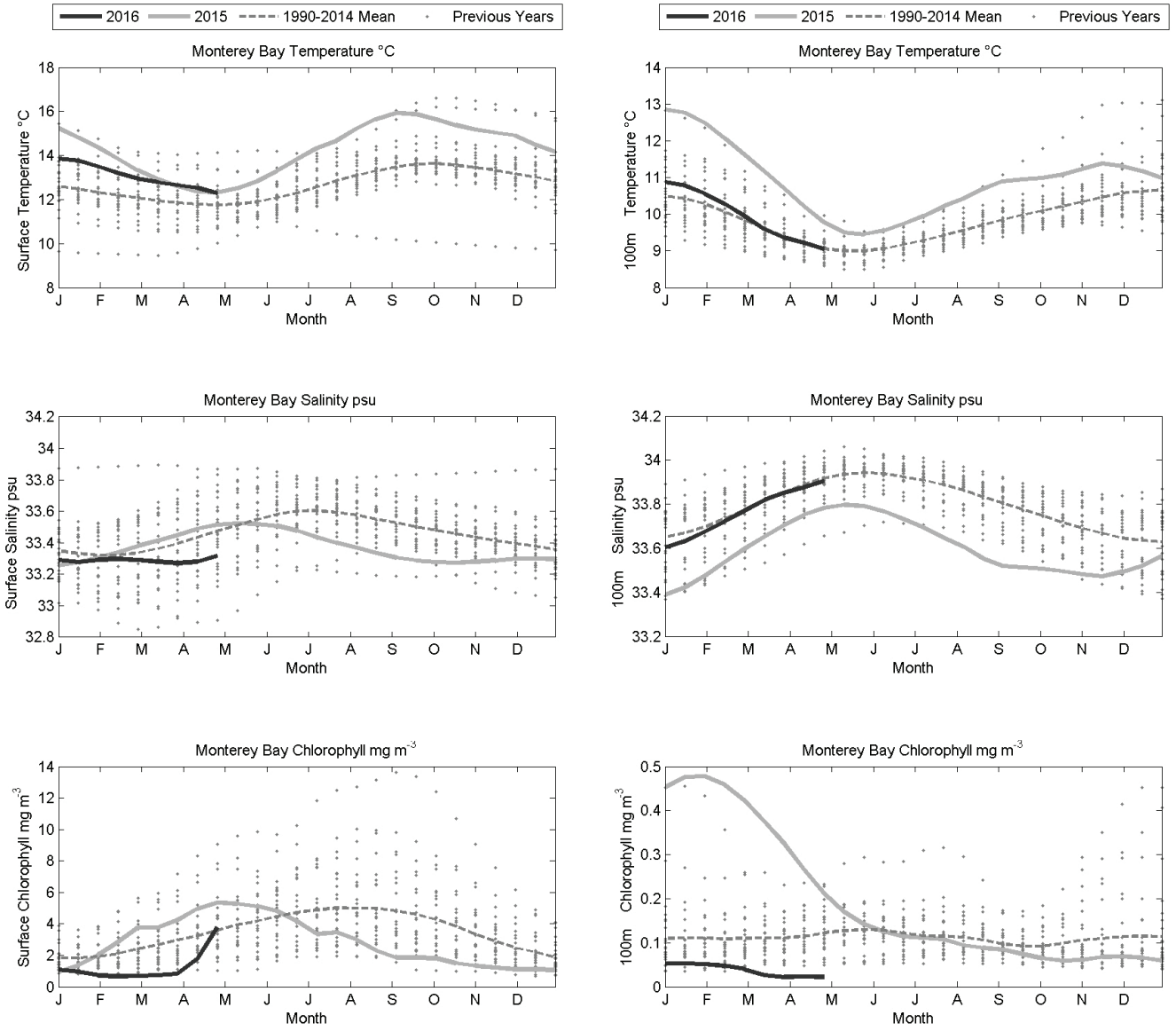

Figure 7. Temperature (top panels), salinity (middle panels) and chlorophyll *a* concentration (bottom panels) at the surface (left-hand column) and at 100 m (right hand column) observed at the M1 mooring in Monterey Bay, CA.

Warm Temperatures, Low Salinities, and Low Chlorophyll Production in Monterey Bay

Surface temperatures at the M1 mooring in Monterey Bay were only slightly above the climatological average, i.e., normal, during the spring of 2015 but began to increase in the Bay with the advent of the El Niño, declining to slightly above normal during the late spring of 2016 (fig. 7). Temperatures at 100 m were above normal during 2015, approaching normal values in the spring of 2016 (fig. 7).

Surface salinities were near the climatological average during this time period, except for the summer-fall of 2015 when extremely fresh waters were observed (fig. 7). Fresher than normal waters had been observed at 100 m throughout 2015, returning to normal values early in 2016. It is thus likely that the fresh surface waters observed during the fall of 2015 were driven by the freshening of the subsurface waters throughout 2015.

Chlorophyll *a* at the surface and at 100 m was unusually low throughout the summer and fall of 2015 and the winter and spring of 2016, only rising to average values in May 2016 (fig. 7). This may have been driven by strong stratification of the surface waters, preventing large fluxes of nitrate into this layer.

Contrasting Effects of the North Pacific Marine Heat Wave and El Niño off Southern California

This report of oceanographic observations off Southern California is based on data collected on four

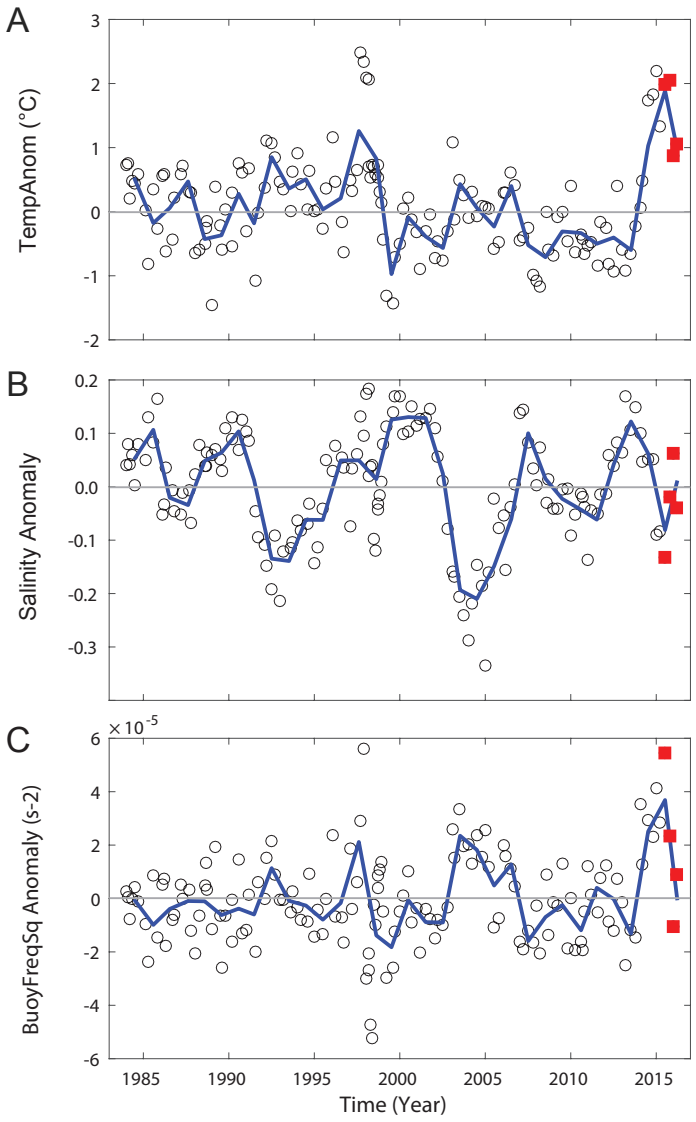

Figure 8. Cruise averages of property anomalies for the mixed layer (ML) of the CalCOFI 66 station standard grid (Figure 1) for 1984 to the spring of 2016. A: ML temperature, B: ML salinity. C: buoyancy frequency squared (N^2) in the upper 100 m. Data from individual CalCOFI cruises are plotted as open circles; data from the four most recent cruises, 201507 to 201604, are plotted as solid red symbols. Blue solid lines represent annual averages, gray horizontal lines the climatological mean, which is zero in the case of anomalies. Anomalies are based on the 1984 to 2012 time period.

CalCOFI cruises in July and November of 2015 and January and April of 2016[8].

Average mixed layer[9] (ML) temperatures during the summer and fall of 2015 in the CalCOFI domain were as high as those observed during 2014 and early 2015 (fig. 8A), likely reflecting the effects of the marine heat wave during the first half of the year and the effects of the El Niño during the second half of the year. ML temperature anomalies cooled by ~1°C during the first half of 2016, consistent with fading of the 2015–16 warming.

The area affected by the marine heat wave and the 2015–16 El Niño in the mixed layer was comparable to the 1997–98 El Niño, but the event lasted longer (fig. 9A). However, as reported previously (Leising et al. 2015), the effects of the marine heat wave on temperatures at depth were small, on the order of 0.5°C, increasing to as much as 1.5°C during the 2015–16 El Niño (fig. 9B, 100 m). This effect was particularly pronounced in the Southern California Bight compared to offshore waters, as was the case during the 1997–98 El Niño, although the effects in 2015–16 were weaker than in 1997–98 (fig. 8B). Such changes in water column properties and depth of the thermocline are thought to be

[8]Each cruise covers 66 stations off southern California (fig. 1), i.e., the CalCOFI domain, a region that encompasses the southern California Current, the Southern California Bight (SCB), the coastal upwelling region at and north of Pt. Conception and the edge of the North Pacific Gyre. At each station a CTD cast and various net tows are carried out. Up to 20 depths are sampled at each station between the surface and, bottom depth permitting, 515 m. Results are presented as time series of averages over all 66 stations (the CalCOFI domain) covered during a cruise or as anomalies of such values with respect to the 1984–2012 time period. When appropriate averages from selected regions are used, i.e., these are based on a subset of the 66 standard CalCOFI stations. The buoyancy frequency was calculated for all depths and averaged for the upper 100 m of the water column. The nitracline depth is defined as the depth where concentrations of nitrate reach values of 1 µM, calculated from measurements at discrete depths using linear interpolation. Methods used to collect samples and analyses carried out on these samples are described in detail at CalCOFI.org/methods.

[9]Mixed layer depth was defined as the depth where density of the water is 0.02 kg m^{-3} larger than density at 10 m depth.

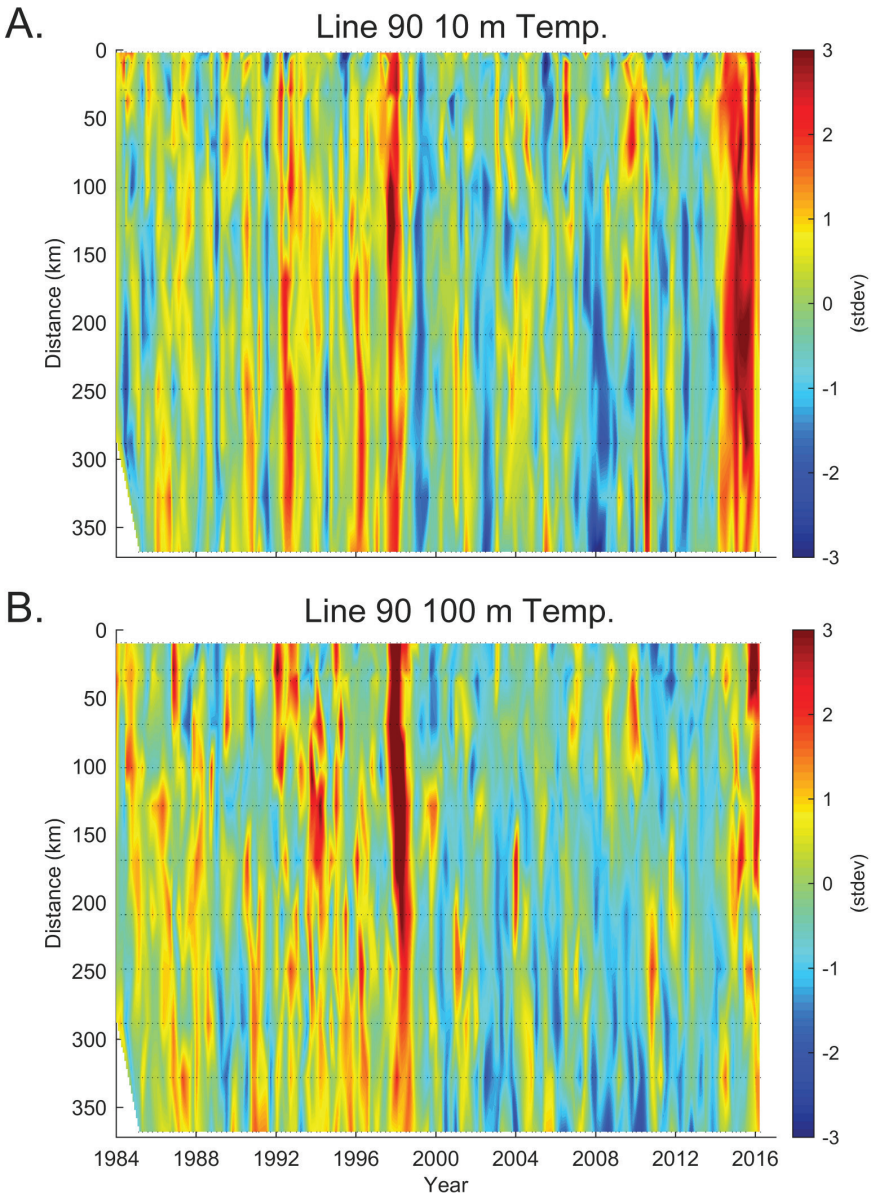

Figure 9. Standardized temperature anomalies for CalCOFI line 90 plotted against time and distance from shore for a depth of 10 m (A) and 100 m (B). Plotted data are deviations from expected values in terms of standard deviations in order to illustrate the strength of the relative changes at different depths.

driven by poleward propagating coastally trapped waves and the northward advection of warm saline water masses (Chelton and Davis 1982; Lynn and Bograd 1992). However, very little warming was observed during the 2015–16 El Niño along Line 80 at depth, in contrast to the 1997–98 El Niño (Supplement fig. S6). These observations suggest that the effects of the 2015–16 El Niño on hydrographic properties in the CalCOFI domain were not as strong as those observed during the 1997–98 El Niño.

Water column stratification in the upper 100 m (fig. 8C) during the 2015–16 marine heat wave was as strong as the most extreme values observed during the 1997–98 El Niño. However, this stratification was primarily driven by the warming of the upper 100 m. Water column stratification was strongest during the marine heat wave, decreasing as the El Niño took hold of the region. The upper ocean was unusually fresh during 2015 in most regions off southern California (Supplement fig. S7), suggesting a strengthening of the California Current.

The depth of the σ_t 26.4 isopycnal (fig. 10), which is usually found at a depth of about 200 m, increased by ~25 m during the 2015–16 marine heat wave and remained there during 2015–16. A similar change in this isopycnal depth was observed during 1997–98 El Niño.

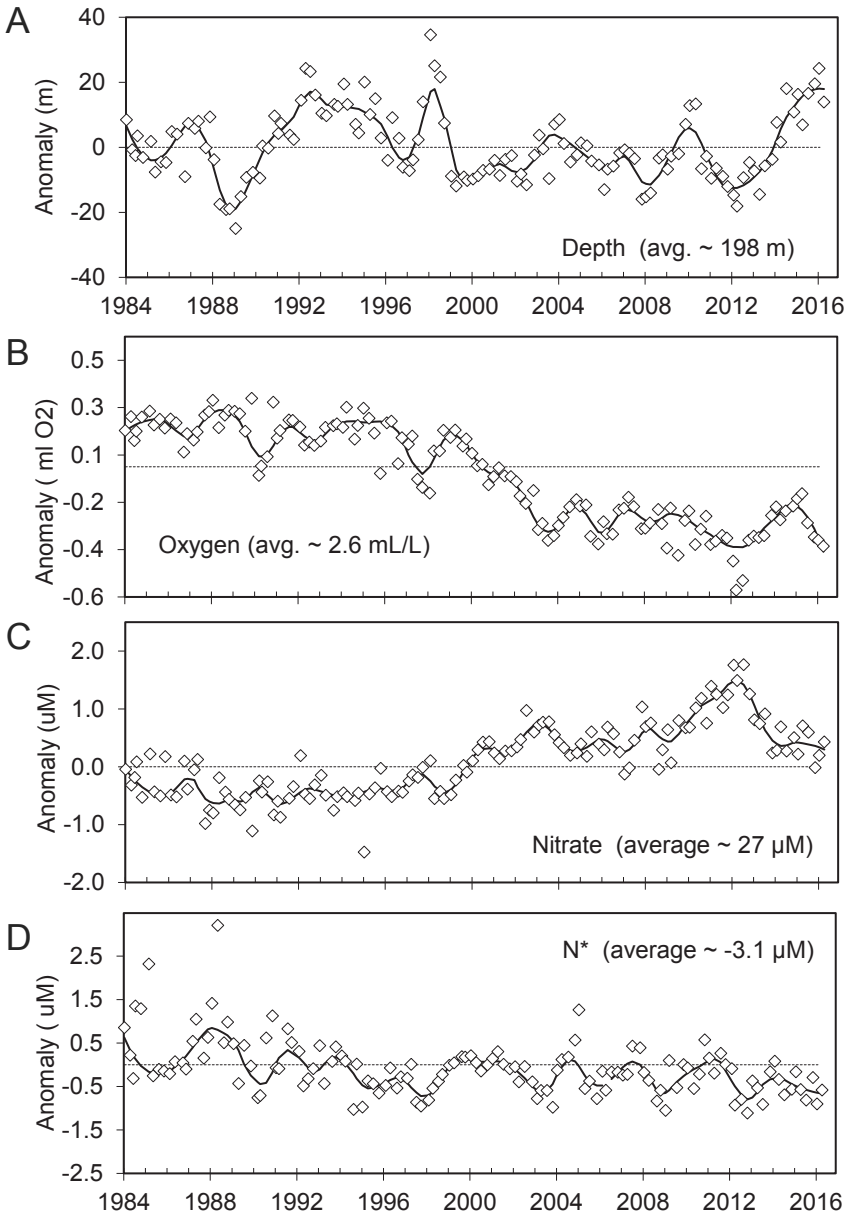

Figure 10. Anomalies of hydrographic properties at the σ_t 26.4 isopycnal (open diamonds) averaged over the standard CalCOFI stations. Shown are anomalies of isopycnal depth, oxygen, nitrate, and N*. The solid line represents a loess fit to the data; average values for the properties are listed.

Changes of spiciness at this isopycnal during 2015–16 suggest that the advection of warm saline waters into the region was likely driven by the El Niño. However, other properties at the isopycnal, such as oxygen, nitrate, and N*, a biogeochemical indicator that reflects the deficit of nitrate in a system relative to concentrations of phosphate (Gruber and Sarmiento 1997), (fig. 10B–D) were not affected by either the marine heat wave or by the El Niño.

Mixed-layer concentrations of chlorophyll *a* have been extremely low over the last three years, similar to those observed during the 1997–98 El Niño (fig. 11A). These low chlorophyll concentrations were likely caused by the low availability of inorganic nutrients such as nitrate (fig. 11B). Mixed-layer nitrate concentrations are controlled by the depth of the nitracline and by stratification. Nitracline depths, compared to the previous 15 years, have been unusually deep over the last two years (fig. 11C), and, as stated above, stratification in the upper 100 m has been unusually strong (fig. 8C). The response of chlorophyll *a* to environmental forcing during the marine heat wave and the 2015–16 El Niño differed significantly between regions within the CalCOFI domain. For example, in 2014 chlorophyll *a* concentrations in the

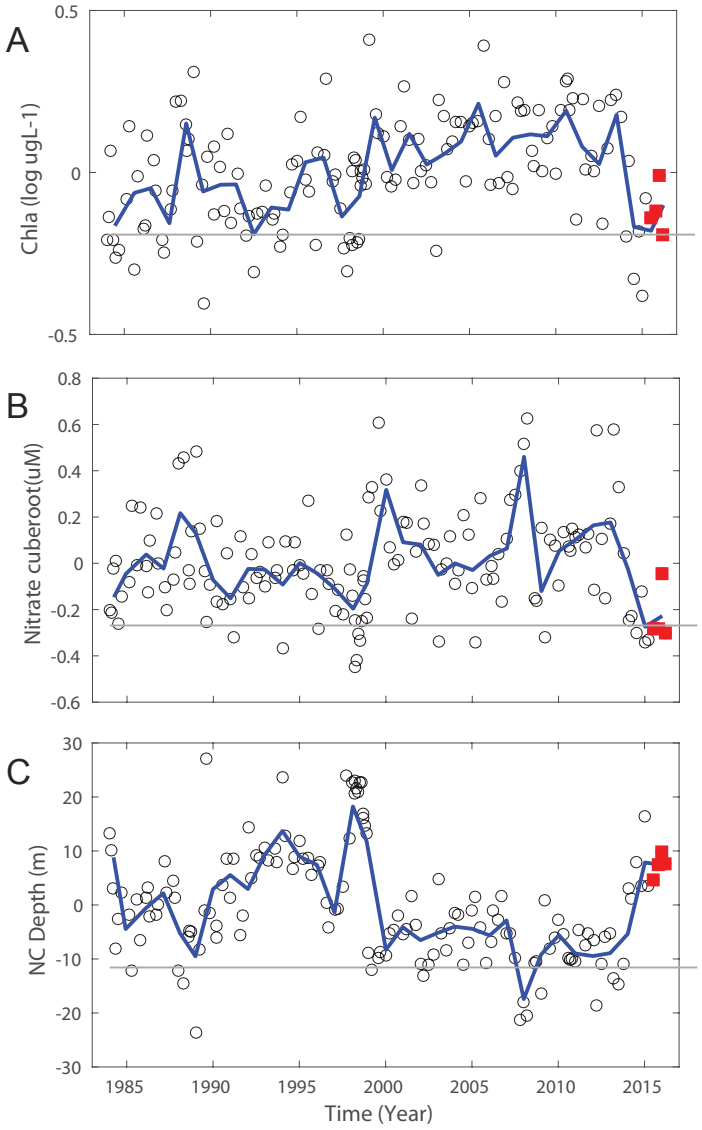

Figure 11. Cruise averages of property anomalies for a depth of 10 m for the CalCOFI standard grid. A: the log10 of chlorophyll *a*, B: the cube root of nitrate, and C: nitracline depth. Data are derived and plotted as described for Figure 8.

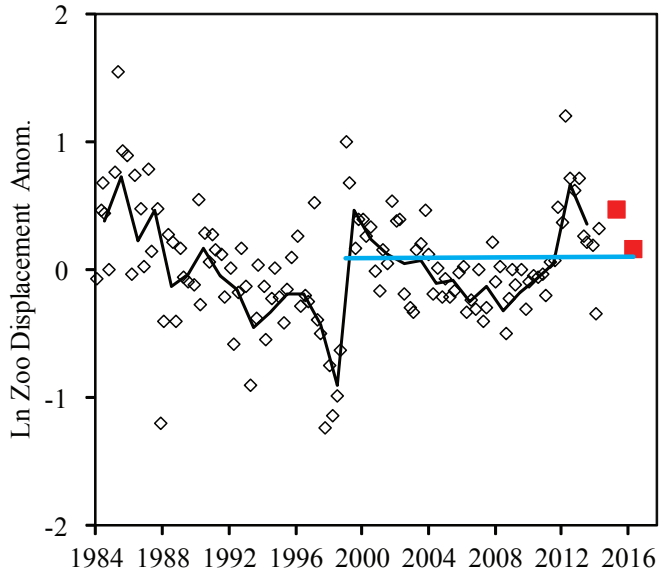

Figure 12. Cruise averages of the anomalies of the log of zooplankton displacement value relative to the 1984 to 2014 time period. Symbols used are as described in Figure 8. The blue lines are linear regressions on data for the time periods 1984 to 1998 and 1999 to the present.

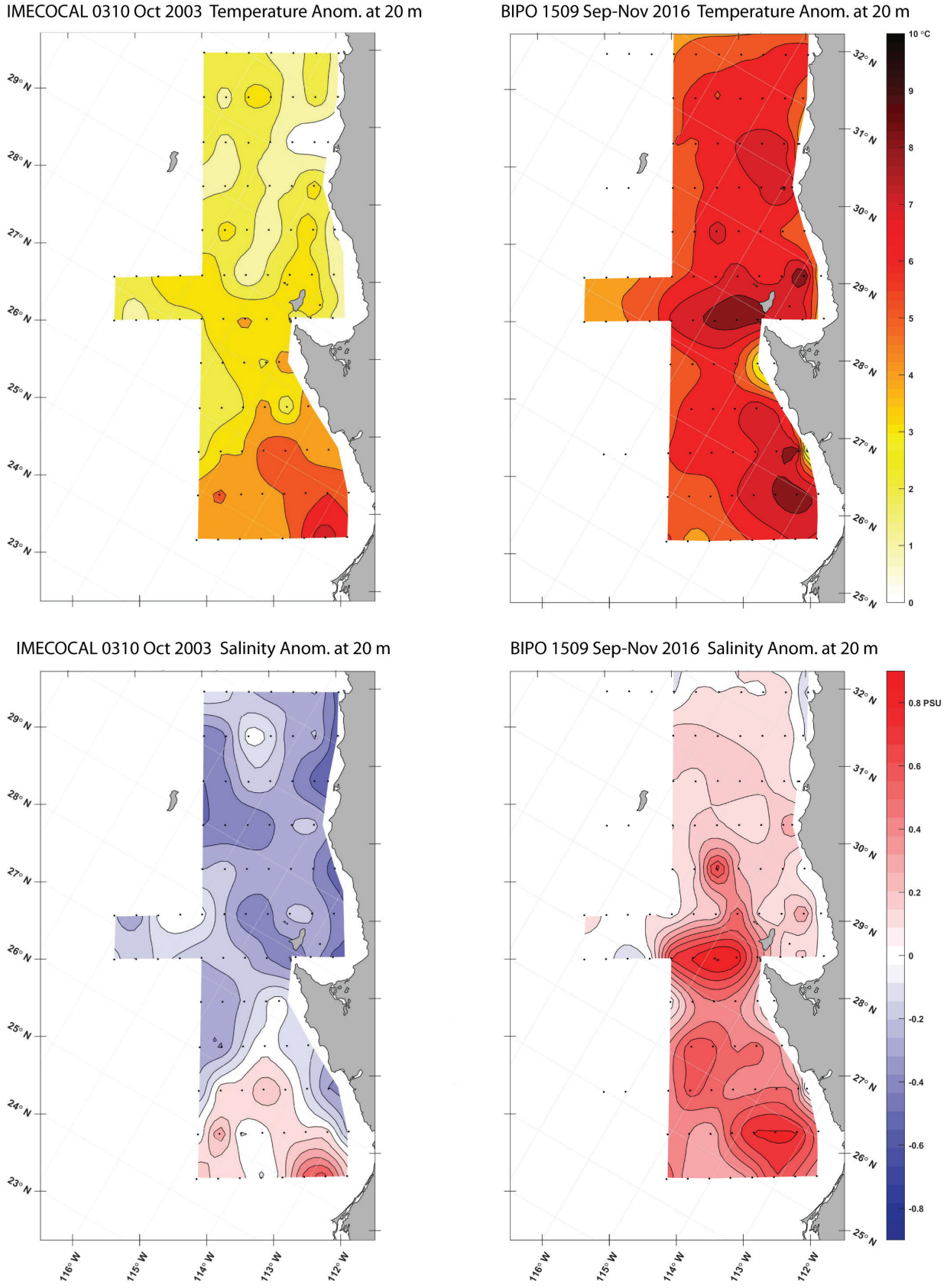

Figure 13. Temperature and salinity anomalies at 20 m depth during October 2003 (IMECOCAL cruise 0310) and September–November 2015 (BIPO cruise 1509).

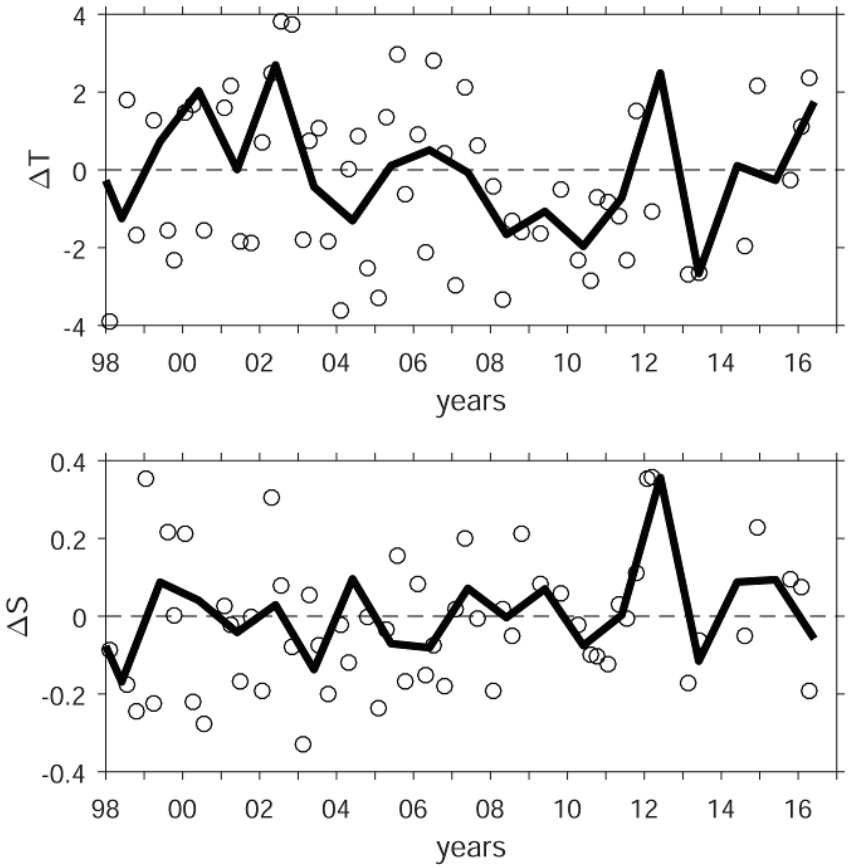

Figure 14. Mixed layer temperature and salinity anomalies in the IMECOCAL region for the period 1998–2016 (white circles) and the mean of each year (thick line).

northern coastal region were significantly below long-term averages, but were similar to these in 2015 (Supplement fig. S8). For the southern coastal area of the CalCOFI domain the opposite holds true. These regional differences are associated with interannual differences in upwelling between 2014 and 2015 (Supplement fig. S2, S4). Upwelling primarily affects the central California coast rather than the southern coastal area, which is sheltered from alongshore winds. In the southern offshore areas that are affected by the North Pacific Central Gyre, chlorophyll *a* maxima were significantly deeper during 2015, and this change was driven by differences in stratification; the temperature–nitrate relationship (data not shown) has been stable in recent years. In contrast to chlorophyll *a*, zooplankton displacement volumes for the spring seasons of 2015 and 2016 were similar to the long-term average observed over the last 15 years, indicating that zooplankton volume did not respond to the marine heat wave and the El Niño (fig. 12).

High Temperatures and High Chlorophyll Production off Baja California

Conditions off Baja California during the 2015–16 El Niño are compared here with those during October 2003[10]. The comparison with the 2003 El Niño was made because there were limited data from the Baja region during the 1997 El Niño. In October 2003, the highest SST anomalies (~6°C) were found south of Punta Eugenia and the lowest anomalies (~2°C) farther north (fig. 13). During the autumn of 2015, temperature anomalies at 20 m depth were also stronger off southern Baja and Punta Eugenia (fig. 13), but conditions were as much as 4°C warmer over the whole region (fig. 13). During the 2015–16 surveys the mean seasonal tempera-

[10]Three IMECOCAL cruises were conducted during 2015–16 aboard the oceanographic vessel *Alpha Helix*. From September 1–5, 2015 coverage was restricted to lines 100–110 off northern Baja California. During 2016, coverage was expanded to Punta Eugenia (lines 100–117) during January 21–28 and April 12–20. The third cruise was carried out during September–November 2015, as part of the INAPESCA program using the vessel *BIPO*. This cruise covered a wide area off Baja California but in the present study, we only used the data from the IMECOCAL region. CTD casts and zooplankton tows were deployed at each station of the IMECOCAL grid. Zooplankton were collected with a bongo net (0.7 m diameter, 0.5 mm mesh) towed obliquely between the surface and 210 m depth.

The mixed layer anomalies were obtained as follows. First, the long-term mean mixed layer temperature or salinity was calculated using each cast in the 1998–2016 IMECOCAL data set. Second, seasonal averages were calculated from each survey. Mixed layer anomalies for each survey were obtained by subtracting the long-term mean from the seasonal means derived from individual cruises. Temperature anomalies were computed as the difference between particular survey's temperatures and the mean temperatures from the IMECOCAL data set (1997–2016).

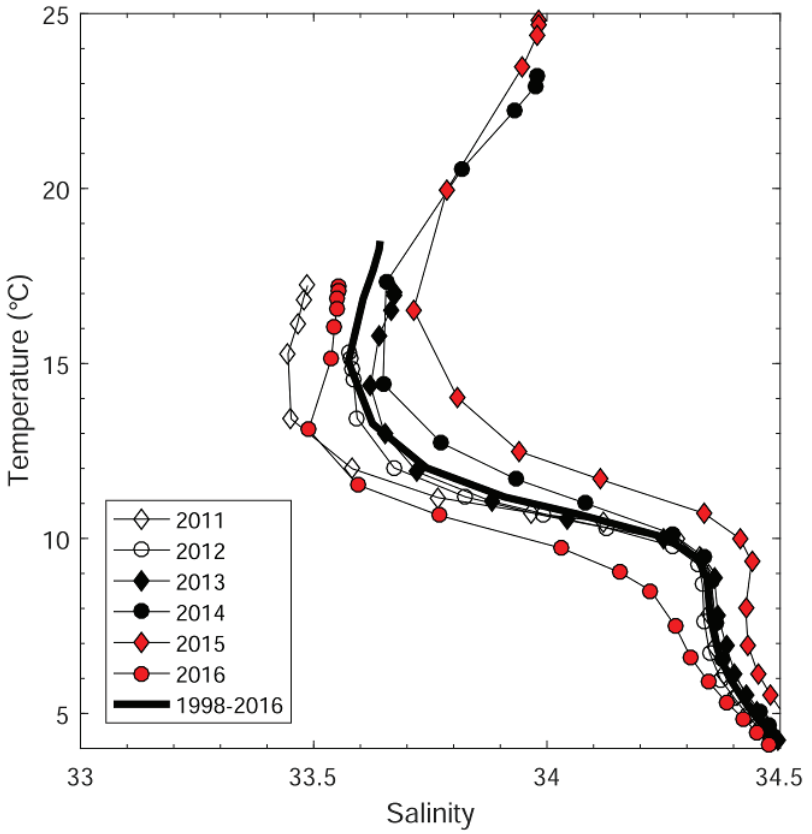

Figure 15. Annual temperature-salinity plots in the IMECOCAL region for 2011–16 compared to the long-term 1998–2016 mean.

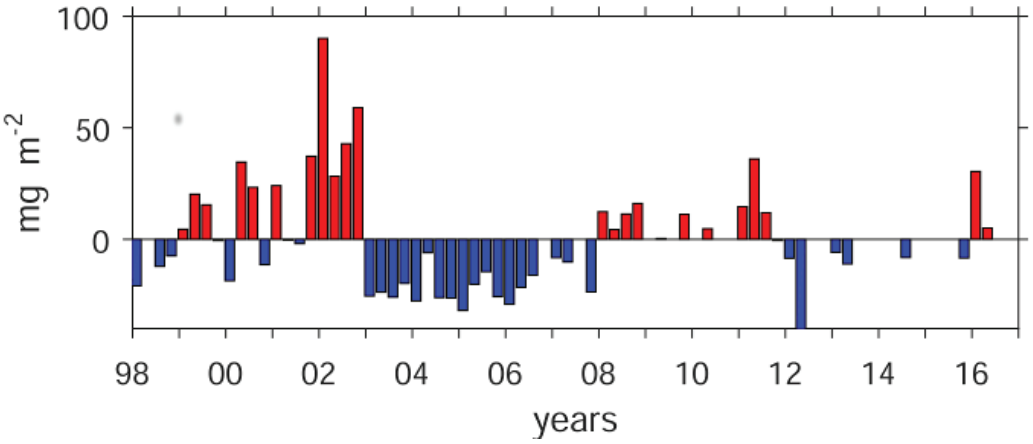

Figure 16. Depth-integrated (0–100 m) chlorophyll *a* anomalies in the IMECOCAL region. Note that chlorophyll concentrations in fall of 2015 only contain data from northern Baja California (30˚-32˚N), and are not directly comparable with the rest of the time series.

ture anomaly was of the order of +2˚C and the salinity anomaly was variable (fig. 14). Temperature-salinity plots for the IMECOCAL region clearly show the presence of anomalously warm, more saline water in 2014, increasing in 2015, before decreasing again in 2016 (fig. 15).

Salinity anomalies at 20 m depth in October 2003 tended to be negative north of Punta Eugenia and nearshore, but positive south of Punta Eugenia, except near shore (fig. 13). In contrast, during autumn 2015, salinity anomalies were positive over the entire region (fig. 13), and the salinity and temperature anomalies (fig. 13) were positively correlated. No evidence of upwelling was seen during either the autumn of 2003 or 2015.

A strong positive chlorophyll anomaly was observed during January 2016 in the IMECOCAL region (fig. 16). This positive chlorophyll anomaly during the peak of the 2015–16 El Niño contrasts with the negative chlorophyll anomaly observed in January 1998 during

the peak of the 1997–98 El Niño. By April 2016 chlorophyll had almost returned to the long-term mean concentration. We note that both chlorophyll and salinity anomalies off Baja were positive in 2015 at the same time that these anomalies were negative off southern and central California.

SUMMARY: DESCRIPTIVE PHYSICAL OCEANOGRAPHY

Warm conditions in the North Pacific, from 2014 to mid-2015, were a result of the continuation of the marine heat wave, a large area of exceptionally high SST anomalies that originated in the Gulf of Alaska in late 2013. Along the coast of North America, high positive SST anomalies due to the marine heat wave started to diminish by December 2015. Positive SST anomalies associated with the El Niño were high across the eastern equatorial Pacific from July 2015 to February 2016. Negative SST anomalies first arose in the summer of 2014 in the region of the Subarctic Frontal Zone. These negative SST anomalies persisted into May 2015. Enhanced westerly wind anomalies in the northwestern Pacific coincided with these negative SST anomalies. Westerly wind bursts are an important driver of the Kelvin waves that propagate across the Pacific, initiating El Niño conditions at the eastern boundary. The Oceanic Nino Index reached the highest positive values since the 1997–98 El Niño during the fall of 2015 and winter of 2015–16.

Positive SST anomalies remained along the coast until late winter and early spring of 2016, with SST anomalies ranging from 0.5° to 1.5°C. Daily SST as measured by NDBC buoys along the West Coast remained above the long-term average since the summer of 2014. Weekly periods of exceptionally high temperature anomalies (greater than 2°C) were observed until the fall of 2015. During the winter and spring of 2015–16, SSTs were still high but not as high as those observed previously. The decrease in SST values seen in the central CCS during the spring of 2015 corresponded with an extended period of upwelling favorable winds. Upwelling associated with the 1997–98 and 2015–16 warming events proceeded similarly, but upwelling during the winter for the 1997–98 event was much weaker than 2015–16.

The impact of recent climate anomalies on the subsurface structure of the CCS was highlighted by temporal variability in the depth of the 26.0 kg m^{-3} isopycnal ($d_{26.0}$). During the 2015–16 warming, $d_{26.0}$ was considerably shallower than during the 1982–83 and 1997–98 events, and also showcased a much different temporal evolution. The past strong El Niño events were characterized by $d_{26.0}$ increasing rapidly beginning in summer, reaching peak anomalies in winter (November to February), and then decreasing again into the spring. In contrast, 2015–16 saw $d_{26.0}$ anomalies that were already positive due to anomalous warming of the North Pacific that began in 2014. In the first half of 2016, $d_{26.0}$ gradually shoaled, as is often the case, approaching climatological values and suggesting the decline of both El Niño and the preexisting warm anomalies.

Mixed layer temperature anomalies off southern California in 2014–16 were significantly higher than those observed during the previous 15 years, and did not begin to cool until the first half of 2016. The area affected by the marine heat wave and the 2015–16 El Niño in the mixed layer was comparable to the 1997–98 El Niño, but the event lasted longer. Water column stratification in the upper 100 m during the 2015–16 marine heat wave was as strong as the most extreme values observed during the 1997–98 El Niño. However, this stratification was primarily driven by the warming of the upper 100 m. The upper ocean was unusually fresh during 2015 in most regions off southern California, suggesting a strengthening of the California Current. We note that this contrasted with higher than normal salinity off Baja California in 2015. Nitracline depths, compared to the previous 15 years, have been unusually deep over the last two years and stratification in the upper 100 m was unusually strong. Despite these notable perturbations, the effects of the 2015–16 El Niño on hydrographic properties in the CalCOFI domain were not as strong as those observed during the 1997–98 El Niño.

UNPRECEDENTED HARMFUL ALGAL BLOOM OF 2015–16

Off central California temperature anomalies exceeding 7°–8°C were observed at shore stations such as the Santa Cruz Municipal Wharf during the marine heat wave. Nutrient data from the Santa Cruz Municipal Wharf (SCMW) in Monterey Bay suggest that associated changes in the mixed layer led to dramatically suppressed nutrient concentrations. Silicic acid, nitrate (fig. 17A), and $Si(OH)_4$:NO_3 were low despite normal upwelling index values throughout the time period (fig. S2). This likely provided perfect conditions for the particularly toxic species, *Pseudo-nitzschia* australis, to bloom in 2015 since it appears to be a good competitor in post-upwelling scenarios where nutrients (particularly Si) are in limiting supply (Sommer 1994; Marchetti et al. 2004; Anderson et al. 2006; 2008). This historic bloom was truly unprecedented given its long duration from mid-April to September (fig. 17B) and its geographic extent along the entire US West Coast—occurring nearly simultaneously from Santa Barbara, CA, to Kodiak, AK—in direct association with the marine heat wave's expansion throughout the North Pacific from 2014 to 2015. This massive bloom led to record-breaking levels of domoic acid

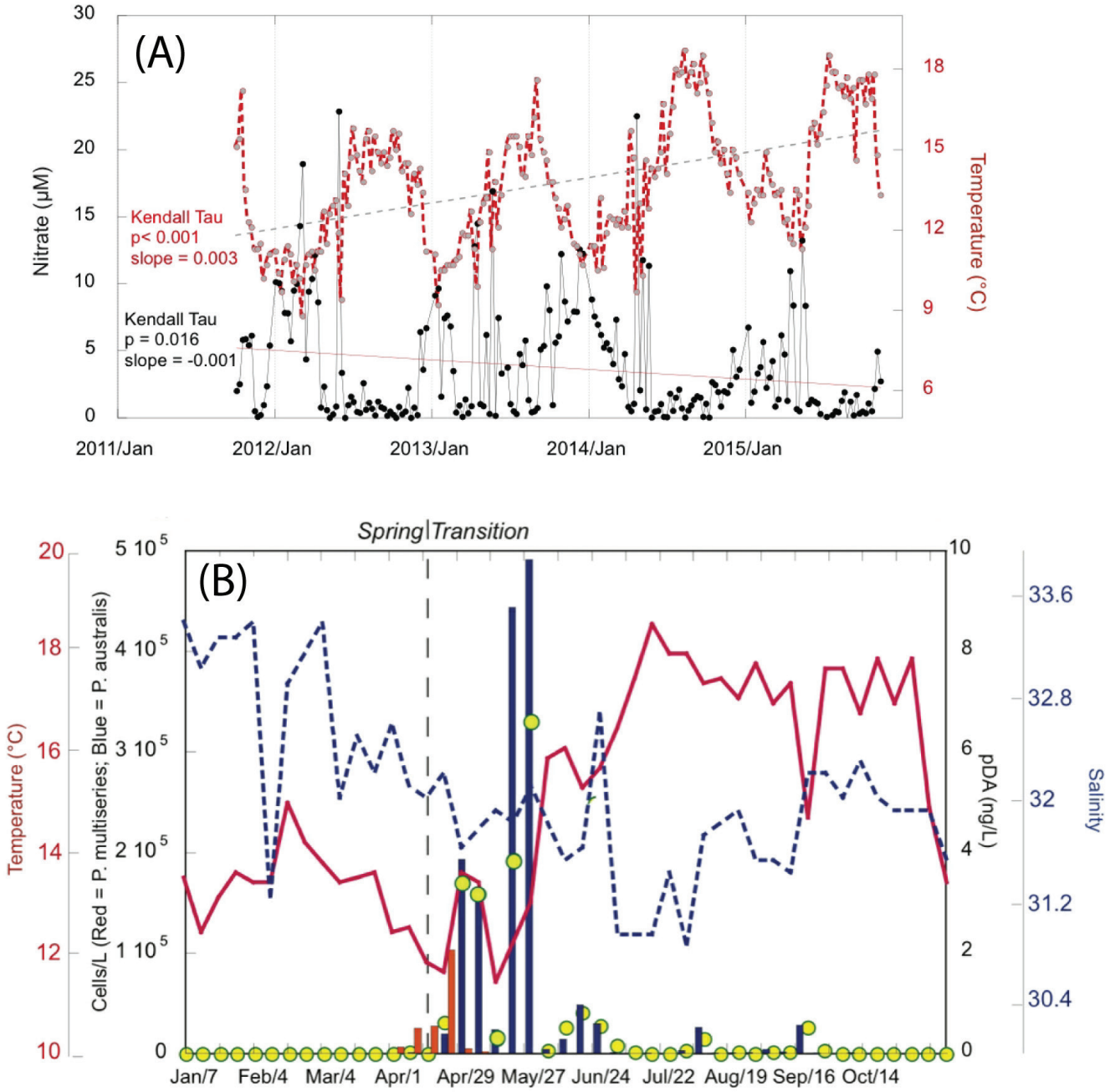

Figure 17. Physical, chemical, and biological properties in the CCS during 2015. (A) SST and nitrate (2011–16) at the Santa Cruz Municipal Wharf (SCMW) in northern Monterey Bay; (B) SCMW records of SST, salinity, *Pseudo-nitzschia* cell counts, and particulate DA in spring to summer 2015 (Kudela, unpublished data).

(DA) in the water column (fig. 18, observations) and extensive food web effects, such as record closures of several economically important fisheries, including the highly lucrative Dungeness crab fishery. Toxin levels hit new highs in dissolved and particulate DA, anchovy, Dungeness and rock crab, and pelicans. DA toxin was found in the fillets of several species of commercially harvested fish (McCabe et al., submitted), and toxin was routinely detected in Monterey Bay Aquarium tanks as well as in the captive sea lion tanks at Moss Landing Marine Laboratory, where one sea lion exhibited symptoms of DA exposure (Kudela et al., unpublished data).

The California Harmful Algae Risk Mapping (C-HARM) System publishes daily nowcasts and 3-day forecasts of *Pseudo-nitzschia* bloom and domoic acid event likelihoods for coastal California on the Central and Northern California Ocean Observing System (CeNCOOS) data portal. C-HARM captured the bloom dynamics at the Santa Cruz Municipal Wharf (SCMW) with 61% and 73% accuracy for

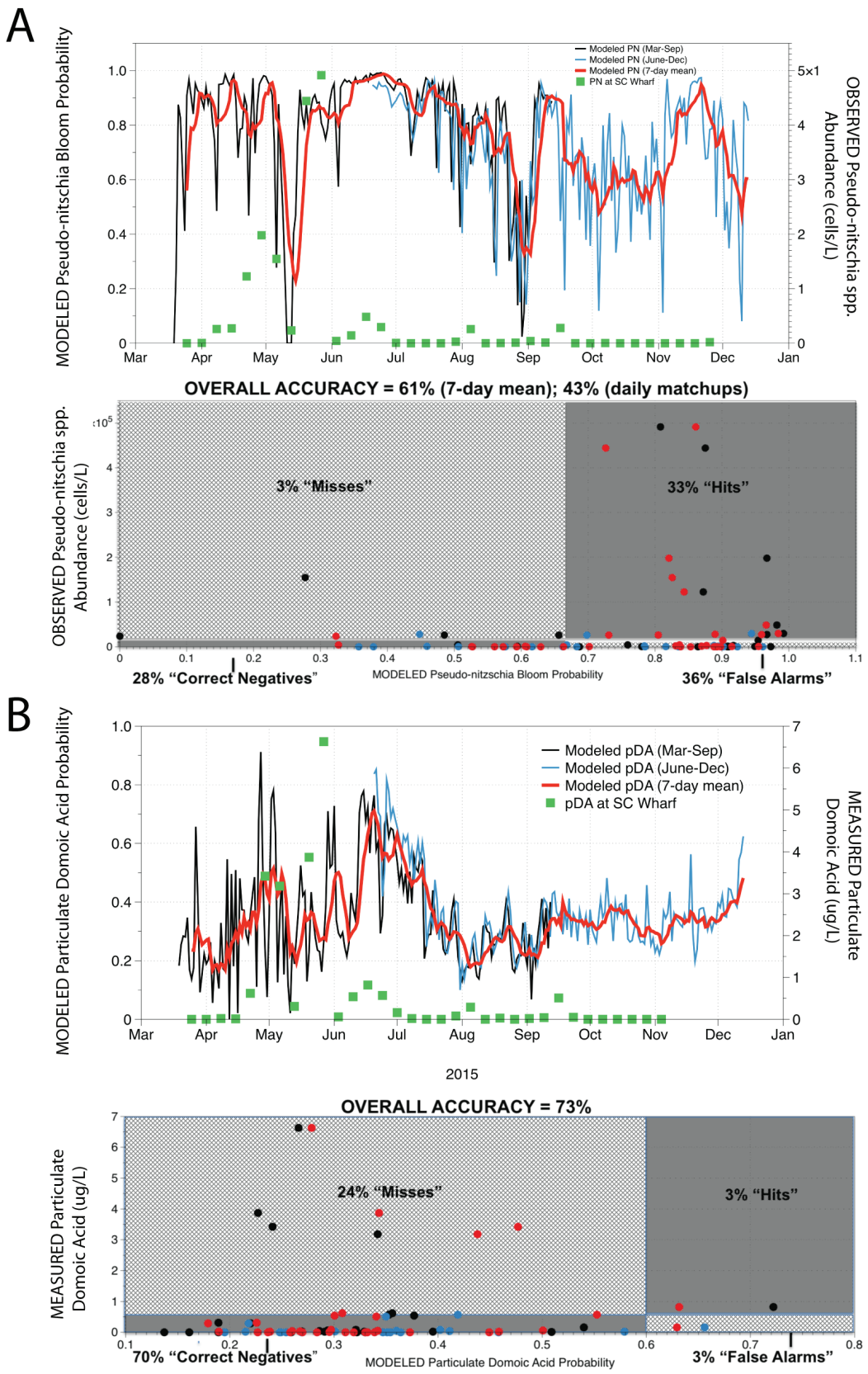

Figure 18. Contingency plots showing the performance of the California HAB model at the Santa Cruz Wharf in 2015. Top = accuracy of *Pseudo-nitzschia* bloom predictions; Bottom = accuracy of the particulate domoic acid (pDA) predictions.

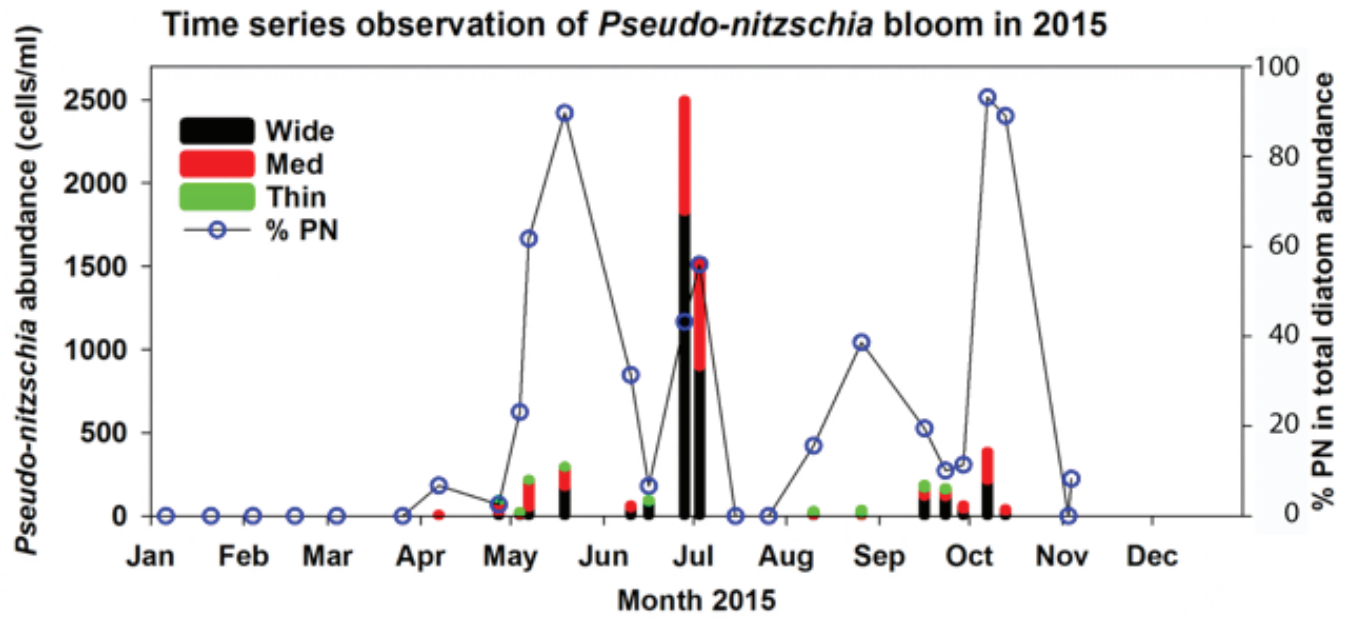

Figure 19. The bloom initiation and development observed at the nearshore station NH5. Bars stacked by the three sized *Pseudo-nitzschia* groups indicate cell abundances (left *y*-axis). Circles connected by dotted lines represent proportions of *Pseudo-nitzschia* (blue circles, right *y*-axis) in the total diatom abundance.

Pseudo-nitzschia and domoic acid, respectively (fig. 18). Interestingly, the abundance of *Pseudo-nitzschia* was not unusually high into the summer at the SCMW (fig. 17B) and total domoic acid levels exceeded 2015 results in both 2014 and 2016. As a result, the 3 km model overpredicted the severity of the bloom at the SCMW, but accurately predicted the high toxin levels exhibited immediately offshore.

In contrast to the central California results, the model successfully identified a new toxic "hot spot" off northern California. Observations from the Southwest Fisheries Science Center's Trinidad Head Line identified maximum total DA concentrations in excess of 15,000 ng/L. Visual inspection of zooplankton samples indicated high concentrations of *Pseudo-nitzschia* from spring through early fall of 2015, coincident with elevated DA concentrations during this period. Record concentrations of DA were observed in razor clams from Humboldt County (340 ppm DA in late 2015), and the waters off Humboldt County were the last to see the crab fishery opened for harvest; both of these observations further attest to the intensity and duration of the HAB off northern California.

The Toxic and Persistent *Pseudo-Nitzchia* Bloom off the Oregon Coast in 2015

The *Pseudo-nitzschia* bloom that developed off Oregon in 2015 led to the closures of razor clam harvest for nearly a year and delayed the opening of the Dungeness crab fishery for only 6 weeks. Oceanographic conditions preceding, during, and following this bloom were tracked from biweekly to monthly field observations of temperature, salinity, nutrients, and *Pseudo-nitzschia* abundance off Newport, Oregon (44.6°N) (Du et al., submitted).

Pseudo-nitzschia cells were first detected in late March nearshore and increased slightly prior to the spring transition in mid-April (fig. 19). After the spring transition, *Pseudo-nitzschia* abundance increased to 105 cells/L in late April but contributed only a low percentage (2.5%) of the total diatom abundance. Following the episodic strong upwelling events in early May, *Pseudo-nitzschia* abundance continued to increase. By late May, the first *Pseudo-nitzschia* bloom peaked at Newport along with a dramatic increase of *Pseudo-nitzschia* percentage from 23% to 90% of total diatoms, indicating the formation of a monospecific bloom. Following this bloom peak, domoic acid concentration in razor clams (Oregon Department of Agriculture) reached its highest level in early June at Newport. The bloom began to decay in mid-June, as inferred from the declines of both the abundance and proportion of *Pseudo-nitzschia*. A second bloom peak was observed in late June and cell abundance remained high in early July with a higher magnitude (106 cells/L) than the first peak. The percentages of *Pseudo-nitzschia* cells were about half of total diatom abundance. However, there was no report of increasing DA in clams even though *Pseudo-nitzschia* abundances were the highest during this time. *Pseudo-nitzschia* cells were absent in mid-late July but recurred following a resurgence of stronger upwelling in early August. A bloom did not form until the end of August albeit with a low magnitude. The bloom continued in

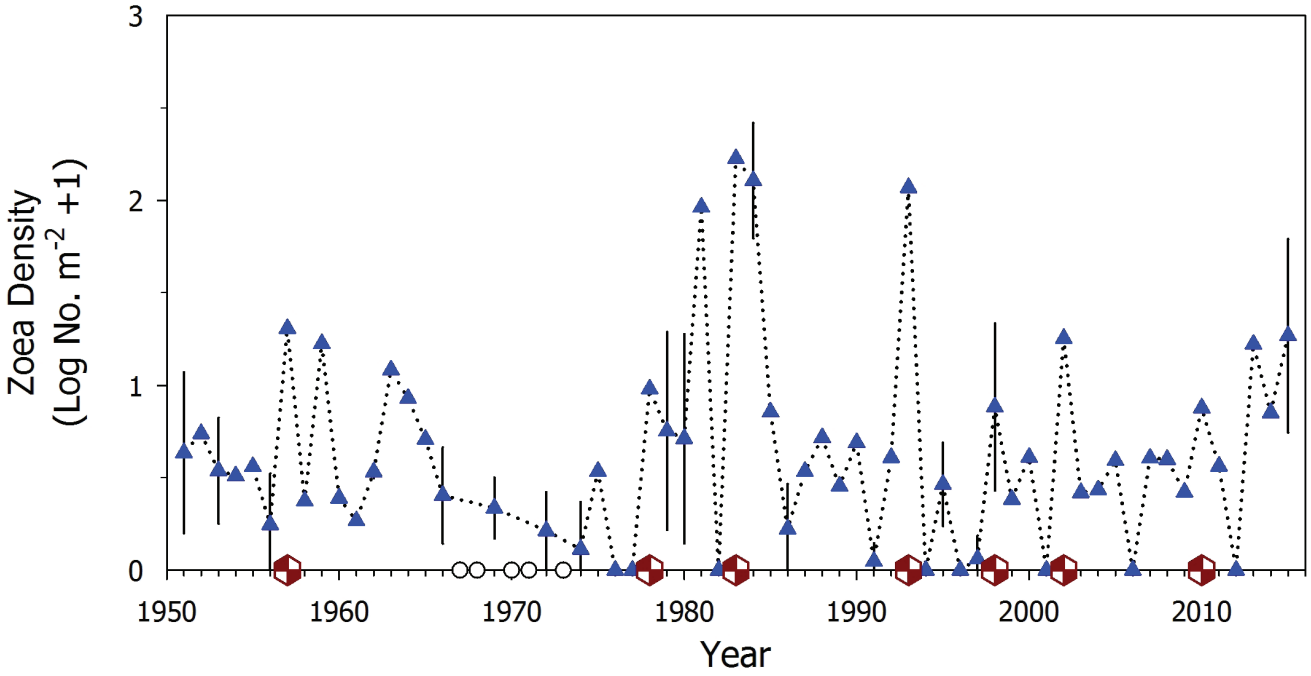

Figure 20. Time series of *Pleuroncodes planipes* total zoeae in nighttime CalCOFI net samples from springtime cruises off southern California, for the region indicated in Figure 21. Density (Log No. m^{-2} +1) of *Pleuroncodes planipes zoeae.* Error bars indicate 95% C.L. when individual samples were enumerated; otherwise pooled samples were enumerated (cf. Lavaniegos and Ohman 2007). Open circles on abscissa indicate years when no CalCOFI spring sampling was conducted. Red semaphores indicate years in which the effects of El Niño were evident in Californian waters. From the SIO Pelagic Invertebrate Collection.

September through early October and then decayed completely shortly after the end of the upwelling season. From July until the end of 2015, DA in clams maintained at a constant level near Newport.

Triggers of the Toxic Bloom

Macronutrient conditions likely played a critical role in triggering the toxic bloom off Oregon. Silicic acid limitation stress is one of the recognized toxin-induction factors. Silicic acid concentrations were <0.3 μM, nitrate concentrations <0.4 μM and Si:N ratios ranged from 0.04 to 0.8 in March and early April. Nutrient stress preceding the toxic bloom was related to two oceanographic events: from September 2014 through 2015 by the marine heat wave, leading to a highly stratified water column and deepening of nutricline, and the drawdown of available nitrate and silicic acid during an intense winter phytoplankton bloom in February and early March 2015. Replenishment of nutrients to the upper water column from upwelling events after the spring transition promoted and sustained the *Pseudo-nitzschia* bloom. For example, at no time in May and June did concentrations of NO_3 fall below 3 μM or SiO_4 below 5 μM. The ratios of Si:N ranged between 1.6–2.3.

The strength of upwelling and associated onshore-offshore Ekman transport regulated the availability of toxic *Pseudo-nitzschia* cells to razor clam beds to some extent and likely contributed to the differences of toxin accumulation in razor clams. Upwelling was intermittent during mid- and late May and toxic *Pseudo-nitzschia* cells were retained very nearshore. The continuous exposure to the toxic cells likely led to the sharp increase of DA level in clams. In contrast, upwelling in June was strongest in 2015. The resultant stronger offshore transport kept most of the toxic *Pseudo-nitzschia* cells away from the nearshore zone and thus reduced the toxic effects.

SUMMARY: UNPRECEDENTED HARMFUL ALGAL BLOOM

Warm ocean conditions and associated stratification combined with nutrient suppression and silicic acid stress likely favored initiation of the *Pseudo-nitzschia* toxic bloom in fall 2014. The winter/spring phytoplankton bloom of February and early March 2015, and higher nutrient concentrations following the spring transition to upwelling, favored explosive growth of the bloom. Local-scale forcing from coastal upwelling driving richer nutrient conditions and cross-shelf transport provided the ultimate explanation for the development of the *Pseudo-nitzschia* bloom and toxic effects.

CHANGES IN THE DISTRIBUTION AND ABUNDANCE OF ZOOPLANKTON

Red Crabs off Southern California

Pleuroncodes planipes (red or tuna crab) is a micronektonic crustacean well adapted to a pelagic life during the larval phase and in the first adult year. During nor-

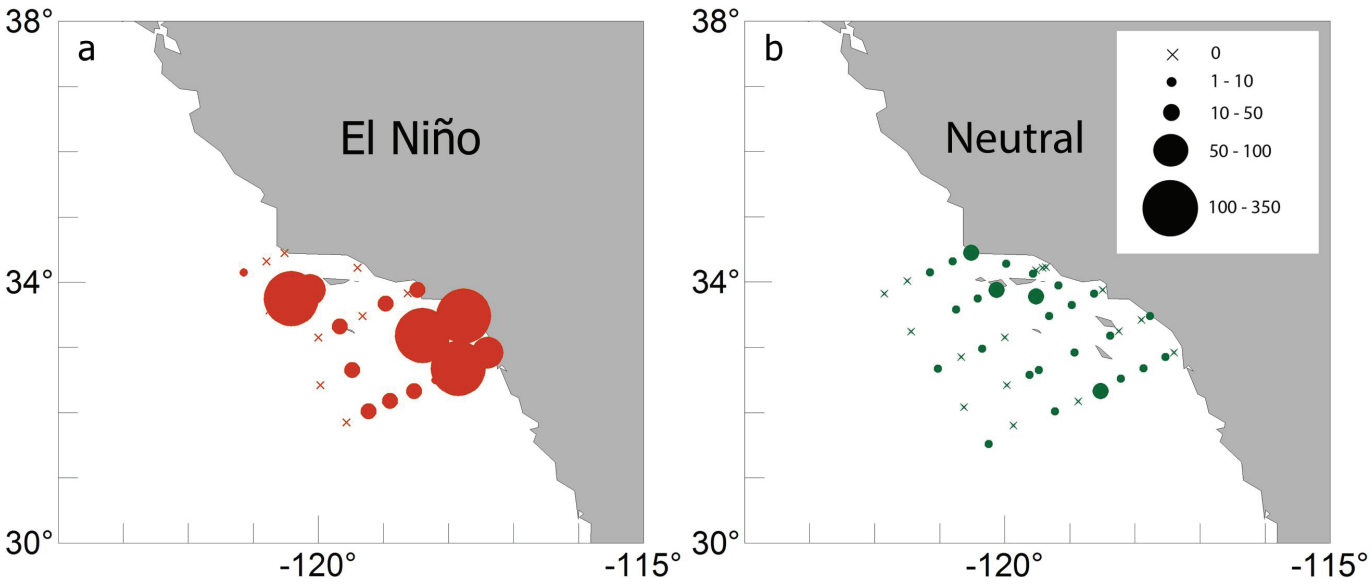

Figure 21. Density of *Pleuroncodes planipes* total zoeae (No. m^{-2}) in nighttime CalCOFI net samples from springtime cruises off southern California, during (a) El Niño-influenced years, and (b) El Niño-neutral years. Only years in which individual stations were analyzed ("unpooled samples," cf. Lavaniegos and Ohman 2007; Niño: cruises 1979, 1984, 1998; Neutral: 1951, 1953, 1956, 1966, 1972, 1974, 1979, 1980, 1986, 1991, 1995, 1997) are included. "X" indicates no specimens found. From the SIO Pelagic Invertebrate Collection.

mal years it forms dense aggregations off southern Baja California and in the offshore region of the Mexican tropical Pacific, but during El Niño years it is often found off southern and central California (Boyd 1967; Gómez-Gutiérrez and Robinson 2006; Longhurst 1967). It's eaten by large predators including yellowfin tuna, skipjack tuna, and many other fishes, birds, turtles, pinnipeds, and whales.

The first observation of an adult *Pleuroncodes planipes* in plankton samples off southern California in 2014 appears to have been on 29 July 2014 off San Diego's Nine Mile Bank (M.D. Ohman, pers. obs.). The first reports in 2015 were from fishers who found pelagic red crabs in the stomach contents of California yellowtail (*Seriola lalandi*) on 1 Jan. 2015 ~8 km west of Mission Bay, San Diego (L. Sala, pers. obs.). Beach strandings of adult *Pleuroncodes planipes* were subsequently widely reported in southern and central California during 2015, beginning on San Clemente Island in January and progressing intermittently northward to San Miguel Island by June, eventually reaching Pacific Grove by October. The northernmost location appears to have been an adult collected in a Tucker trawl off Cordell Bank in September 2015 (J. Jahncke, pers. comm.). Adults were common in the water column at Nine Mile Bank in June 2015 (to densities of 5–15 individuals m^{-2} visible at the sea surface, usually at night, M.D. Ohman, pers. obs.). Many accounts of occurrence at sea and beach strandings of adults were subsequently reported during the El Niño of 2015–16.

Turning to larval stages sampled in the plankton by CalCOFI, a multidecadal springtime time series shows that zoea stages of *P. planipes* have been present in the southern California region in spring in nearly all years in the last 6½ decades (fig. 20). Of a total of 60 spring surveys enumerated, in only 8 years (1976, 1977, 1982, 1994, 1996, 2001, 2006, 2012) were no zoeae detected. However, densities are typically very low, averaging 3.3 zoeae m^{-2} (untransformed range: 0–163 m^{-2}; note log scale in fig. 20) across the time series. Average density increases during and/or immediately after El Niño years (e.g., 1957–58, 1977–78, 1983–84, 1992–93, 1998, 2009–10; red semaphores in fig. 20) but also during warm water years that are not linked to El Niño. The major El Niño of 1957–59 showed moderately high densities of *P. planipes* zoeae, despite the widespread occurrence of adults in CalCOFI samples (Longhurst 1967).

The historical (i.e., prior to 2015) spatial distribution of zoea stages of *P. planipes* in springtime reveals that during El Niño years, zoea larvae are typically most abundant nearshore in the Southern California Bight and in the vicinity of the Channel Islands (fig. 21a). Densities decrease in offshore waters. This spatial distribution is consistent with an influx of larvae in coastal waters originating to the south, possibly followed by offshore transport in the Southern California Eddy. In contrast, during El Niño-neutral springs, densities of zoea larvae are nearly an order of magnitude lower in abundance ($p < 0.01$, Mann-Whitney U) and show less tendency to be elevated near the coast (fig. 21b).

In spring 2015 *P. planipes* total zoeae showed a generally coastal distribution, with some zoeae extending to station 86.7 60 (fig. 22f), although few nighttime samples were available from cruise 1504NH to resolve distributions close to shore or in proximity to the Channel

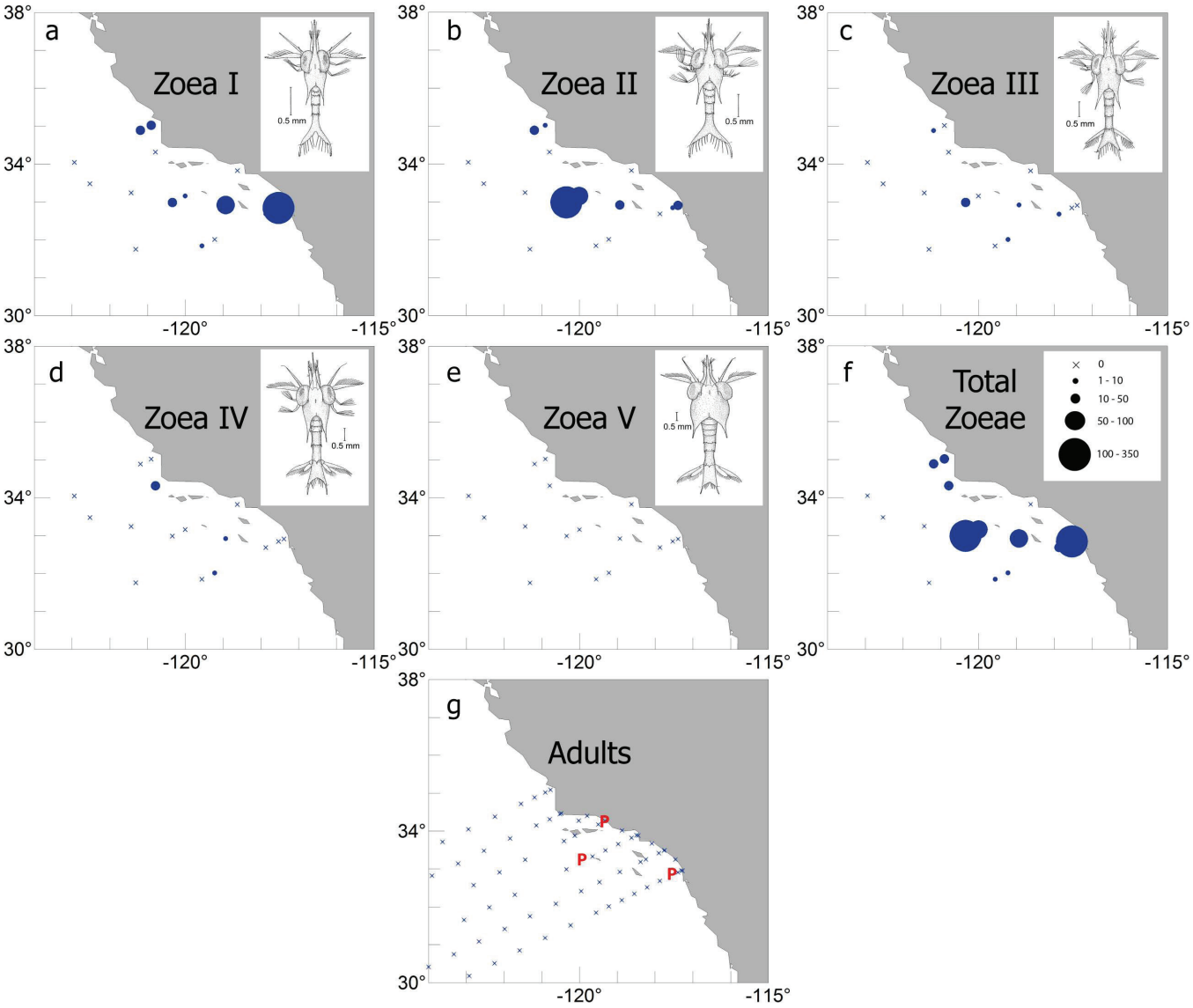

Figure 22. Occurrence of *Pleuroncodes planipes* in CalCOFI bongo net samples on cruise 1504NH (April 2015). Panels (a)–(f) indicate density (No. m^{-2}) of zoea stages I–V and the sum of all zoea stages, respectively, enumerated only from nighttime samples. Panel (g) indicates the presence ("P") of adults enumerated from both day and night samples, although all three positive records occurred at night. "X" indicates no specimens found. Illustrations of zoeae reproduced from Boyd (1960). From the SIO Pelagic Invertebrate Collection.

Islands. Analysis of the spatial distribution of the five zoea stages of *P. planipes* treated separately shows that stages I and II were the most abundant, with markedly lower abundances of zoea stages III and IV, and no stage Vs detected (fig. 22a–e). Adults were found in net samples at only three locations, all toward the southeastern part of the sampling pattern (fig. 22g).

It is highly unlikely that the proliferation of larval and adult *P. planipes* in southern California in spring 2015, when beach strandings of adults were common, can be attributed to in situ population growth alone without preceding advection from more southern waters. The adults found at sea and on beaches were in size classes typical of 2-year old *P. planipes* (Boyd 1962, 1967), suggesting that a very protracted period of favorable conditions in situ would have been necessary to lead to such abundances. However, in April 2015 larval stages were dominated by zoea I and II, with few zoea IV and no zoea stage V detected, suggesting inhospitable conditions for larval survival and population growth. It is more likely that adults had been advected into the region from the southeast in northward coastal flows, followed by advection offshore and relatively high mortality of later zoea stages. While Zaba and Rudnick (2016) concluded that there was no evidence of anomalous northward advection in this region in 2014–15, they averaged glider-derived velocity data over the nearshore 200 km. In contrast, coastally located moorings in southern

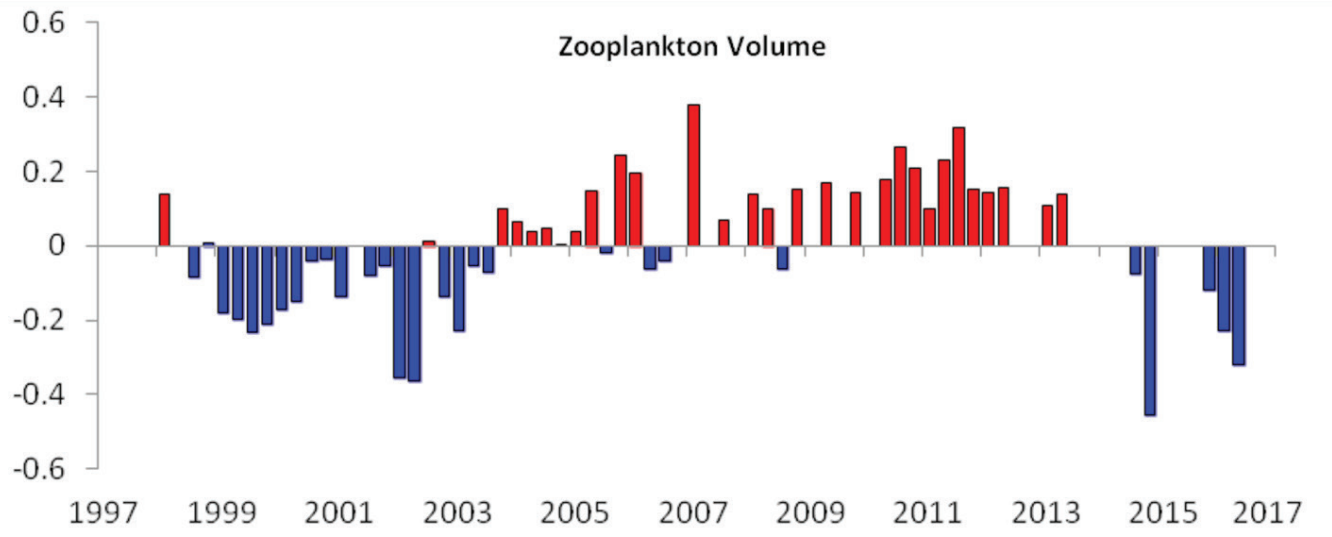

Figure 23. Zooplankton biomass anomalies (Log µl m^{-3}) off Baja California from January 1998 to January 2016.

California indicate anomalously large northward flows at two locations close to the continental shelf (U. Send, pers. comm.). Furthermore, mean advection close to the coast is typically northward, especially in fall–winter (the Inshore Countercurrent, Lynn and Simpson 1987). Satellite altimetry averaged across 200 km from the coast suggests anomalous northward flows off Baja California from April–Nov 2014, resuming weakly northward in Feb–March 2015 (P.T. Strub, pers. comm.), indicating a southern source for *P. planipes* during this event.

Expansion of Tropical Species off Baja California

The high positive temperature anomalies recorded off Baja California in 2015–16 were associated with extremely low zooplankton displacement volumes (fig. 23). Note that low zooplankton volumes were observed in 2014 before the onset of the 2015–16 El Niño, ending a period (2004–13) of positive zooplankton volume anomalies. Despite high SST during the El Niños of both 1997–98 and 2015–16, the response of zooplankton volume was quite different, reflecting the unique character of each El Niño. Low zooplankton volume in fall 2015 and January 2016 (fig. 23) was caused by low abundance of gelatinous plankton, copepods, and euphausiids. It is possible that lower grazing pressure contributed to higher chlorophyll in 2016 (fig. 16). In contrast, during the 1997–98 El Niño, zooplankton volume was close to the average, with abundant copepods, euphausiids, and salps at some stations.

During autumn 2015, tropical species such as *Pleuroncodes planipes* (red crabs) expanded into the northern IMECOCAL region and extended their distribution offshore south of Punta Eugenia (fig. 24). During a typical autumn such as October 2003, adult red crabs were observed only over the southern shelf (fig. 24). The expanded distribution during fall 2015 resembled that seen during the 1958–59 El Niño (Longhurst 1967), when the entire Baja California region and parts of southern California were occupied by adult red crabs. In contrast, during 1955–57, before the 1958–59 El Niño, red crabs remained south of Punta Eugenia (28°N). Interestingly, red crabs were absent on the shelf during autumn 2015 (fig. 24) although in the prior seasons (spring–summer of 2015), and subsequently in spring 2016, red crabs washed up on the beaches of Baja California and California (Durán 2016).

Vinciguerria lucetia is the most abundant mesopelagic fish species all year round off Baja California (Jiménez-Rosenberg et al. 2007, 2010). *V. lucetia* and *Triphoturus mexicanus* increased in abundance during the 2015–16 El Niño. The mean abundance of *V. lucetia* during October 2003 was 172 larvae/10 m^2; in contrast during September 2015 mean abundance increased by a factor of five (938 larvae/10 m^2). The highest abundances during October 2003 were concentrated in oceanic waters (fig. 24), while the high abundances of *V. lucetia* larvae during September 2015 included the shelf stations (fig. 24). Similar to the 2015–16 El Niño, a notable increase in the abundances of *V. lucetia* larvae was also observed during the 1997–98 El Niño (Jiménez-Rosenberg et al. 2007, 2010). There was also a notable shift northwards in the distribution of *V. lucetia* larvae in 2015 relative to 2003 (fig. 24).

Persistence of a Low-Lipid, Diverse, Warm Water Copepod Assemblage off Oregon

The warm water that intruded onto the Oregon shelf in Sept 2014, the coastal expression of the marine heat wave, remained throughout 2014–15 and continued

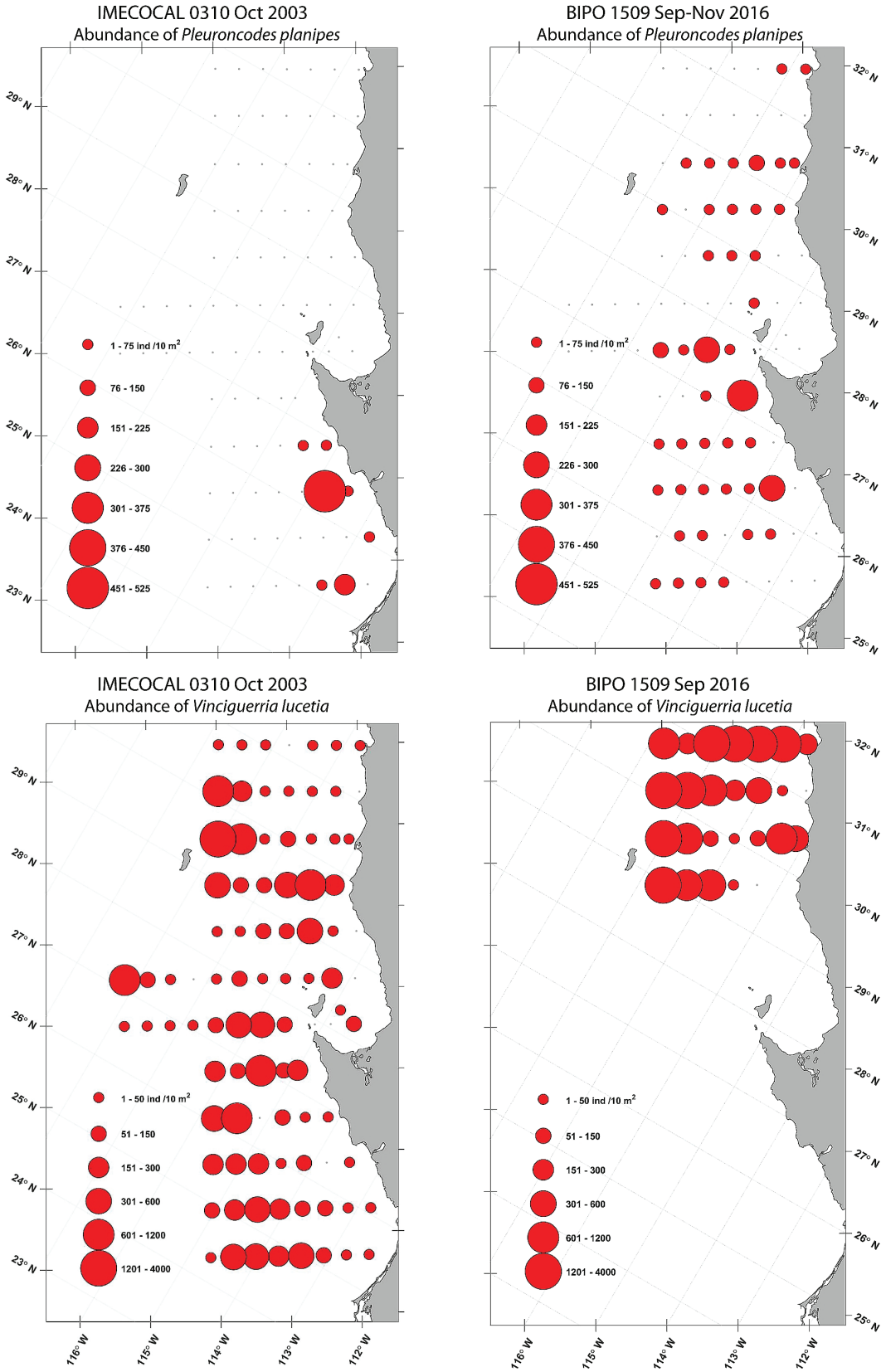

Figure 24. Distribution of adult galatheid crab (*Pleuroncodes planipes*) and larval Panama lightfish (*Vinciguerria lucetia*) during October 2003 (IMECOCAL cruise 0310) and September–November 2015 (BIPO cruise 1509).

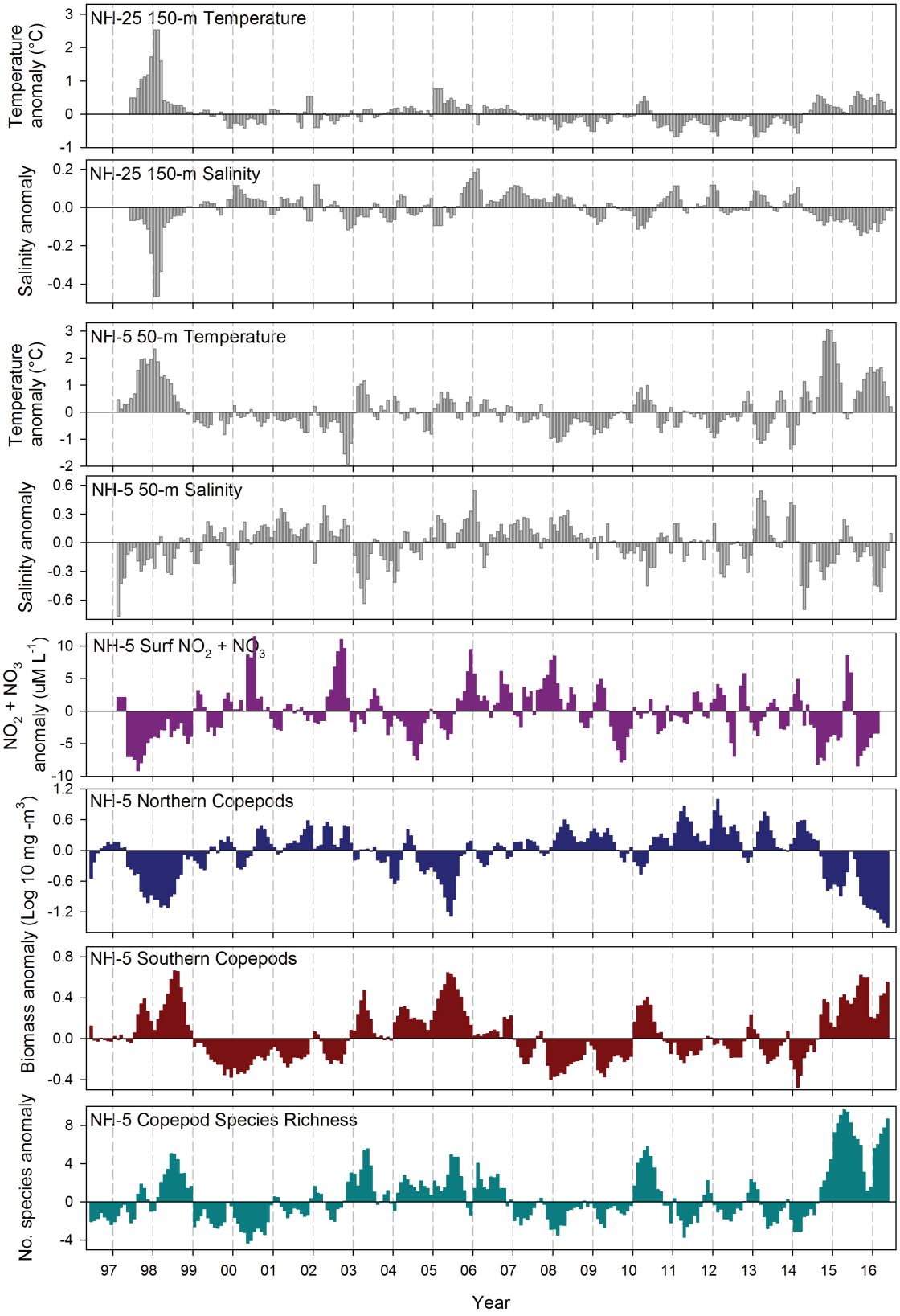

Figure 25. Time series plots of local physical and biological anomalies (monthly climatology removed) from 1997–present at NH-25 (Latitude: 44.6517 N Longitude: 124.65 W; top two panels) NH-5 (Latitude: 44.6517 N Longitude: 124.1770 W; lower six panels) along the Newport Hydrographic Line. Temperature and salinity from 150 m and 50 at NH-25 and NH-5 respectively, NO_2 + NO_3 from the surface, and copepod biomass and species richness anomalies are integrated over the upper 60 m. All data were smoothed with a 3-month running mean to remove high frequency variability.

into 2016, affecting local hydrography and pelagic communities. Despite the unusual ocean conditions during 2015 on the Newport Hydrographic Line (see fig. 2), the duration of the upwelling season (13 April–5 October) was similar to its long-term average. Cumulative upwelling over the season was the highest in the past 20 years (fig. S4, latitude 45°N). Despite strong inferred cumulative upwelling, temperatures at 50 m at the shelf station (NH-5) and 150 m at the slope station (NH25) remained warmer than average (fig. 25), surface nitrate was anomalously low (fig. 25) and chlorophyll (not shown) was lower than average throughout most of 2015. In May and June 2015, during the strongest upwelling period, shelf waters at both 50 and 150 m cooled, salinity increased, and nitrate increased greatly (fig. 25). However, positive temperature anomalies and lower than average nitrate and chlorophyll returned quickly in July and persisted into 2016. Dissolved oxygen at depth on the Oregon shelf remained average or higher than average throughout both 2015 and 2016 (not shown).

During this time period, the zooplankton community was dominated by lipid-poor tropical and subtropical copepods and gelatinous zooplankton. This generally indicates poor feeding conditions for small fishes which are prey for juvenile salmon. With the exception of June and July 2015, following strong upwelling, the biomass of lipid-rich northern or "cold water" copepods was the lowest observed in the 20-year time series (fig. 25). The biomass of southern ("warm water") copepods fluctuated greatly but was generally higher than average throughout 2015 and 2016 (fig. 25). We also observed 17 copepod species with Transition Zone and North Pacific Gyre affinities that have rarely been observed off Newport since sampling began in 1969. The presence of these species greatly increased copepod species richness which exceeded the number of species observed during the strong El Niño in 1998 (fig. 25). In 2015 and in 2016, the usual seasonal shift from a winter copepod community to a summer community, which is associated with strengthening of the Davidson Current in winter and its disappearance in spring, did not happen (data not shown). This seasonal transition in the copepod community also did not occur during the 1997–98 El Niño or during the anomalously warm year of 2005. Euphausiid biomass during 2016 was also among the lowest in 20 years (data not shown).

Despite a strong El Niño signal at the equator during much of 2015 and into 2016, we did not encounter the copepod or euphausiid species that have occurred off Oregon during other El Niño events. Copepods are good indicators of large-scale transport. We know that the unusual copepod species observed off Oregon in 2015–16 have Transition Zone and North Pacific Gyre affinities. Thus it is unlikely that these copepods have southerly coastal origins, as is usual during El Niño events. It is also unlikely that they were transported north by the California Undercurrent because the T-S properties at 150 m during this time period were unusually warm and fresh, rather than warm and more saline (fig. 25). The biogeographic affinities of the copepods in anomalously warm, fresh water suggest offshore intrusion Central Pacific water and mixing with subarctic Pacific water of the California Current. This suggests that the unusual copepod vagrants of 2015–16 originated from an offshore and southwesterly source.

Shelf waters off Oregon in mid-2016 remain warm, northern copepod biomass is the lowest, and copepod species richness remains the highest in the 20-year time series (fig. 25). We know from past warm events such as the 1997–98 El Niño, that the return to a lipid-rich copepod community following warm ocean conditions is strongly dependent on the magnitude and the duration of the event (Fisher et al. 2015). The Oregon shelf has been in an anomalously warm state since September 2014 (22 months as of this writing), far exceeding the duration of the 1997–98 El Niño that lasted 13 months. The copepod community recovered after 17 months following the 1997–98 El Niño (Peterson et al. 2002). Given that the PDO is still in a positive (warm) phase, and that a change in the copepod community lags the PDO by 2–6 months, we expect that we will not see a transition to a northern copepod community for at least a year to come.

Copepods and Krill Respond to Warm Conditions off Trinidad Head, Northern California

Coastal waters off northern California (Trinidad Head Line, station TH02, fig. 2) cooled during the first half of 2015 (fig. 26a) in response to mild winter upwelling events, reinforced by average upwelling during the spring and above-average upwelling during the summer of 2015 (Supplement fig. S4, latitude 41°N). Near-bottom temperatures returned to slightly warmer than average conditions during the summer and into the fall as upwelling weakened (fig. 26a and b).

Elevated phytoplankton concentrations developed over the inner to middle shelf in spring and persisted throughout the summer of 2015 (fig. 26c). The toxic species *Pseudo-nitzschia* was common, producing elevated concentrations of domoic acid (DA) (fig. 26d; see previous discussion of HAB). Shelf waters warmed during winter 2016, driven by persistent southerly winds, and remained relatively warm into spring 2016. Early observations of the phytoplankton bloom in spring 2016 indicated that *Pseudo-nitzschia* was again abundant.

Throughout much of 2015 and early 2016, the copepod community was dominated by warm-water species while the biomass of northern species was lower than usual (fig. 26e, f). Copepod community structure in this area reflects changes in water temperature. Copepod spe-

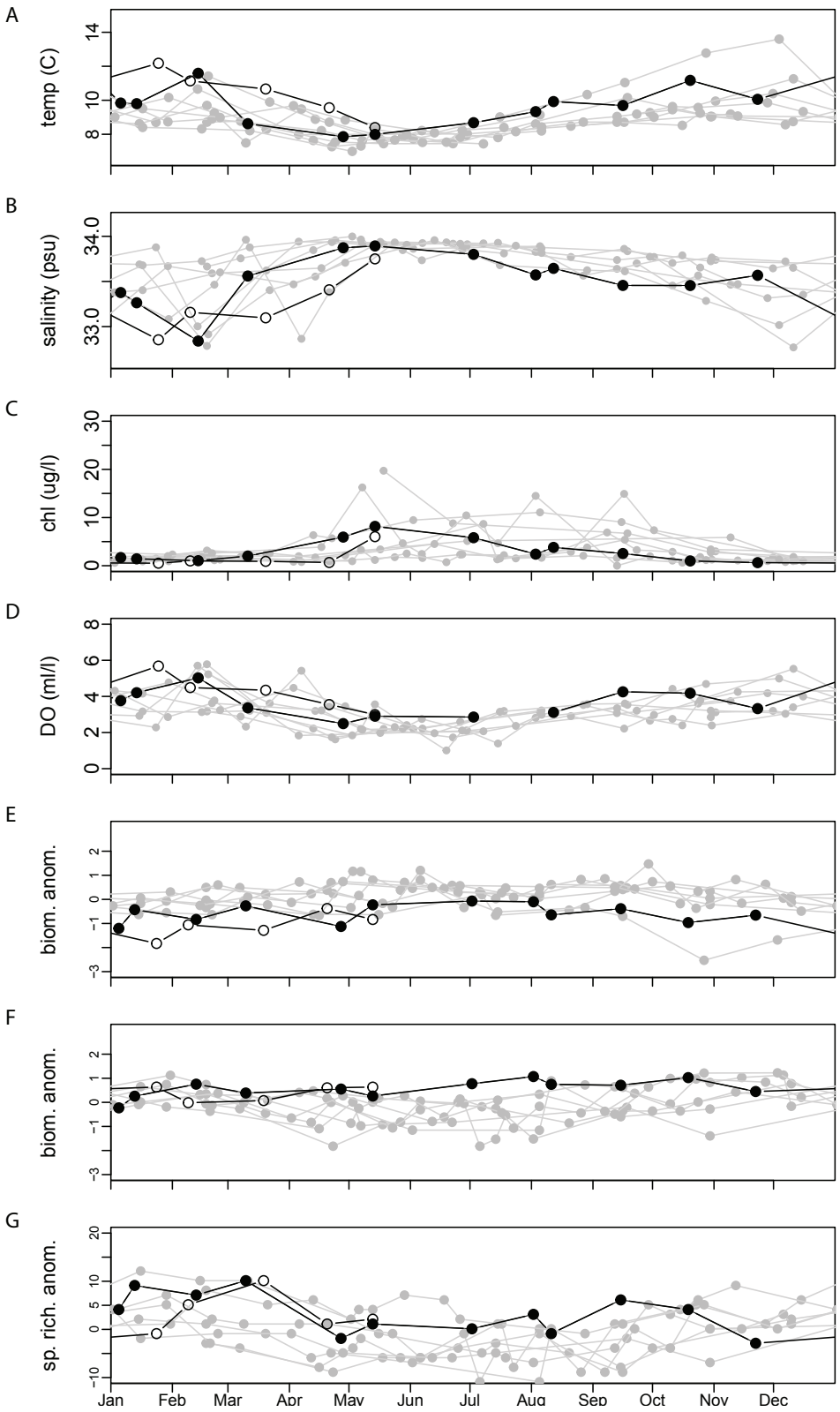

Figure 26. Hydrographic and ecosystem indicators at midshelf along the Trinidad Head Line (station TH02; 41 03.5'N, 124 16'W, 75 m depth). Panels from top to bottom show (A) near-bottom (68 m) temperature, (B) near-bottom (68 m) salinity, (C) mean chlorophyll *a* concentration over the upper 30 meters of the water column, (D) near-bottom (68 m) dissolved oxygen concentrations, (E) biomass anomalies for northern copepod species (ln g C m^{-3}), (F) biomass anomalies for southern copepod species (ln g C m^{-3}), and (G) species richness anomalies (N). All assemblages are defined following Hooff and Peterson (2006), and all anomalies are calculated using means from the full time series (2006–16). For all plots, gray symbols indicate historical observations (2006–14), filled circles indicate observations during 2015, and unfilled symbols indicate observations in 2016.

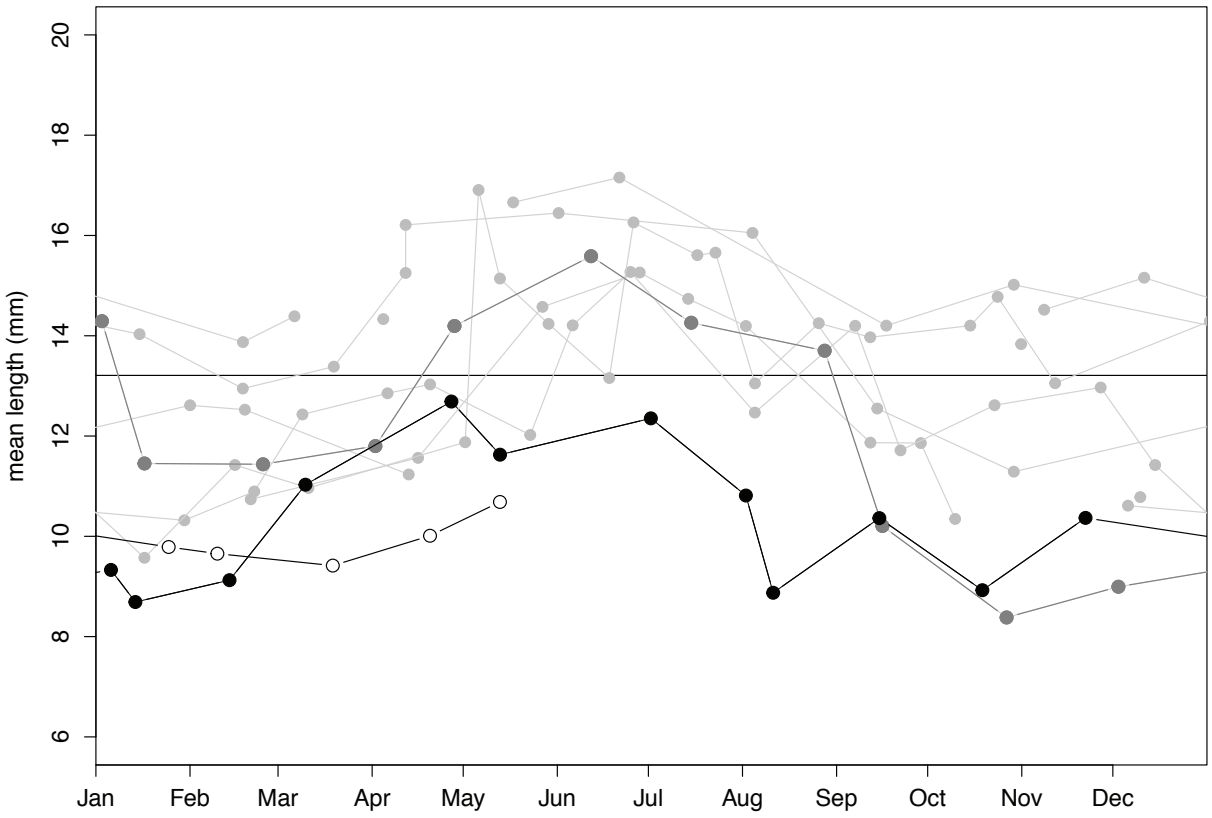

Figure 27. Mean rostral-dorsal length of adult *Euphausia pacifica* (males and females combined) captured along the Trinidad Head Line. Light gray symbols indicate observations from late 2006 through 2013. Dark gray symbols indicate observations for 2014, black symbols, for 2015, and open symbols for early 2016.

cies richness was high throughout much of 2015 when the marine heat wave was evident over the shelf. Richness peaked again in early 2016 (fig. 26g) associated with increased poleward transport. These diverse, warm-water copepod assemblages included several southern and offshore species not reported from this area prior to 2014.

Among the euphausiids, the abundance of *Thysanoessa spinifera* declined while both the subtropical *Euphausia recurva* and the warm water-associated *Nyctiphanes simplex* increased throughout 2015 and early 2016. *N. simplex* was the most abundant adult euphausiid observed in January 2016 in a region normally dominated by *E. pacifica* and *T. spinifera* (data not shown). In addition to their low abundance, adult *E. pacifica* were small relative to sizes observed prior to summer 2014 (fig. 27). Mean size of *E. pacifica* remained small through early 2016, and growth during spring and summer months was slower than normal.

Changes in Gelatinous Zooplankton off Oregon

The numerically dominant large jellyfish[11] off Oregon and Washington is cool-water associated scyphozoan species *Chrysaora fuscescens*. In June 2015, *Chrysaora* abundance was the second lowest of the time-series (fig. 28). These jellyfish were only found at 25% (11/44) of the stations sampled the following year, in June 2016, mostly nearshore, north of the Columbia River (fig. 2b). Although the time series is relatively short (18 years), and does not extend across the 1997–98 El Niño years, the data do show a notable decline in *Chrysaora* in other warm years (2003, 2005, and 2010) similar to that observed in 2015 and 2016 (fig. 28).

The more offshore taxa of hydromedusae, *Aequorea* spp. (Suchman et al. 2012), shows a less convincing relationship between abundance and warm years compared to *Chrysaora* (fig. 28). One plausible explanation for this may be that abundance of offshore species is more related to intrusion of offshore waters rather than to temperature. As described elsewhere in this paper, advective forcing differs between anomalously warm years, and this would affect the distribution of offshore species. The offshore hydroid, *Velella velella*, which lives in the pleuston, occurred in much lower abundances in June 2016 than in 2015, suggesting less onshore intrusion of offshore water in June 2016 than in the previous "warm blob" year.

Southern species such as the large scyphozoans *Phacellophora camchatica* and *Aurelia aurita* and the colonial

[11]Large gelatinous zooplankton taxa have been quantified from pelagic surface trawls off Oregon and Washington every June since 1999 (see Suchman et al. 2012 for collection methods).

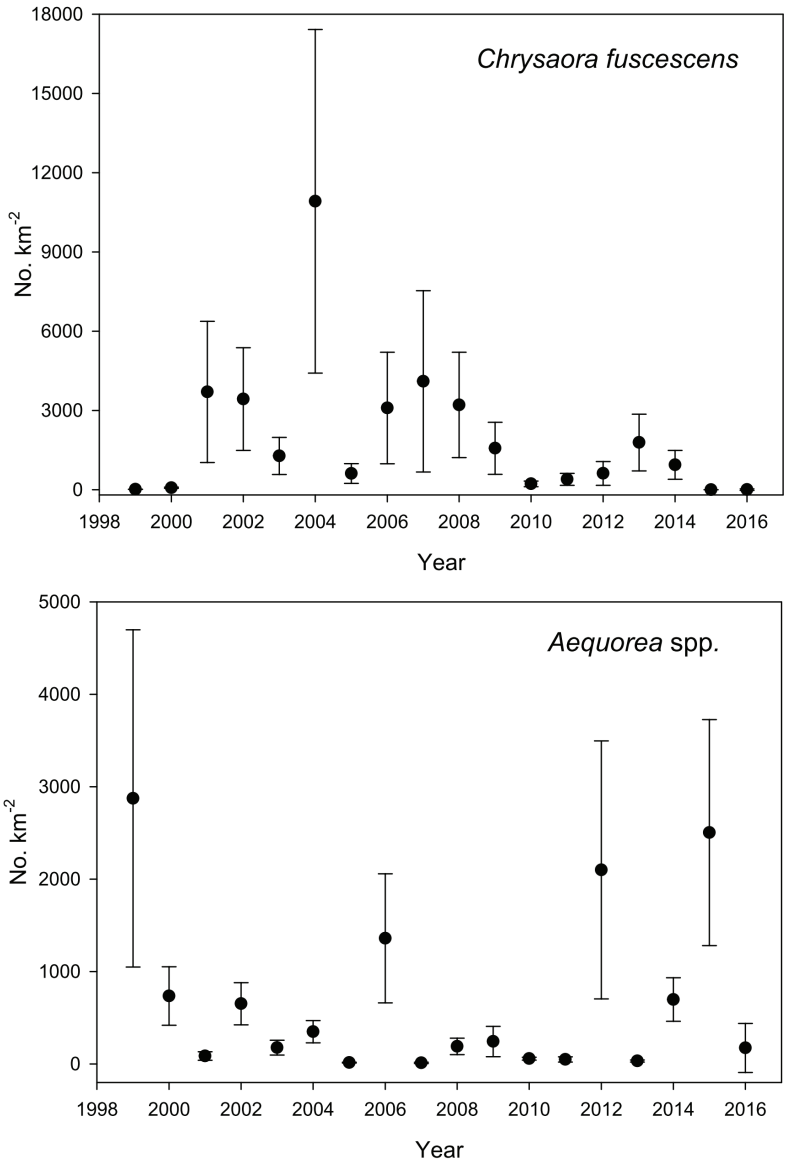

Figure 28. The abundance of the large jellyfish *Chrysaora fuscescens* and the hydromedusae, *Aequorea* spp. off Oregon and Washington during June.

salps (*Salpa* and *Thetys*) were found in higher abundances during the June 2016 cruise and the June NOAA Pre-recruit survey (data not shown) conducted during the warm ocean conditions of 2016, suggesting increased northward transport due to the El Niño event.

The combined data support the idea that offshore intrusion during the anomalous North Pacific warming of 2015 increased the occurrence of the offshore *Aequorea* spp., but that as the 2015–16 El Niño developed, advection from more southern sources increased the occurrences of southern gelatinous species.

SUMMARY: CHANGES IN THE DISTRIBUTION AND ABUNDANCE OF ZOOPLANKTON

The anomalies of temperature and salinity at 20 m depth in the IMECOCAL region off Baja California were higher during 2015–16 El Niño than during the 2003 year. The distribution of near-surface temperature and salinity during the 2015–16 El Niño suggests that warm, more saline waters typically found south of Punta Eugenia, extended to the north during the 2015–16 El Niño. Anomalously warm and saline surface waters off Baja California were associated with very low zooplankton displacement volumes in 2015–16. In contrast, during the 1997–98 El Niño, zooplankton volume was close the average, with abundant copepods, euphausiids, and salps at some stations. Tropical species such as red crab and the mesopelagic fishes *V. lucetia* and *T. mexicanus* increased in abundance and extended their range northwards in 2015–16, a phenomenon also seen during the 1997–98 El Niño.

Off California, pelagic red crab (*Pleuroncodes planipes*) adults were abundant in the water column and frequently washed up on beaches of southern California in winter

and spring 2015. They were reported in central California by September–October 2015. Zoea larval stages are found in southern California waters in most springtimes of the CalCOFI time series, although typically at very low abundances. However, during springs of historical El Niño years, zoea abundances increased dramatically, with a coastal distribution suggestive of northward transport from Baja California in the Inshore Countercurrent. In spring 2015, the presence of only adults and the youngest zoea stages, together with their coastal distribution, is suggestive of advective transport from Baja California waters.

Despite strong cumulative upwelling, temperatures at 50 m on the Oregon shelf remained warmer than average, surface nitrate was anomalously low, and chlorophyll was lower than average throughout most of 2015. Throughout 2015 and 2016, the zooplankton community was dominated by lipid-poor tropical and subtropical copepods and gelatinous zooplankton. This generally indicates poor feeding conditions for small fishes that in turn are prey for juvenile salmon. The biomass of southern copepods fluctuated greatly but was generally higher than average throughout 2015 and 2016. Seventeen copepod species with Transition Zone and North Pacific Gyre affinities that have rarely been collected off Newport, Oregon, were also observed. The presence of these species greatly increased copepod species richness which exceeded the number of species observed during the strong El Niño in 1998. Despite a strong El Niño signal at the equator during much of 2015 and into 2016, copepod or euphausiid species that have occurred off Oregon during other El Niño events were not encountered. Temperature-salinity properties at 150 m during 2015 indicated unusually warm and fresh waters, consistent with water properties of the upper 80–100 m over the slope. The conditions off Newport, Oregon, appear to have been influenced by intrusion of offshore waters. This suggests that the unusual copepods vagrants of 2015–16 originated from an offshore and southwesterly source, which is an important difference from the southerly origin of vagrants during the 1997–98 El Niño.

Coastal waters cooled off Trinidad Head in northern California due to winter upwelling events, reinforced by more sustained upwelling in spring and summer. A bloom of toxic *Pseudo-nitzschia* developed, producing high levels of domoic acid. Similar to the Oregon shelf, the copepod assemblage was dominated by a more diverse, warm water assemblage in 2015. Krill species common off northern California were diminished in size and abundance as subtropical and warm water species became more abundant. For a brief period near the end of the anomalously warm period, the dominant krill species was *Nyctiphanes simplex* rather than *Euphausia pacifica*.

The large cool water associated jellyfish (*Chrysaora fuscescens*) showed reduced abundance in warm years (2003, 2005, 2010, 2014, and 2015) off Oregon. In contrast, an offshore species (*Aequorea* spp.) showed a less convincing relationship between abundance and warm years, compared to *Chrysaora*. We speculate that intrusion of offshore waters during the anomalous North Pacific warming of 2015 increased the occurrence of the offshore *Aequorea* spp., but that as the 2015–16 El Niño developed, advection from more southern sources increased the occurrences of southern gelatinous species.

CHANGES IN THE DISTRIBUTION AND ABUNDANCE OF FISH

Changes in Ichthyoplankton Assemblages Associated with Anomalous Warming

Coastal pelagic fish egg abundance has declined off central and southern California in the last 16 years (2000–16) (Supplement fig. S9, fig. 29). Sardine, anchovy, and jack mackerel eggs were found at very low concentrations in the spring of 2016 consistent with this decadal-scale trend[12].

Jack mackerel eggs were an order of magnitude more abundant than sardine off southern California in spring 2016, but were less abundant than in spring 2015. The distribution of jack mackerel eggs in 2016 extended farther offshore than in 2015 (fig. 29). Offshore spawning of mackerel, which is commonly regarded as being typical, nevertheless occurred at low densities in spring 2016 (fig. S9, fig. 29). Anchovy eggs were an order of magnitude more abundant in spring 2016 compared to 2015, but the increase was spatially restricted to small areas off Ventura, California, and Newport, Oregon (Supplement fig. S9, fig. 29). We see no evidence in the distribution of anchovy eggs of a coast-wide recovery of anchovy abundance. The spawning distribution of sardine eggs was centered even further north in 2016 (43°–44.5°N, off Oregon) than in spring 2015 (41°–43°N, California-Oregon border). Sardine eggs are rarely found north of San Francisco in spring, meaning that the spring spawning distribution was again much farther north than usual. Sardine egg densities off Oregon in spring 2016 were <3 eggs m^{-3} (compared to <1.5 eggs m^{-3} in spring 2015), which was extremely low compared to spring 2000–13 (fig. 29).

Conditions off central and southern California were unusually warm in spring 2016 (see elsewhere in this report). Sardine spawning, centered off Oregon in a band about 50–60 nm from shore as well as nearshore, occurred in surface water temperatures of 12°–13°C (Supplement fig. S9, fig. 29). Mackerel eggs were found in water with surface temperatures of 14°–18°C,

[12]Ichthyoplankton sampling methods used by CalCOFI were summarized in McClatchie (2014).

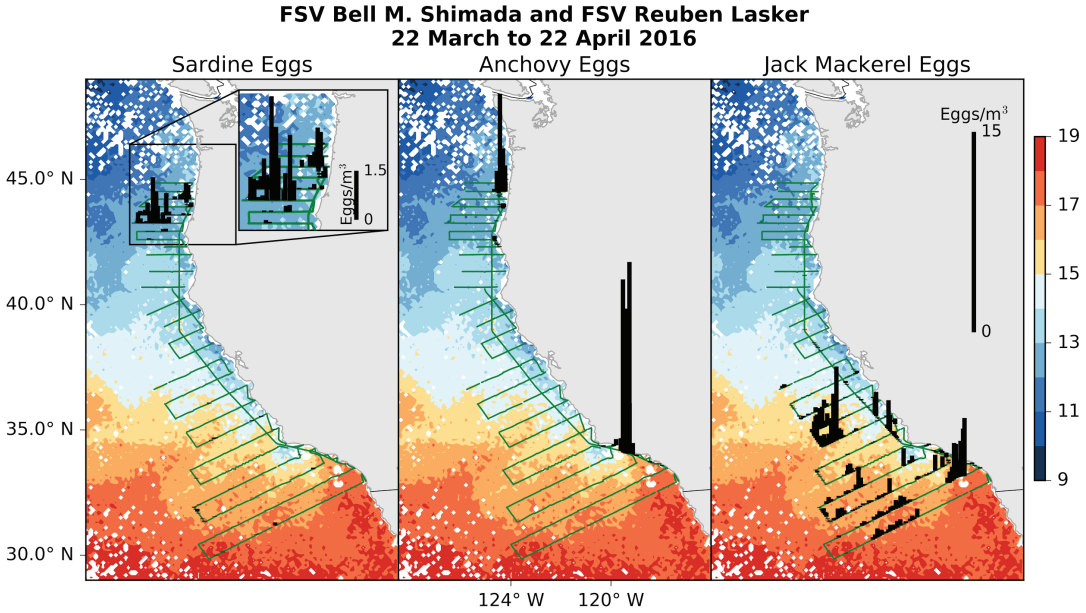

Figure 29. Density of eggs of sardine, anchovy, and jack mackerel collected with the continuous underway fish egg sampler (CUFES) during the spring 2016 CalCOFI and coastal pelagic fish cruises overlaid on satellite sea surface temperatures (°C).

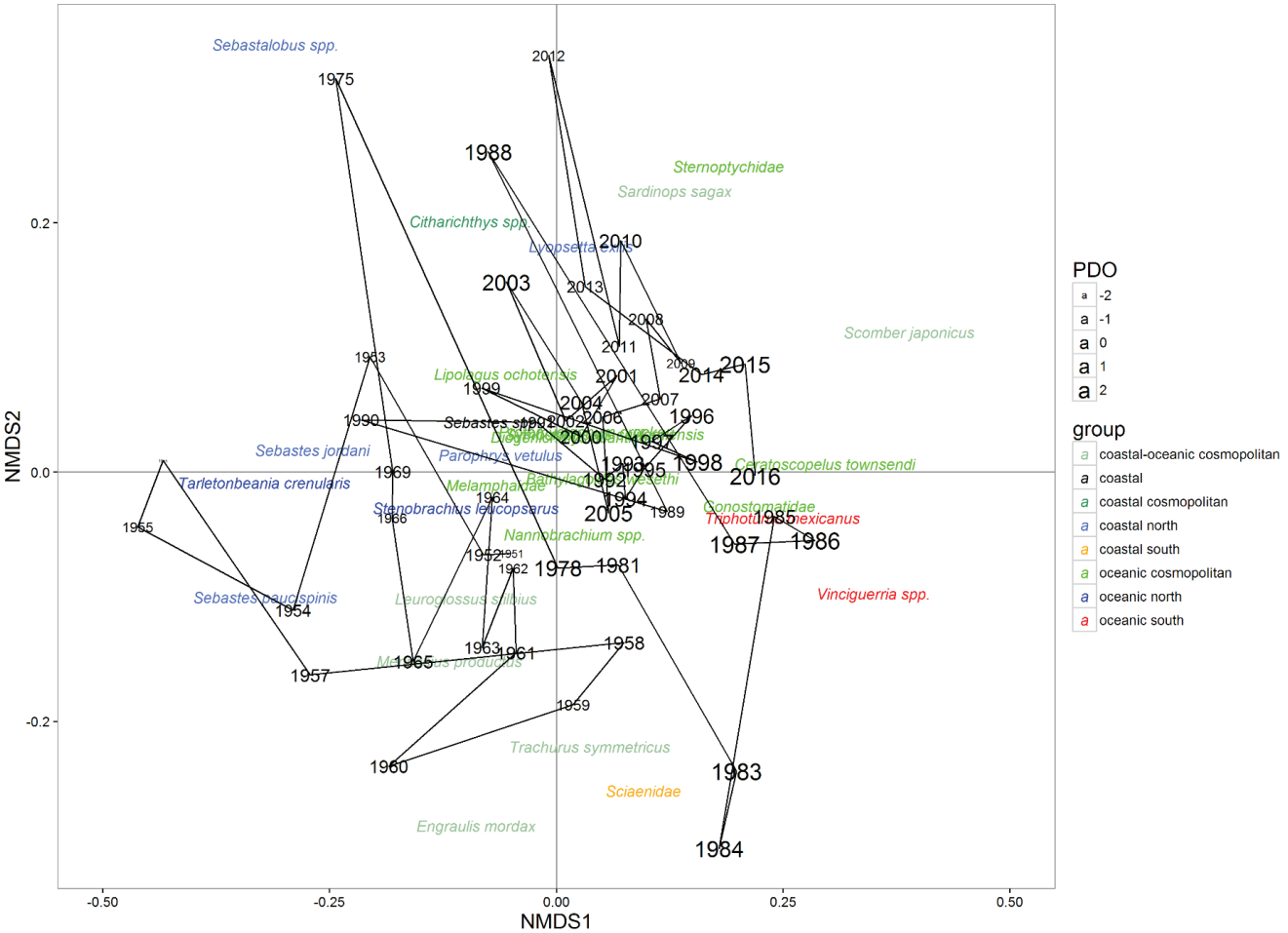

Figure 30. Nonmetric multidimentional scaling plot of the ichthyoplankton assemblage. The nMDS analysis utilized square-root transformed delta mean abundances for each year. Only taxa whose mean sums across the time series were at least 50 are included. Species are color coded based on their habitat (coastal, coastal-oceanic, and oceanic) and biogeographic range relative to the CalCOFI region (cosmopolitan, northern, and southern). Font size of the years is scaled by the PDO value in March of that year. Taxa that were not consistently identified to the species level since 1951 were grouped to either genus or family. The stress value for the analysis is 0.20.

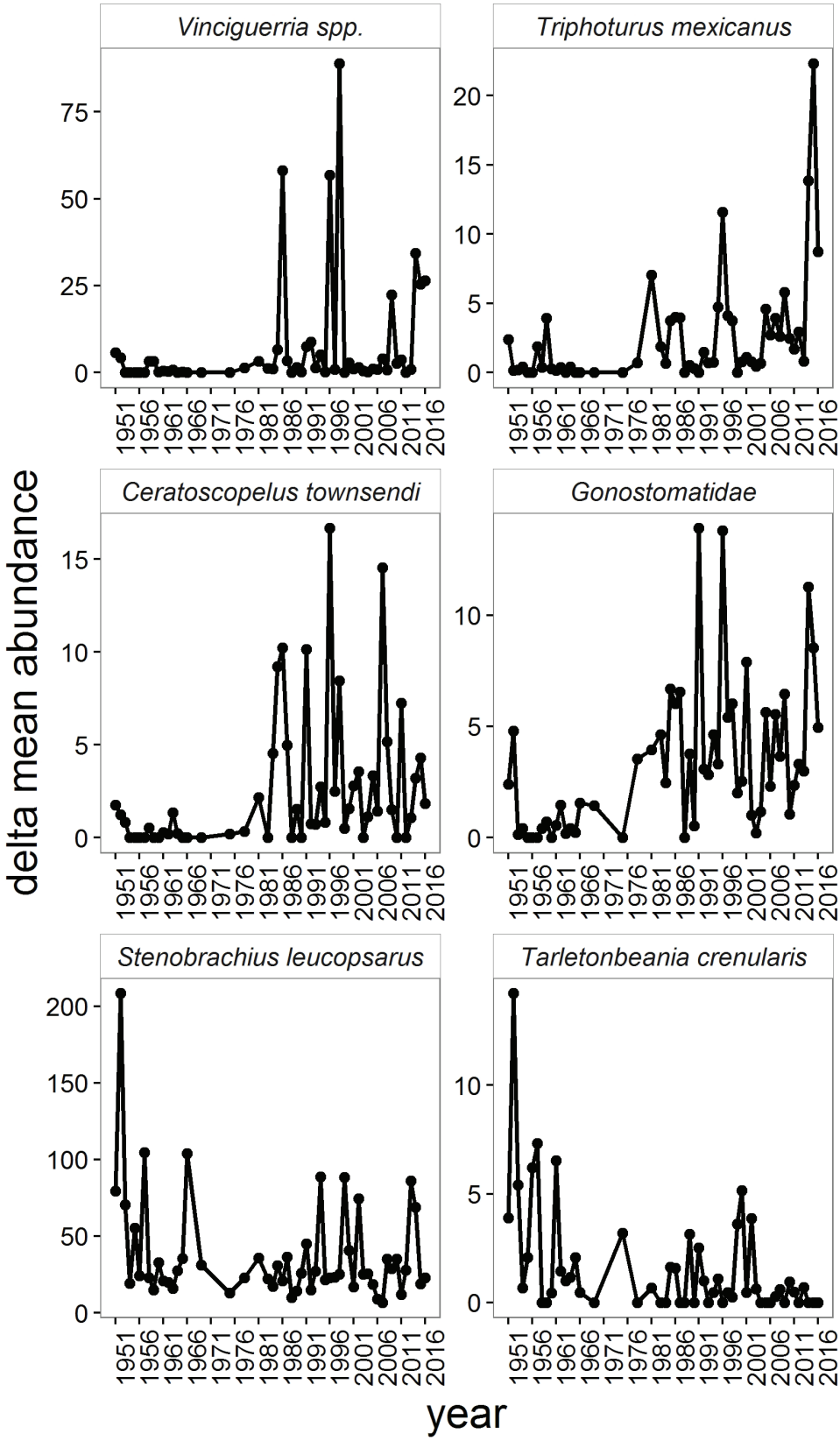

Figure 31. Delta-mean abundances of common mesopelagic taxa that drive the nMDS analysis. Delta mean was used rather than simple averaging because it is better suited for data with many zero values. *Vinciguerria* spp., *Triphoturus mexicanus*, *Ceratoscopelus townsendi*, and Gonostomatidae have southerly biogeographic ranges while *Stenobrachius leucopsarus* and *Tarletonbeania crenularis* are have northerly ranges. Note that southern taxa have high nMDS1 scores and the northern taxa low nMDS1 values.

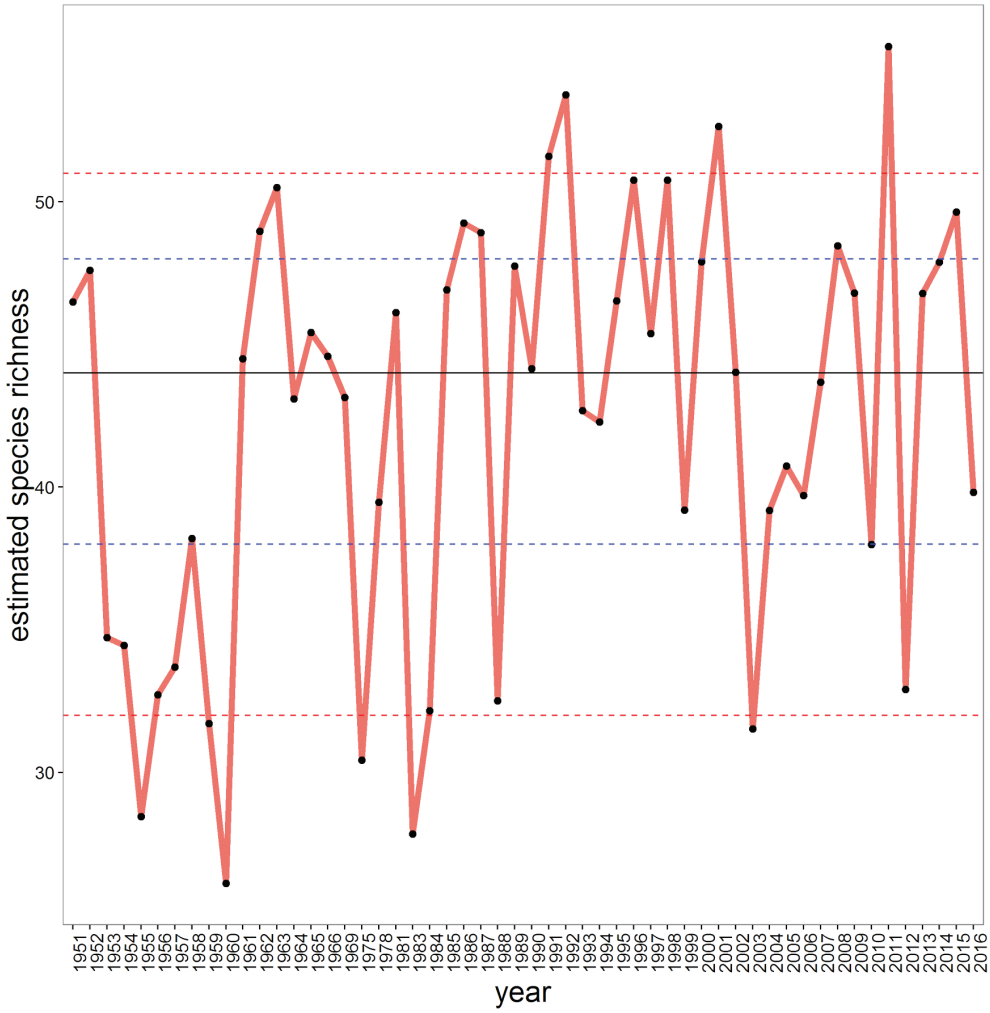

Figure 32. Estimated species richness based on a bootstrap species accumulation curve. The solid, black horizontal line depicts the long-term median, the dashed blue lines the 25th and 75th quantiles, and the dashed red the 5th and 95th quantiles.

and anchovy spawned in temperatures ranging from 12°–17°C. Both mackerel and anchovy spawned in a wider range of temperatures than sardine.

The ichthyoplankton assemblage in 2014–16 (based on spring samples from lines 80 and 90) was similar to previous years when there was either an El Niño or anomalously warm waters (fig. 30). Under these oceanographic conditions the assemblage tends to have high abundances of mesopelagic species with southerly or cosmopolitan biogeographic ranges such as *Ceratoscopelus townsendi*, Gonostomatidae (mostly in the genus *Cyclothone*, predominantly *C. signata*), *Triphoturus mexicanus*, and *Vinciguerria* spp. (mostly *V. lucetia*) and low abundances of midwater species with northern biogeographic affinities such as *Stenobrachius leucopsarus* and *Tarletonbeania crenularis* (fig. 31).

Species richness was down in 2016 relative to 2014 and 2015 but still between the 25th and 50th percentile of the long-term median (fig. 32). The 2016 drop in species richness was due in part to the complete lack of a few species that are typically common such as *Bathylagus pacificus*, *Citharichthys* spp. (mostly *C. sordidus* and *C. stigmaeus*), and *Sebastes paucispinis*.

Ichthyoplankton composition and relative concentrations of dominant taxa off Newport, Oregon, in June–July 2015 was similar to the previous seven years (fig. 33)[13]. Mean larval concentration for all species combined was the third highest in the nine-year time-series.

[13]Oregon ichthyoplankton samples were collected from 3–4 stations representing coastal (<100 m in depth), shelf (100–1000 m), and offshore (>1000 m) regions along both the Newport Hydrographic (NH; 44.65°N, 124.35°–125.12°W) and Columbia River (CR; 46.16°N, 124.22°–125.18°W) lines off the coast of Oregon during June–July in 2007–15 (for complete sampling methods, see Auth [2011] cited in the main paper). In addition, post-larval (i.e., juvenile and adult) fish were collected using a modified Cobb midwater trawl (MWT) with a 26 m headrope and a 9.5 mm codend liner fished for 15 min at a headrope depth of 30 m and ship speed of ~2 kt. MWT collections were made at 4–6 evenly-spaced, cross-shelf stations representing coastal, shelf, and offshore regions along nine half-degree latitudinal transects between 42.0° and 46.0°N latitude in the northern California Current region during June–July in 2011–16 (although no sampling was conducted in 2012). Sampled volume was assumed to be uniform for all hauls. All fish collected were counted and identified to the lowest taxonomic level possible onboard, although prerecruit rockfish were frozen and taken back to the lab for identification using precise meristic and pigmentation metrics.

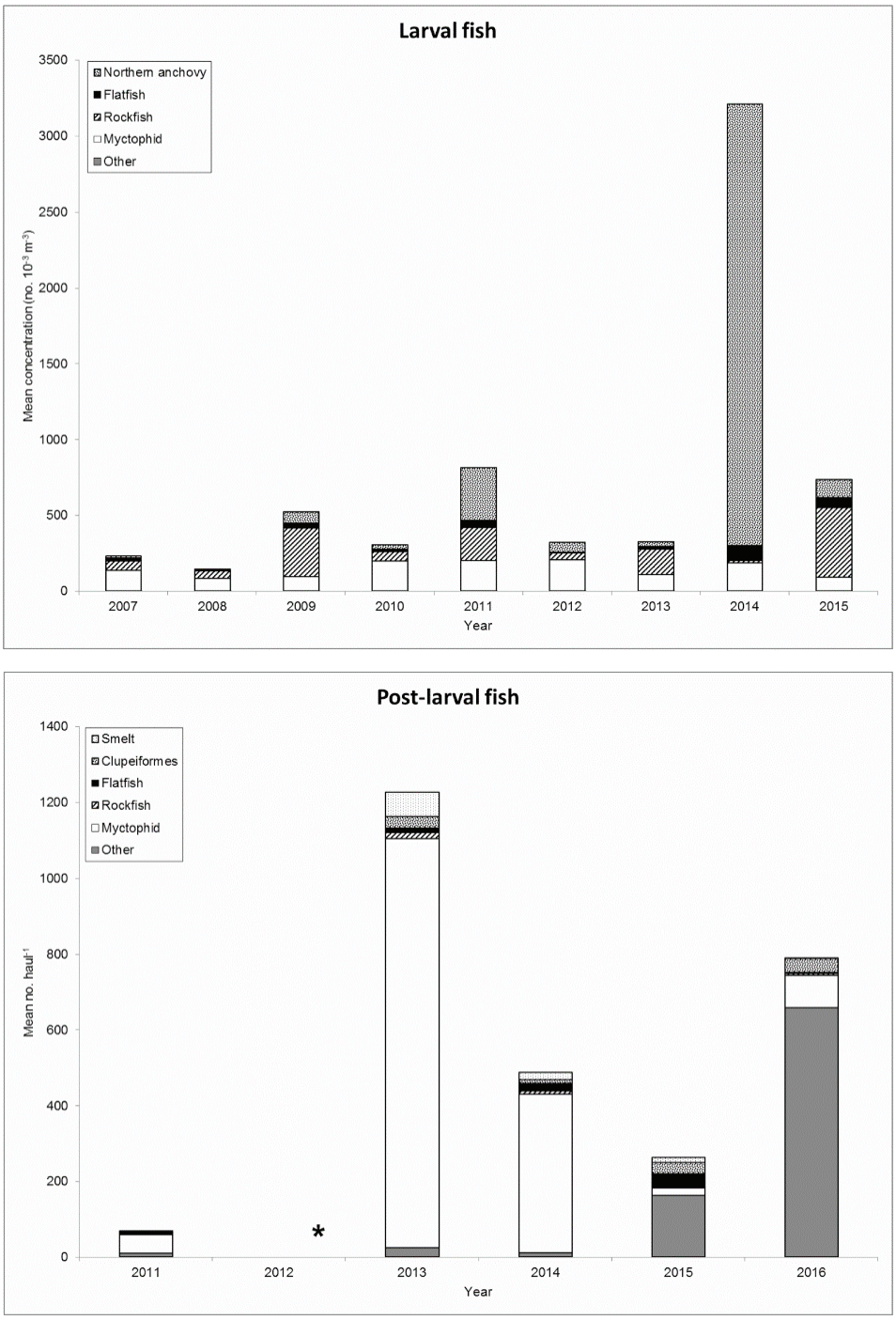

Figure 33. (Upper) Mean concentrations (no. 10^{-3} m^{-3}) of the dominant larval fish taxa collected during June–July in 2007–15 along the Newport Hydrographic (NH; 44.65°N, 124.35°–125.12°W) and Columbia River (CR; 46.16°N, 124.22°–125.18°W) lines off the coast of Oregon. (Lower) Mean catches (no. $haul^{-1}$) of the dominant post-larval fish taxa collected during June–July in 2011–16 along nine half-degree latitudinal transects between 42.0° and 46.0°N latitude in the northern California Current region. * = no samples were collected in 2012.

Larval rockfish in 2015 were found in the highest concentration of the time-series, while flatfish concentration was second only to that of 2014. Similar to flatfish, but even more exaggerated, northern anchovy were also present in unusually high concentrations in 2014, declining again in 2015 (fig. 33).

The post-larval fish assemblage in 2016 differed from the assemblage structure found in the same area and season in 2011–15, primarily due to the dominance of Pacific hake, (*Merluccius productus*). Post-larval hake comprised 82% of the total mean abundance of all post-larval fish (fig. 33). At the other extreme, the abundances

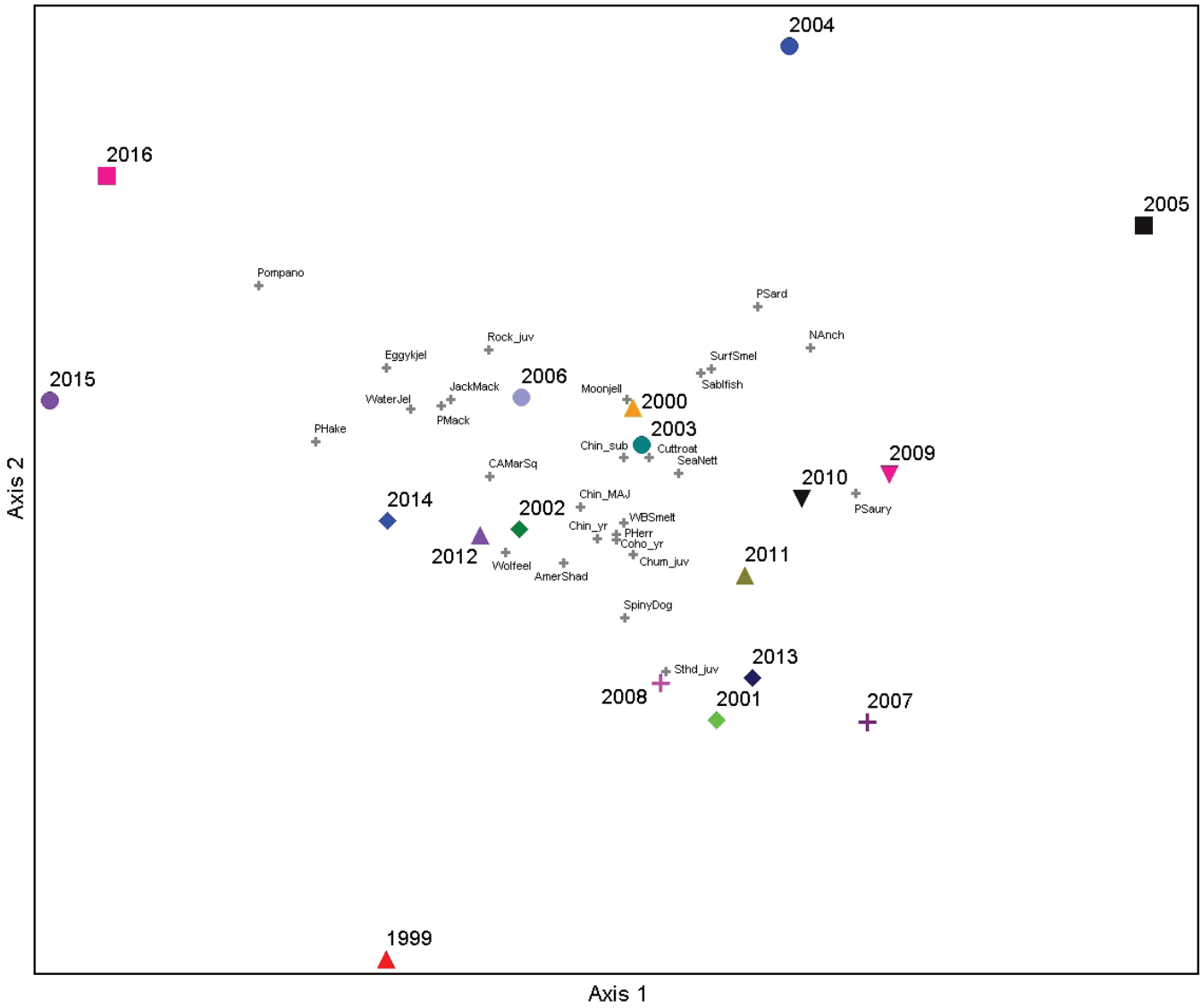

Figure 34. NMS ordination of northern California Current pelagic assemblages. The NMS ordination explained 87.0% of the total variability in the first two dimensions.

of flatfish and smelt in 2016 were the lowest of the five-year time series. Myctophids were another group showing strong interannual variability. It is notable that post-larval myctophids were numerically dominant prior to the anomalous warming of 2014–16, but that hake dominated the assemblage during the anomalous warming. This may be because the dominant myctophid taxa off Oregon are cool water-associated species.

Northern California Current Nekton and Fish

The June fish and invertebrate assemblage[14] in the northern California Current during 2016 was unusual and dominated by species that normally occur in warmer ocean waters to the south of the study area. An NMS ordination clearly showed that the 2015 and 2016 assemblages were outliers, distinct not only from the 1999 La Niña assemblages, but also from the assemblage sampled during the 2005 warm event in the northern California Current (fig. 34).

[14]Pelagic fish and invertebrate catch data were collected by the NWFSC NOAA/Bonneville Power Administration surveys using surface trawls on standard stations along transects between northern Washington and Newport, OR, in June from 1999 to 2016 (fig. 2b). All tows were made during the day at predetermined locations along transects extending off the coast to the shelf break (Brodeur et al. 2005). We restricted the data set to stations that were sampled consistently over the sampling time period (>9 y). Large sharks, ocean sunfish (*Mola mola*), and adult salmonids were removed from the dataset as a Marine mammal excluder device that has been used in the trawl since June 2014, has been shown to exclude these taxa from the catch. Numbers of individuals were recorded for each species caught in each haul and were standardized by the horizontal distance sampled by the towed net as CPUE (number/km towed). A log(x+1) transformation was applied to the species at each station and then averaged by year for each species. The species data matrix included the 27 most abundant species captured over the 18 years sampled years (27 species x 18 years). A nonmetric multidimensional scaling (NMS) ordination was used to describe the similarity of each year's community in species space.

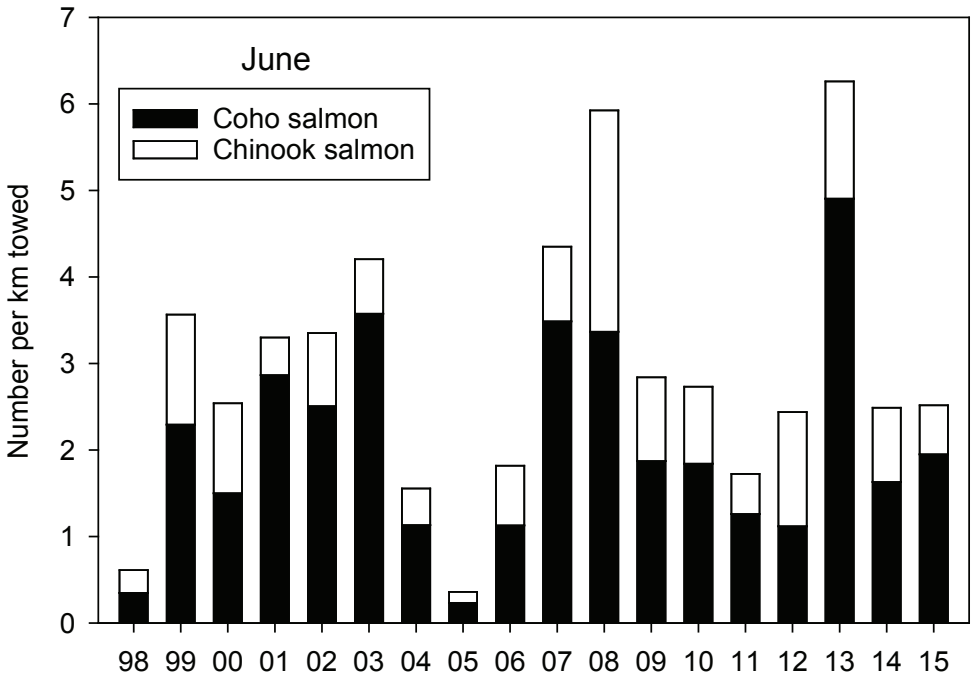

Figure 35. Catches of juvenile coho (black bars) and Chinook (white bars) salmon off the coast of Oregon and Washington in June from 1998–present.

The fish and invertebrate community in 2016 was more similar to 2015 than to any of the previous years (fig. 34). Taxa indicative of 2016 included Pacific pompano (*Peprilus simillimus*), California market squid (*Doryteuthis opalescens*), water jellyfish (*Aequorea* sp.), egg yolk jellyfish (*Phacellophora camtschatica*), age-0 Pacific hake (*Merluccius productus*), Pacific chub mackerel (*Scomber japonicus*), and jack mackerel (*Trachurus symmetricus*). Age-0 rockfishes (*Sebastes* spp.) were also extremely abundant in 2016, especially off the Washington coast. However, it should be noted that age-0 rockfish are not well quantified by the sampling gear. Forage fish species typically found in these surveys, such as Pacific herring (*Clupea pallasii*), northern anchovy (*Engraulis mordax*), and Pacific sardines (*Sardinops sagax*) were much less abundant in 2015 and 2016 than in previous years.

Catches of yearling salmon off Washington and Oregon in June may be a good indicator of early ocean survival of yearling Chinook (*Oncorhynchus tshawytscha*) and coho salmon (*O. kisutch*). The abundance of yearling Chinook salmon during June surveys has a significant and positive relationship to spring Chinook jack counts at the Bonneville Dam the following spring, as does the abundance of yearling coho salmon to subsequent coho smolt to adult survival (Morgan et al. 2016). Catch per unit effort (CPUE, number per km trawled) of yearling Chinook and coho salmon during the June 2016 survey was about average compared to the 18 previous June surveys 1998–2015 (fig. 35). Catches of yearling Chinook salmon in June 2016 were eleventh of the 19 years of sampling, and catches of yearling coho salmon were ranked 13 out of the 18 years.

Shifts in Forage and Gelatinous Plankton off Central and Southern California

Very high catches[15] of young-of-the-year (YOY) rockfish (fig. 36) were collected off central California (fig. 2b) in summer 2016, as was the case in 2015. In contrast, catches of YOY rockfish in the north central region were lower than previous years and catches in the south region were very low. Catches of YOY anchovy,

[15]The Fisheries Ecology Division of the SWFSC has conducted a late spring midwater trawl survey for pelagic juvenile (young-of-the-year, YOY) rockfish (*Sebastes* spp.) and other groundfish off central California (approximately 36 to 38°N) since 1983, and has enumerated most other epipelagic micronekton encountered in this survey since 1990 (Ralston et al. 2015; Sakuma et al. in prep). The survey expanded the spatial coverage to include waters from the US/Mexico border north to Cape Mendocino in 2004 (fig. 2b). The results here include time series of anomalies of some of the key species or groups of interest in this region since 1990 (core area) or 2004 (expanded survey area), and an update of a principal component analysis (PCA) of the pelagic micronekton community in the core area developed by Ralston et al. (2015), all of which have also been reported in earlier SoCC reports. The data for the 2016 survey are preliminary, corresponding oceanographic information (CTD casts, continuous data on surface conditions and productivity, and acoustic data) and seabird and marine mammal abundance data are also collected but not reported here. Catches are shown as standardized anomalies from the mean of the log transformed catch rates.

In addition to the six species shown in Figure 36, an additional 14 species and groups were included in the analysis of the forage assemblage within the core (1990–2015) area developed by Ralston et al. (2015), and are subsequently represented in the PCA of this assemblage (fig. 38). The results of the PCA for the core area (fig. 38, 1990–2016) were comparable to those originally reported by Ralston et al. (2015) and Leising et al. (2015), with a greater fraction of the total variance explained by the first two principal components (due to the smaller number of time series included).

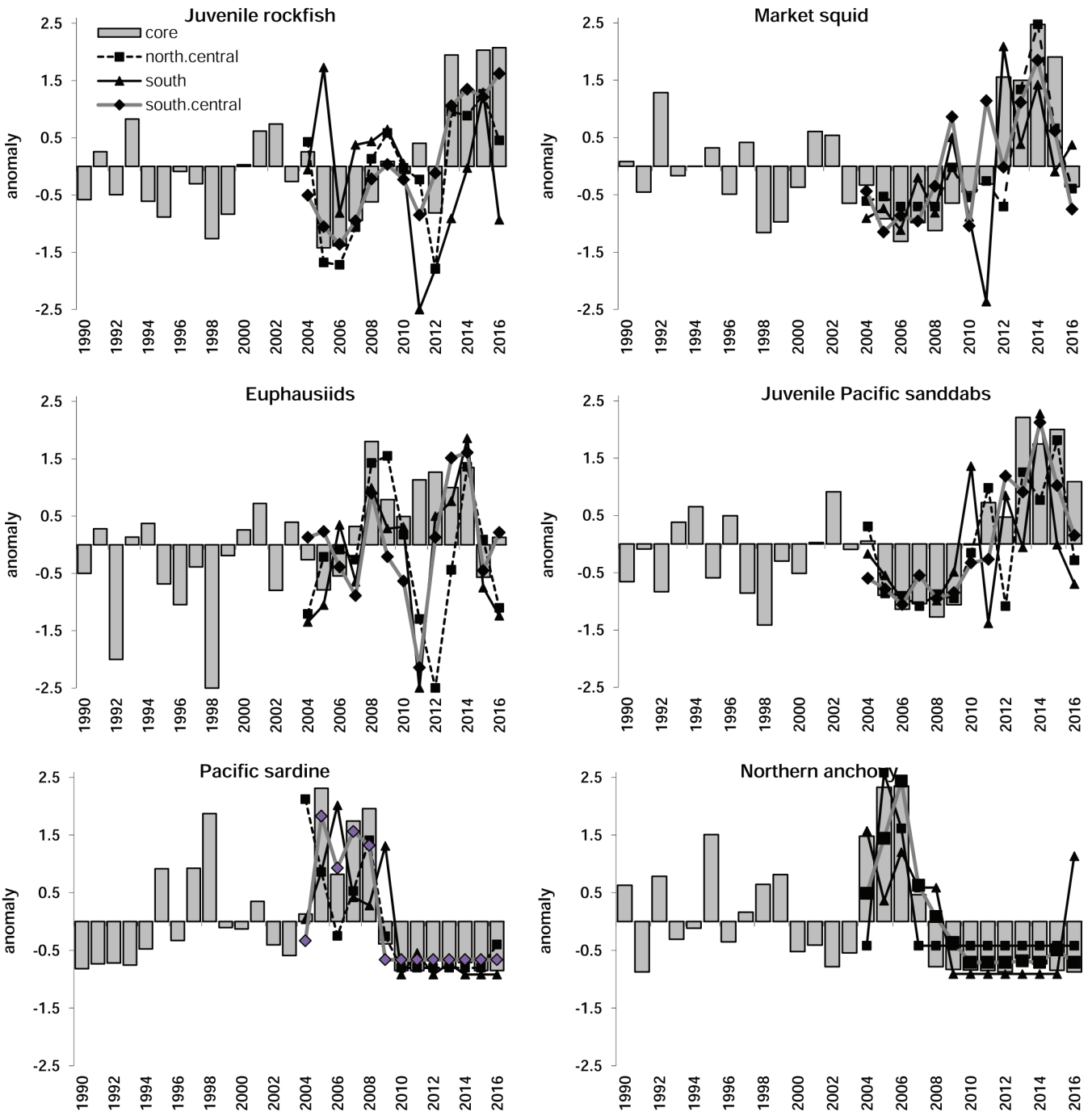

Figure 36. Long-term standardized anomalies of several of the most frequently encountered pelagic forage species from rockfish recruitment survey in the core (central California) region (1990–2014) and the southern, south-central and north-central survey areas (2004–15). Forage groups are YOY rockfish, market squid (*Doryteuthis opalescens*), krill (primarily *Euphausia pacifica* and *Thysanoessa spinifera*), YOY Pacific sanddab (*Citharichthys sordidus*), Pacific sardine (*Sardinops sagax*) and young-of-the-year Northern anchovy (*Engraulis mordax*).

which are enumerated separately from age 1+ anchovy, were the highest ever observed in the Southern California Bight, while in other regions of the California Current their numbers in summer 2016 were reduced compared to 2015 (unpublished data). *Thetys vagina* and *Pyrosoma* spp. were caught in large numbers, but other salps (i.e., non-*Thetys* salps) were less abundant compared to the past several years (fig. 37). As in summer 2015 (Leising et al. 2015), high numbers of pelagic red crabs (*Pleuroncodes planipes*) and California lizardfish were captured in summer 2016. These species are typically associated with warm water.

The abundance of both krill and market squid declined in summer 2016 in most areas relative to

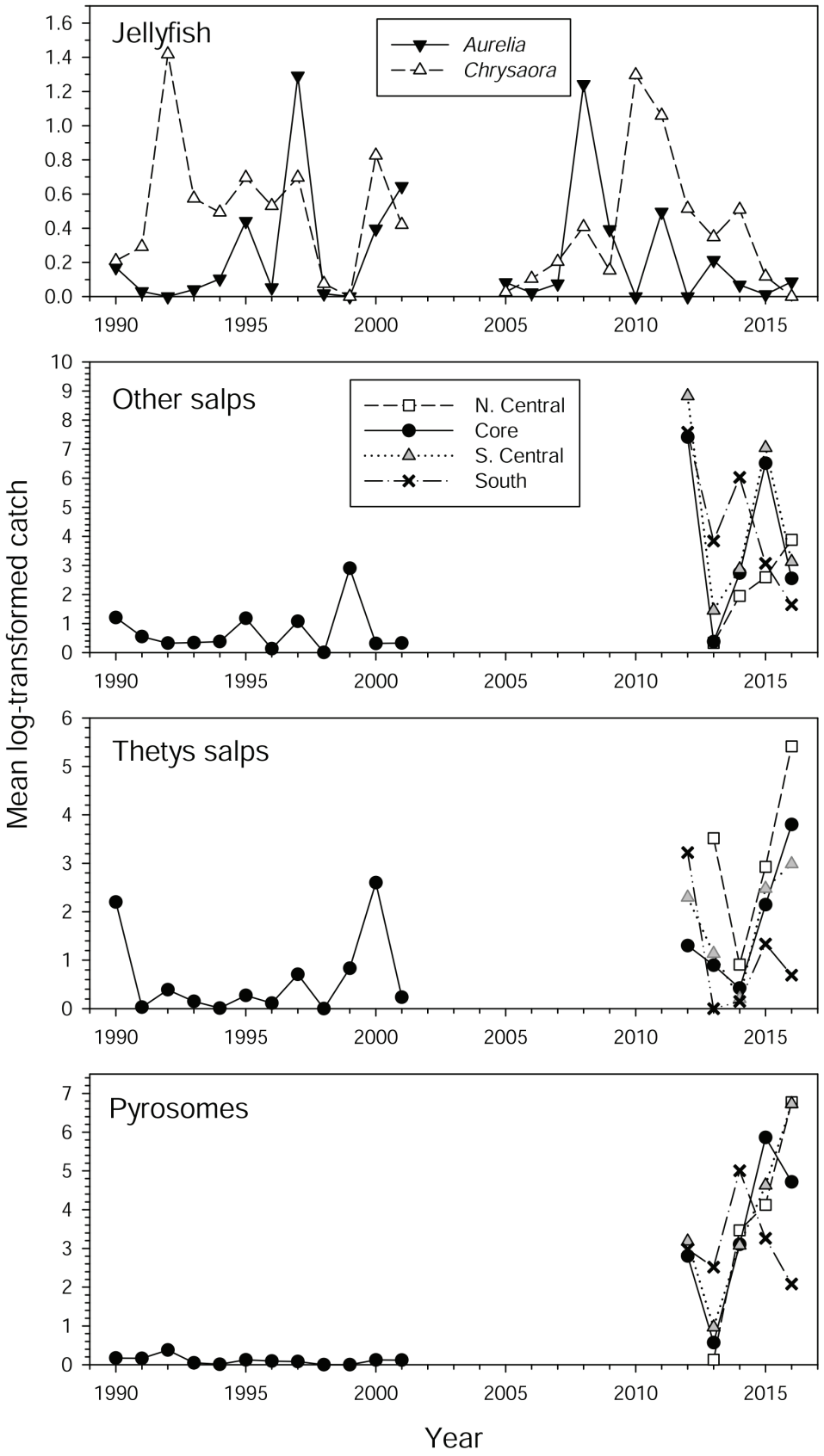

Figure 37. Standardized catches of jellyfish (*Aurelia* and *Chrysaora* spp.) and pelagic tunicates in the core and expanded survey areas.

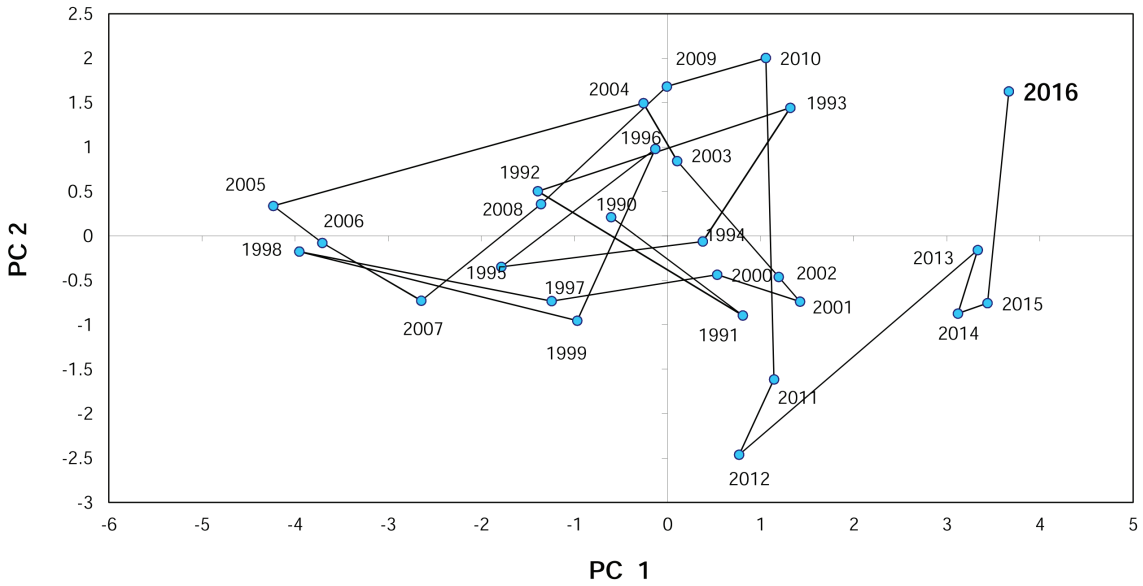

Figure 38. Principal component scores plotted in a phase graph for the nine key taxonomic groups of forage species sampled in the central California core area in the 1990–2016 period.

2015, with abundance close to or below average levels, and catches of juvenile Pacific sanddabs also declined to lower levels relative to previous years (fig. 36). The abundance of adult Pacific sardine and northern anchovy remained very low for most regions as well. Both of these species have rarely been encountered in most of the times and regions monitored since 2009, with the exception of adult anchovy in the Southern California Bight in 2016. This suggests that the biomass may be too low to be meaningfully indexed by the survey, or that a substantial fraction of the biomass is primarily located in nearshore or offshore habitats not sampled by the survey. Catches of scyphozoan jellyfish (primarily *Aurelia* spp. and *Chrysaora* spp.) continued to be unusually low in 2016 (fig. 37). Many of the more rare and unusual species that were encountered in summer 2015 (discussed in Leising et al. 2015 and Sakuma et al., in review) were not observed in the 2016 summer survey.

As in past analyses, there were sharp differences in principal component (PC) loadings between coastal pelagic (Pacific sardine, northern anchovy) and mesopelagic species (myctophids) relative to most of the YOY groundfish, krill and cephalopods. The two leading PCs for the assemblage are shown in a phase plot (fig. 38). The dramatic (and apparently ongoing) separation of the 2013 through 2016 period is apparent from these years being extremely orthogonal to the low productivity years of 1998, 2005, and 2006. Such shifts in the forage base have important implications for seabirds, marine mammals, salmon, and adult groundfish that forage primarily, or exclusively, on one or another component of the forage assemblage.

SUMMARY: CHANGES IN THE DISTRIBUTION AND ABUNDANCE OF FISH

The very warm conditions were not associated with a large spawning of sardine, but were associated with a northern shift of the sardine spawning area from central California to Oregon. Anchovy larvae were very abundant off Newport, Oregon, in 2014, but not subsequently. The ichthyoplankton assemblages off southern California and Oregon were similar to those seen in other anomalously warm or El Niño years. The mesopelagic fish assemblage off southern California exhibited higher abundances of species with southern affinities, and lower abundances of species with northern affinities. The increase in abundance and northward shift of southern species off southern California was similar to what was observed for mesopelagic fish species and red crabs off the Baja Peninsula. Off Oregon, post-larval fishes exhibited shifting dominance from myctophids prior to and at the beginning of the anomalous warming to hake becoming numerically dominant during the warming.

Fish and nekton assemblages in 2015 and 2016 were different from assemblages present during the 1997–99 El Niño/La Niña and the 2005 warm event. Forage fish such as Pacific herring, northern anchovy, and Pacific sardine were much less abundant in 2015–16 compared to previous years. In contrast, catches of salmon were close to average off northern California. Catches of young-of-the-year rockfishes were high off central California, but low off both northern and southern California. High numbers of warm water species like red crabs and lizardfish were captured in 2016, but many rare species encountered in summer 2015 were absent in 2016.

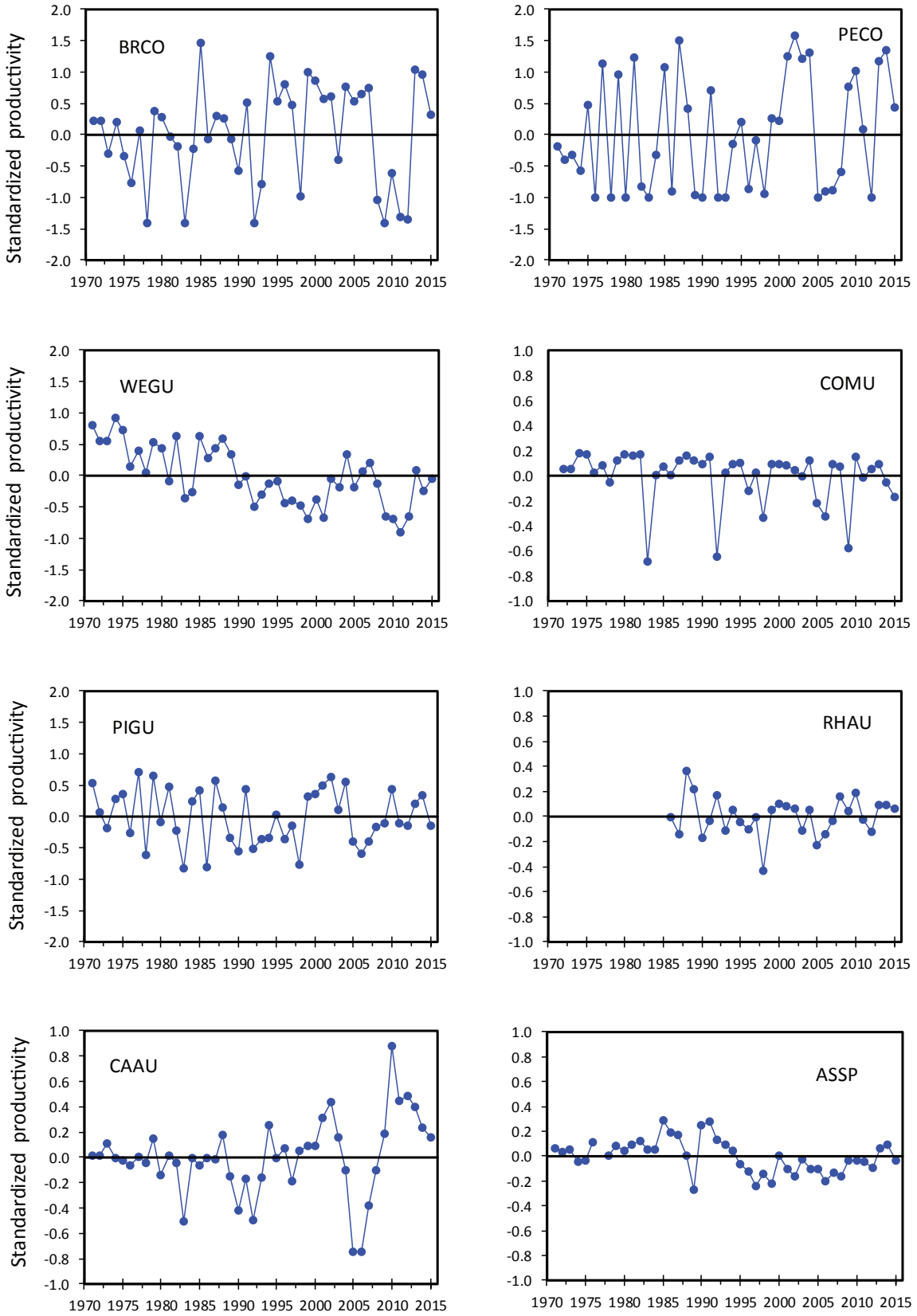

Figure 39. Standardized productivity anomalies (annual productivity minus 1971–2015 mean productivity) for 8 species of seabirds on Southeast Farallon Island. The species are: BRCO – Brandt's cormorant, PECO – pelagic cormorant, WEGU – western gull, COMU – common murre, PIGU – pigeon guillemot, RHAU – rhinoceros auklet, CAAU – Cassin's auklet, ASSP – ashy storm-petrel.

Similarly to northern California, numbers of adult sardine and anchovy were very low in summer 2016, and the survey may not provide reliable estimates at such low abundances. Multivariate analyses suggest that there may have been a shift in the composition of the forage base since 2013, and this has important implications for predators feeding exclusively on one or another component of the forage base.

SEABIRD BREEDING, PHENOLOGY, AND DIET

Reduced Seabird Breeding Populations and Breeding Success off Central California

During 2015, seabird breeding populations at Southeast Farallon Island (fig. 2a) decreased relative to 2014 for all species (data not shown) except tufted puffin (*Fratercula cirrhata*). Tufted puffins continued to increase, establishing a new high count. The upward trend for puffins contrasted with other species. The number of breeding western gulls was the lowest observed during 45 years of monitoring. Breeding populations of pigeon guillemots (*Cepphus columba*), pelagic cormorants (*Phalacrocorax peligacus*), Brandt's cormorants (*Phalacrocorax penicillatus*), and Cassin's auklets (*Ptychoramphus aleuticus*) also exhibited significant declines relative to 2014, although all except Brandt's cormorants were above long-term means. Double-crested cormorants (*Phalacrocorax auritus*) had their lowest breeding populations since 1974.

Standardized productivity (fig. 39) was lower for most species in 2015 when compared to 2014, but remained near or above long-term mean values. Chicks generally took longer to grow and fledged at lower weights than in the past few seasons. Common murres (*Uria aalge*) and pigeon guillemots were the only species below the long-term mean breeding success, while western gulls were the only species to have higher success relative to 2014. Black oystercatchers (*Haematopus bachmani*) had the lowest productivity and population ever observed for this colony, due primarily to disturbance caused by sea lions. In both 2014 and 2015, Cassin's auklets failed to produce any successful second broods resulting in their lowest productivity in six years. However, a high success rate for first broods ultimately resulted in a productive season.

A shift in chick diets from rockfish to anchovies was observed. Juvenile rockfish (*Sebastes* spp.), was still important in chick diets at Southeast Farallon Island colonies comprising 51% of the common murre chick diet and 29% of the rhinoceros auklet (*Cerorhinca monocerata*) chick diet, but rockfish were much less prominent in the diet compared to the previous two years. Anchovies returned as a major prey item for the first time since 2008 (Warzybok et al. 2015). Northern anchovy comprised 33% of common murre chick diet and 62% of rhinoceros auklet chick diet in 2015.

The Gulf of the Farallones was characterized by very warm sea-surface temperatures (SST) throughout most of the 2015 breeding season. Mean seasonal SST measured at the island in 2015 was the warmest since 1992 and joins 1992, 1998, and 2014 as the only years in which the seasonal mean was greater than 13°C (Warzybok et al. 2015). While April and May were close to the long-term average temperatures, mean monthly values for both July and August were the highest ever recorded at the Farallones. It appears that early breeding birds, in particular Cassin's auklets, fared better than later breeding species, which appear to have been affected by changed prey availability in late summer.

Warm water brought unusual bird species into the region. These included the first island records for wedge-rumped storm-petrel (*Oceanodroma tethys*) and kelp gull (*Larus dominicanus*), as well as record numbers of brown boobies (*Sula leucogaster*).

Breeding Success, Nesting Phenology, and Diet of Common Murres and Brandt's Cormorants Nesting in Far Northern California

Castle Rock National Wildlife Refuge (hereafter Castle Rock) is the most populous single-island seabird breeding colony in California (Carter et al. 1992). This island is located off the coast of Crescent City, just south of Point St. George, in the northern California Current System (fig. 2b). Here we describe the reproductive performance of common murre and Brandt's cormorants. For common murre, we also document prey composition delivered to chicks between 2007 and 2015[16].

Common murre are the most abundant surface-nesting seabird at Castle Rock and their reproductive success, nesting phenology, and chick diet have been studied since 2007. The percent of nesting pairs that successfully fledged young in 2015 was based on 87 nest sites that were monitored every other day for the entire breeding season. During 2015, fledging was 10% lower than the long-term average for this colony (63% of nests fledged young) (fig. 40A). Hatching was also 4% lower than the long-term average. The cause of depressed hatching success at Castle Rock in 2015 is not known, although hatching success at this colony is commonly influenced by egg dislodgment, egg abandonment, and inclement weather (e.g., rain) during incubation. In 2015 we infer that inadequate prey reduced the ability of murres to raise chicks to fledging age at Castle Rock because (1) chicks were observed dead at their nest site and (2) alternate sources of chick mortality (e.g., colony disturbance, predation of chicks) were not observed. Although murres do not respond directly to upwelling,

[16]To facilitate long-term monitoring of seabirds nesting at this colony, a remotely-controlled video monitoring system was installed in 2006.

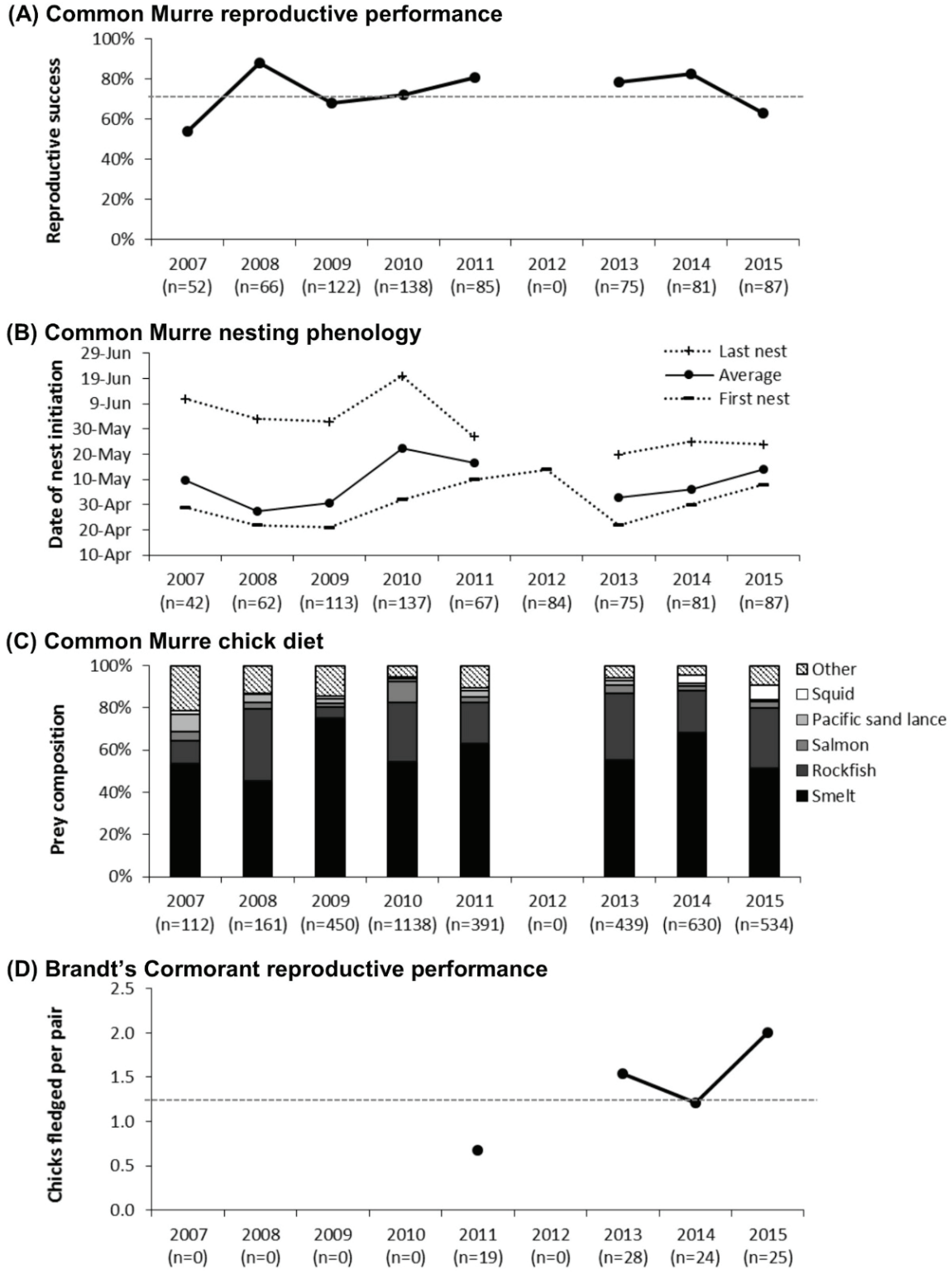

Figure 40. Reproductive performance, phenology, and chick diet of seabirds nesting at Castle Rock National Wildlife Refuge, Del Norte County, CA, between 2007 and 2015. (**A**) Percent of common murre nesting pairs that successfully fledged young. The dashed line represents the long-term (2007–15) average in reproductive success for first-clutches at this colony and the sample size (n) represents the total number of nesting pairs observed per year. (**B**) First, average, and last dates for nests initiated by common murre where the sample size (n) represents the total number of nests observed each year where nest initiation dates were accurate to ±3.5 days. (**C**) Composition of prey delivered to chicks by common murre where the sample size (n) represents the total number of prey identified each year. (**D**) Chicks fledged per each Brandt's cormorant nesting pair. The dashed line represents the long-term (2011–15) average in reproductive success for first-clutches at this colony and sample size (n) represents the total number of nesting pairs observed per year. For all subplots, data from 2012 is missing due to early failure of the video monitoring system.

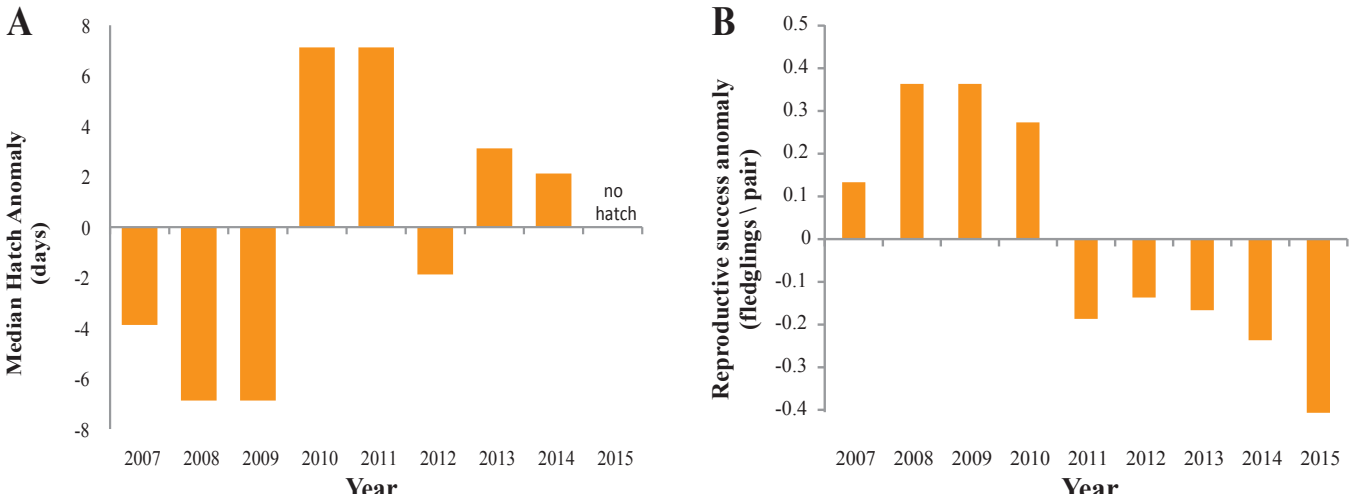

Figure 41. Anomalies of median chick hatch date and reproductive success for common murres nesting at Yaquina Head, Oregon, 2007–15. 2015 was the first year that all pairs in our reproductive plots failed to produce chicks.

increased availability of food associated with upwelling improves the body condition of egg-laying females and thereby influences the timing of nesting (Perrins 1970; Reed et al. 2006; Schroeder et al. 2009). In 2015, average nest initiation date was 5 days later (14 May) than the long-term average observed at this colony (fig. 40B), suggesting female body condition was suboptimal for early breeding.

In 2015, 16 prey types were identified[17]. All prey types had been observed in previous years with the exception of one octopus observed in 2015. Prey composition in 2015 was generally similar to other years, with smelt (Osmeridae) being the predominant prey fed to chicks and rockfish (*Sebastes* sp.) being the second-most common prey (fig. 40C). Market squid (*Doryteuthis opalescens*) were 4.2 times more frequent in murre chick diets than the long-term average and were the third most common prey type fed to chicks in 2015. Unusually in 2015, murres fed their chicks many subadult (as opposed to young-of-the-year) rockfish.

Brandt's cormorants are the second-most abundant surface-nesting seabird at Castle Rock and their reproductive success has been studied since 2011. The reproductive success of Brandt's cormorants, measured as the number of fledglings produced per pair, was determined by monitoring 26 nests every three days throughout the entire breeding season. In 2015, in contrast to the murres, cormorant breeding pairs produced 2.0 chicks on average which was 47% more than the long-term average at this colony and 29% greater than the year with the most successful reproduction (2013; fig. 40D). This illustrates an important species-specific difference between the reduced breeding success of murres and increased breeding success of cormorants during the anomalously warm conditions.

[17]Prey composition was monitored using 2-hour diet surveys conducted 6 days per week during the murre chick-rearing period (approximately 62 hours surveyed in 2015).

Reproductive Failures of Most Seabirds at Yaquina Head, Oregon: Bottom-Up Impacts Under Top-Down Control

Common murres (*Uria aalge*) and pelagic cormorants (*Phalocrocorax pelagicus*) at Yaquina Head (fig. 2b) experienced complete reproductive failure in 2015. Murre eggs were laid, but none were incubated long enough to hatch chicks. This was the first time that no murre chicks were produced in 14 years of data collection, maintaining a 5-yr run (2011–15) of low reproductive success that is less than half the success for the first four years of the study (2007–10, fig. 41). Murre reproductive success during the 1998 El Niño (Gladics et al. 2015), and 2010, 2014, and 2015 were the lowest on record. Pelagic cormorants had the lowest brood size and reproductive success in 2015 for our 8-year record (only 2011 was similarly low; fig. 42B). In contrast, Brandt's cormorants (*P. penicillatus*) had the highest reproductive success and second-highest brood size during our 8 year record (fig. 42A). Median hatch date for cormorants was over a week later than the mean (fig. 43).

Since 2011 much of the reproductive loss for murres has been due to egg and chick predators (Horton 2014). In 2015, however, the disturbance by primarily bald eagles (*Haliaeetus leucocephalus*) was so intense early in the breeding season that no eggs were incubated long enough to hatch chicks. Persistent eagle disturbance early in the season is also in part responsible for the later laying and hatching dates of murres and cormorants.

The three main forage fish species fed to murre chicks are smelt (Osmeridae), Pacific herring or sardine

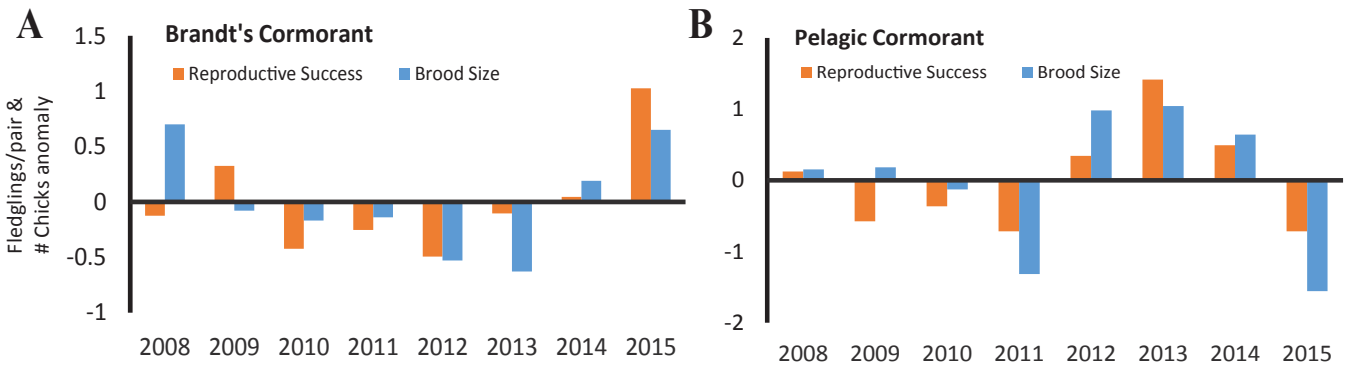

Figure 42. Anomalies of reproductive success and brood size for cormorants nesting at Yaquina Head, Oregon, 2007–15. Brandt's cormorants had an above average year for chick production, but pelagic cormorants, like murres, had a complete reproductive failure.

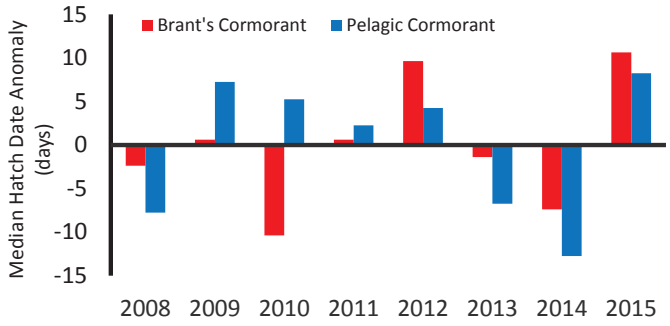

Figure 43. Anomalies of median hatch dates for Brandt's and pelagic cormorants at Yaquina Head, Oregon, 2007–15. Both species experienced one of the latest hatch dates recorded.

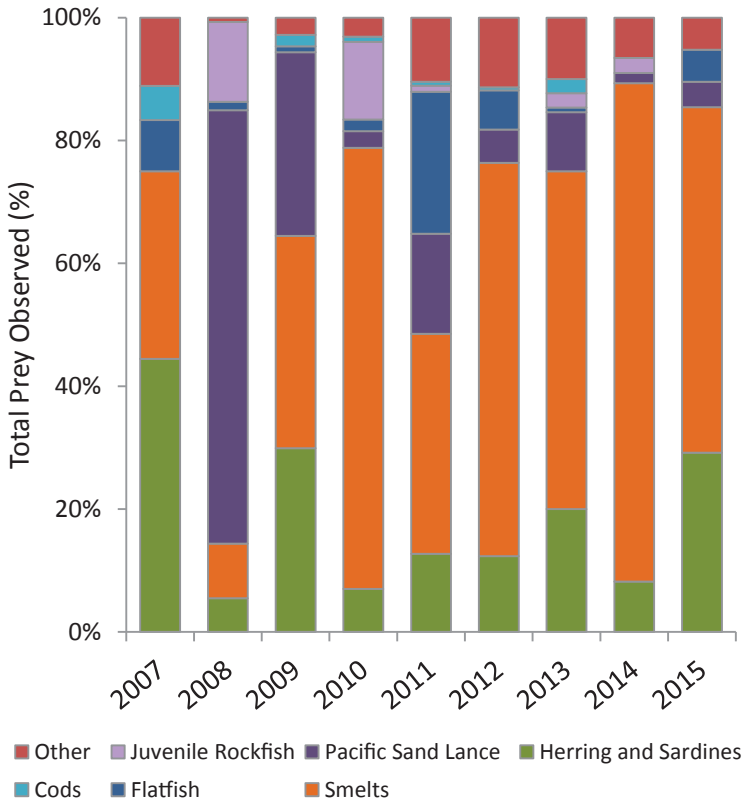

Figure 44. Prey fed to common murres chicks (% occurrence) at Yaquina Head, Oregon, 2007–15.

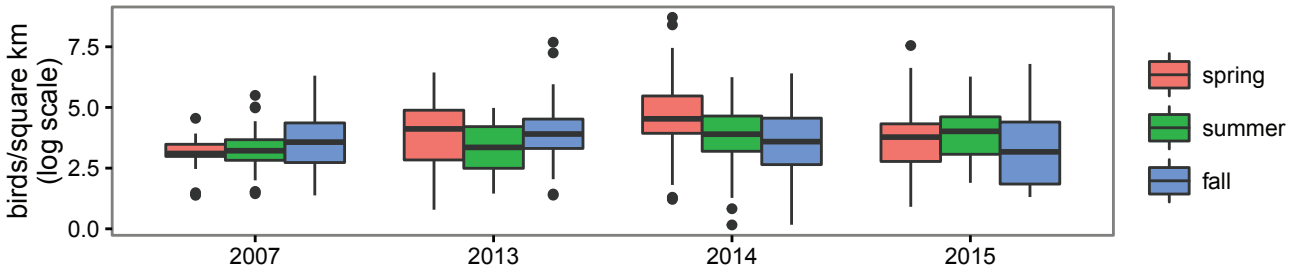

Figure 45. Boxplots of overall seabird density from vessel-based surveys off Newport, Oregon, including along the Newport Hydrographic Line and adjacent nearshore waters.

(Clupeidae), and Pacific sand lance (*Ammodytes hexapterus*). The relative proportion of the three species can be similar or one species may be numerically dominant in a given year. Smelt was the main prey item in 2015, continuing a trend of smelt-dominated diets for 4 of the past 5 years (fig. 44). In 2015, however, there was an increase in Clupeids (herring/sardine) compared to recent years. Pacific sand lance continues to be minimal in diets since 2010. The dominance of smelt and lack of herring and sand lance is notably different than diets during the 1998 El Niño (Gladics et al. 2015). Sand lance are generally more prominent in murre diets during cold water years (Gladics et al. 2014, 2015), as highlighted by their prevalence in 2008 (fig. 44). Clupeids, primarily Pacific herring (*Clupea pallasii*), are generally associated with warmer water and positive PDO (Gladics et al. 2015), although their occurrence in recent warm water years has been lower than expected.

Vessel-based seabird surveys off Newport, Oregon, indicated reduced seabird densities in spring 2015 relative to 2014 (especially for common murre, Brandt's and pelagic cormorants), but average or above average densities in nearshore waters during summer 2015 (fig. 45).

SUMMARY: SEABIRD BREEDING, PHENOLOGY, AND DIET

Seabirds at Southeast Farallon Island in 2015 exhibited reduced breeding populations, reduced breeding success, lower chick growth rates, and lower fledging weights. Chick diets shifted from a high proportion of rockfish to more anchovies compared with the previous two years. Coincident with reduced breeding and the dietary shift, the temperatures in the Gulf of Farallones were anomalously warm. Unusual bird species were observed in the region during these anomalously warm conditions. Common murre reproductive success was lower than average in northern California, similar to observations from central California during 2015, and a complete reproductive failure in central Oregon. Reduced prey availability was likely the cause as chick mortality resulted primarily from starvation, with the added pressure of increasing bald eagle predation in central Oregon. Murre chick diets were similar to other warm years, with anchovies dominating in the central and smelt dominating in the northern California Current, with another year of notable lack of sand lance off central Oregon. Fewer rockfish were consumed by murres in central California and an older age class was consumed in northern California. An increase in California market squid that began in 2014 continued in 2015 potentially indicating northward shift in these squid populations due to the prevalence of warm sea-surface temperatures across the CCS in 2015. Unlike murres and Pelagic cormorants, Brandt's cormorants were more successful in 2015 than previously observed indicating that seabird response to conditions in the CCS are species specific.

FEW PUPS AND LOW GROWTH AT SAN MIGUEL SEA LION ROOKERIES

California sea lions (*Zalophus californianus*) are permanent residents of the CCS, breeding in the California Channel Islands and feeding throughout the CCS in coastal and offshore habitats. They are also sensitive to changes in the CCS on different temporal and spatial scales and so provide a good indicator species for the status of the CCS at the upper trophic level (Melin et al. 2012). Two indices are particularly sensitive to prey availability, pup production, and pup growth during the period of maternal nutritional dependence. Pup production is a result of successful pregnancies and is an indicator of prey availability to and nutritional status of adult females from October to the following June. Pup growth from birth to 7 months of age is an index of the transfer of energy from the mother to the pup through lactation between June and the following February, which is related to prey availability to adult females during that time.

After a 12% increase in pup births at San Miguel Island in 2014, pup births declined 26% in 2015 and were 16% lower than the long-term average between 1997 and 2015 (fig. 46). Pup condition and pup growth for the 2015 cohort was the lowest observed over the time series. The average weights of three-month-old pups were 27% and 30% lower than the long-term average for female and male pups, respectively (fig. 47). Pup growth rates from three to seven months of age were 79% below average

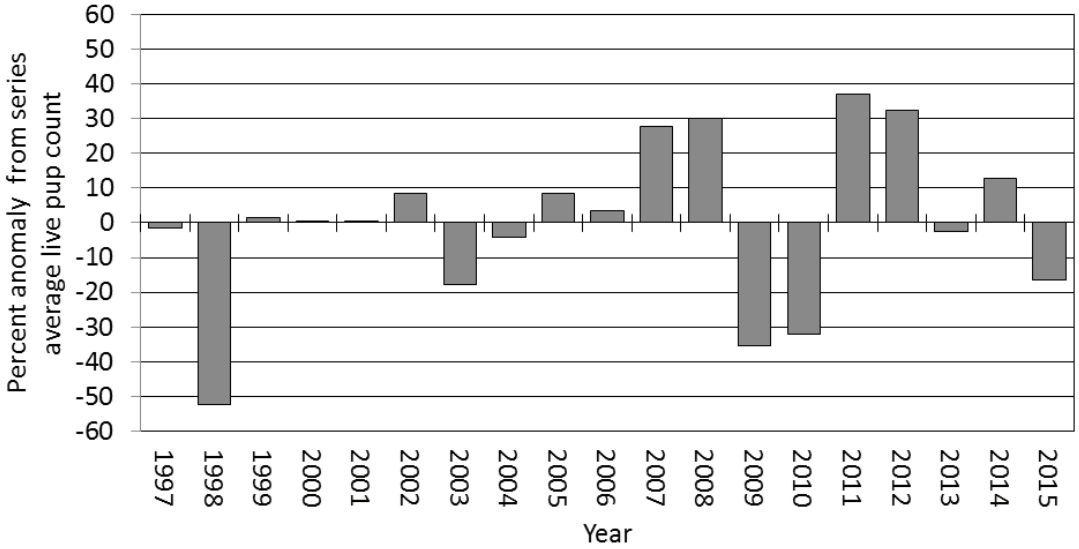

Figure 46. The percent anomaly of live California sea lion pup counts at San Miguel Island, California, based on a long-term average of live pup counts between 1997-2015 in late July when surviving pups were about 6 weeks old.

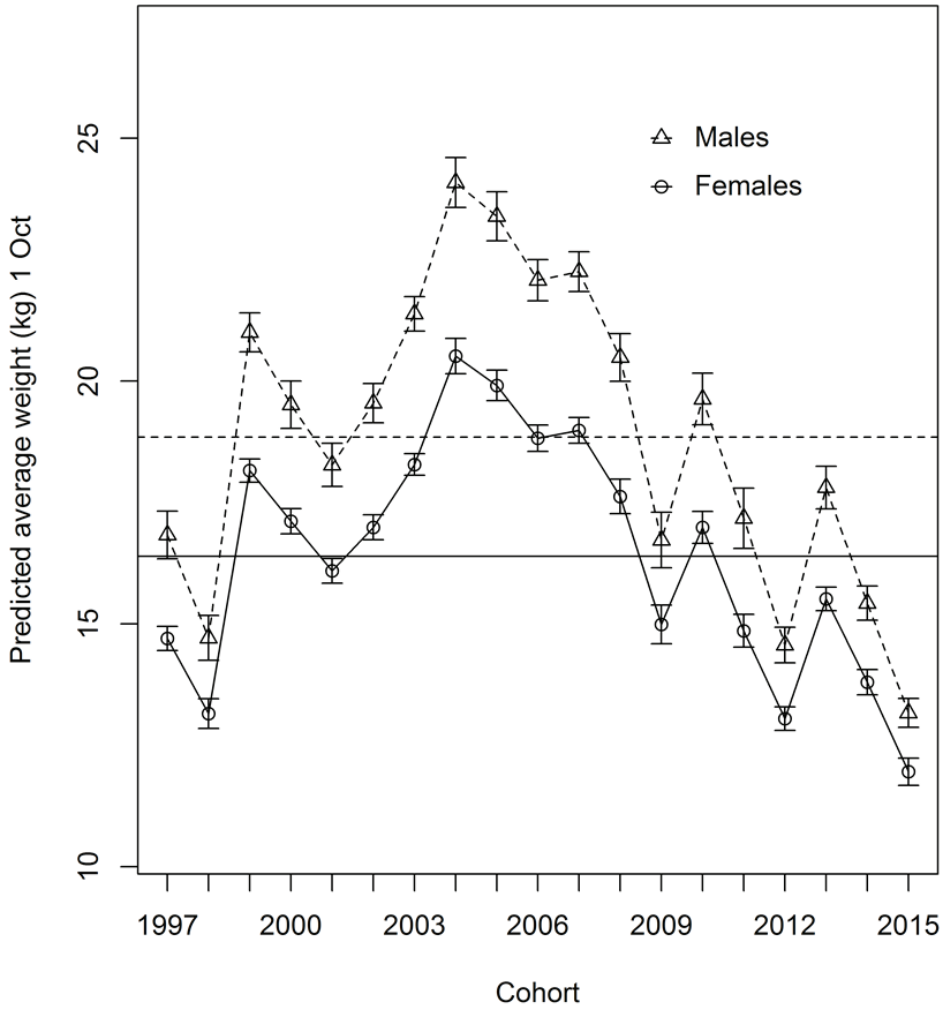

Figure 47. Predicted average weights of 3-month-old female (open circle) and male (open triangle) California sea lion pups at San Miguel Island, California, 1997–2015 and long-term average between 1997 and 2015 for females (solid line) and males (dashed line). Error bars are ± 1 standard error.

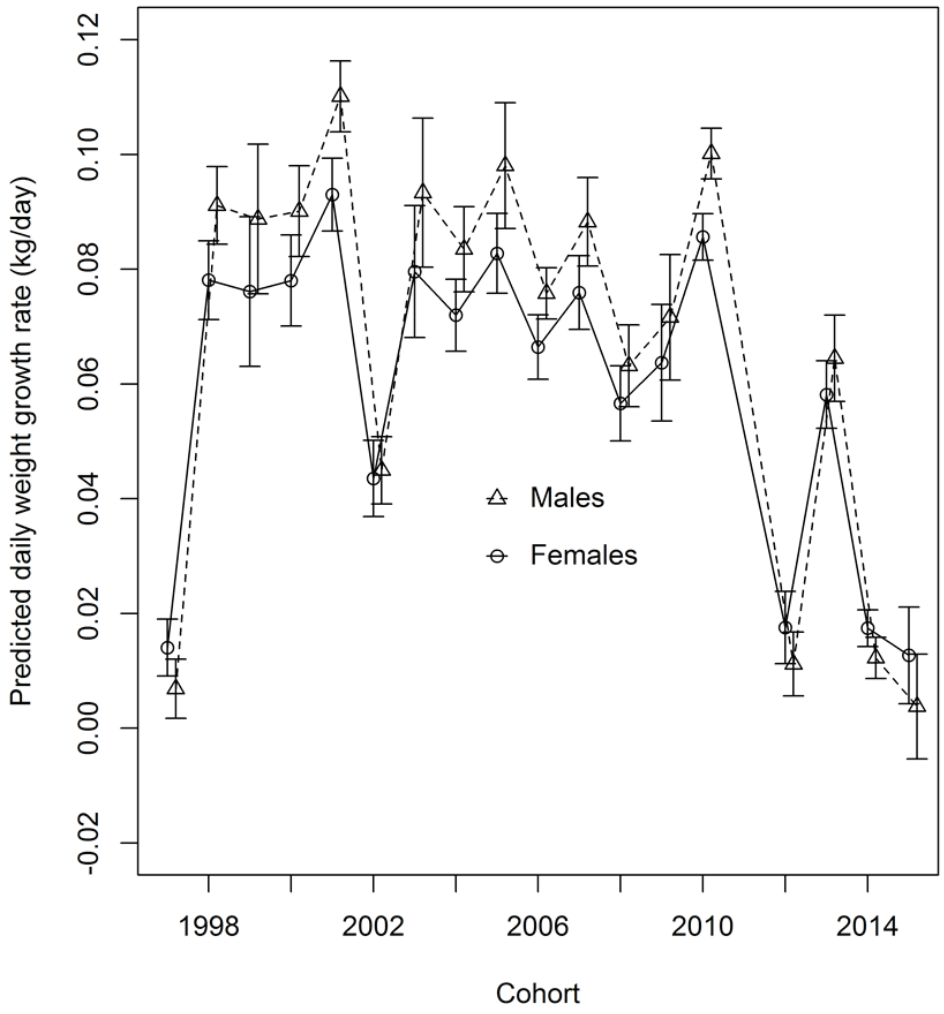

Figure 48. Predicted average daily growth rate of female (open circle) and male (open triangle) California sea lion pups between 3 and 7 months old at San Miguel Island, California, 1997–2015, and long-term average between 1997 and 2015 for females (solid line) and males (dashed line). Error bars are ± 1 standard error.

for female pups and 94% lower than average for male pups in 2015, indicating that male pups had almost no growth over the four month period (fig. 48).

Since 2009, the California sea lion population has experienced low pup survival, low pup births or both (Melin et al. 2010, 2012; Leising et al. 2014). An unusual mortality event (UME) was declared for California sea lions in southern California in response to unusually high numbers of young pups from the 2012, 2014, and 2015 cohorts stranding along the coast between January and April and poor condition of pups at San Miguel Island and other rookeries during the winter (Wells et al. 2013; Leising et al. 2014). Since 2013, fisheries surveys during the springs each year indicated that several of the primary fish prey of California sea lions that typically are associated with years of normal or better pup condition (Melin et al. 2012), including Pacific sardine (*Sardinops sagax*), northern anchovy (*Engraulis mordax*), and Pacific hake (*Merluccius productus*), were not abundant along the central California coast in the foraging range of nursing females (Wells et al. 2012, 2013, 2014; Leising et al. 2014, 2015). Analysis of scat contents of California sea lion females during these periods indicated increased consumption of rockfish (*Sebastes* spp.) and market squid (*Doryteuthis opalescens*) (Melin et al., in review). Thus, the composition of the prey community available to nursing females during the UME period was quite different from previous years when pups were in better condition (Melin et al. 2012; McClatchie et al. 2016). The combination of the residual effects of the marine heat wave and the El Niño conditions during the fall and spring of 2014–15 continued to influence the availability of prey to nursing females. Consequently, nursing females were not able to provide enough energy for their pups to grow, pups weaned too early or weaned in poor condition, and large numbers of pups stranded along the California coast contributed to the continuation of the UME in 2015. We anticipate low numbers of births,

poor condition and survival of pups, and elevated strandings along the coast to continue until the composition and abundance of the prey community increases and provides sufficient food for nursing females to support pregnancies and the energetic demands of pup growth from birth to weaning.

LOWER NUMBERS OF BALEEN WHALES AND DOLPHINS BUT CLOSER INSHORE

Marine mammal surveys were only initiated as part of the CalCOFI cruises in 2004 so it is not possible to compare distribution and abundance between the 2015–16 and the 1997–98 El Niños. This contribution focuses on the spatial distribution patterns of cetaceans off southern California and their seasonal variability in the last 5 years (2012–16) derived from visual monitoring using standard line-transect survey protocols. Methods are described in detail in Campbell et al. (2015).

The spatial distribution of several species of baleen whales differed both seasonally and interannually (fig. 49). During winter and spring, most baleen whale sightings occurred within ~370 km of the shoreline. During summer and fall, baleen whales were sighted primarily along the continental slope and in offshore waters. The exception was the fall 2015 cruise when baleen whales were mainly seen in the coastal areas of Southern California Bight. However, minke whales (*Balaenoptera acutorostrata*) and gray whale (*Eschrichtius robustus*) sightings were restricted to the continental shelf. Sightings of baleen whales in fall 2015 were significantly fewer than usual. The timing and the reduced number of sightings of baleen whales during fall 2015 coincided with anomalously warm conditions, but was prior to the winter peak of the 2015–16 El Niño.

Among the toothed (Odontocete) whales, short-beaked common dolphins (*Delphinus delphis*) were detected more frequently offshore in contrast to long-beaked common dolphins (*D. capensis*) that were more commonly seen inshore (fig. 50). During summer and fall 2015, short-beaked common dolphins extended their distribution inshore. There were fewer sightings of odontocetes during fall 2015, as was also the case for baleen whales.

Both baleen whales and odontocetes were sighted less frequently during anomalous warming off southern California prior to the peak of the 2015–16 El Niño. Baleen whales and short-beaked common dolphins normally occur offshore (e.g., over the continental slope), but in fall 2015 baleen whales (except minke and gray whales) and short-beaked common dolphins extended their distribution inshore.

OVERALL SUMMARY

Warm conditions in the North Pacific in 2014–15 were a result of the continuation of the marine heat wave, a large area of exceptionally high SST anomalies that originated in the Gulf of Alaska in late 2013. The North Pacific heat wave conditions interacted with an El Niño developing in the equatorial Pacific in 2015. Along the coast of North America, high positive SST anomalies due to the marine heat wave and the El Niño started to diminish by December 2015. The ONI reached the highest positive values since the 1997–98 El Niño during the fall of 2015 and winter of 2015–16.

Positive SST anomalies remained along the coast in late winter and early spring of 2016, with SST anomalies ranging from 0.5° to 1.5°C. Weekly periods of exceptionally high temperature anomalies (greater than 2°C) occurred until the start of the 2015–16 El Niño (winter of 2015), when SSTs were still high but not as high as those due to the marine heat wave. The decrease in SST values seen in the central CCS during the spring of 2015 corresponded with an extended period of upwelling favorable winds.

PDO values during December 2014 until March 2015 were all higher than 2, which are some of the highest values in the time series. These high winter PDO values can be attributed to the marine heat wave since they preceded the onset of the 2015 El Niño event, and modulated the regional expression of the El Niño event on the California Current (Jacox et al. 2016). High PDO values persisted during the El Niño event and reached their highest value in the past 15 years in May 2016.

During the 2015–16 warming, the depth of the 26.0 kg m^{-3} isopycnal ($d_{26.0}$) was considerably shallower than during the 1982–83 and 1997–98 events, and also showcased a much different temporal evolution. The past strong El Niño events were characterized by $d_{26.0}$ increasing rapidly beginning in summer, reaching peak anomalies in winter (November to February), and then decreasing again into the spring. In contrast, 2015–16 saw $d_{26.0}$ anomalies that were already positive due to anomalous warming of the North Pacific that began in 2014. In the first half of 2016, $d_{26.0}$ gradually shoaled, as is often the case, approaching climatological values and suggesting the decline of both El Niño and the pre-existing warm anomalies.

Mixed layer temperatures off southern California in 2014–15 were significantly higher than those observed during the previous 15 years, and did not begin to cool until the first half of 2016. The area affected by the marine heat wave and the 2015–16 El Niño in the mixed layer was comparable to the 1997–98 El Niño, but lasted longer. Water column stratification in the upper 100 m during the 2015–16 marine heat wave was as strong as the most extreme values observed during the 1997–98 El Niño. However, this stratification was primarily driven by the warming of the upper 100 m. The upper ocean was unusually fresh during 2015 in most regions off

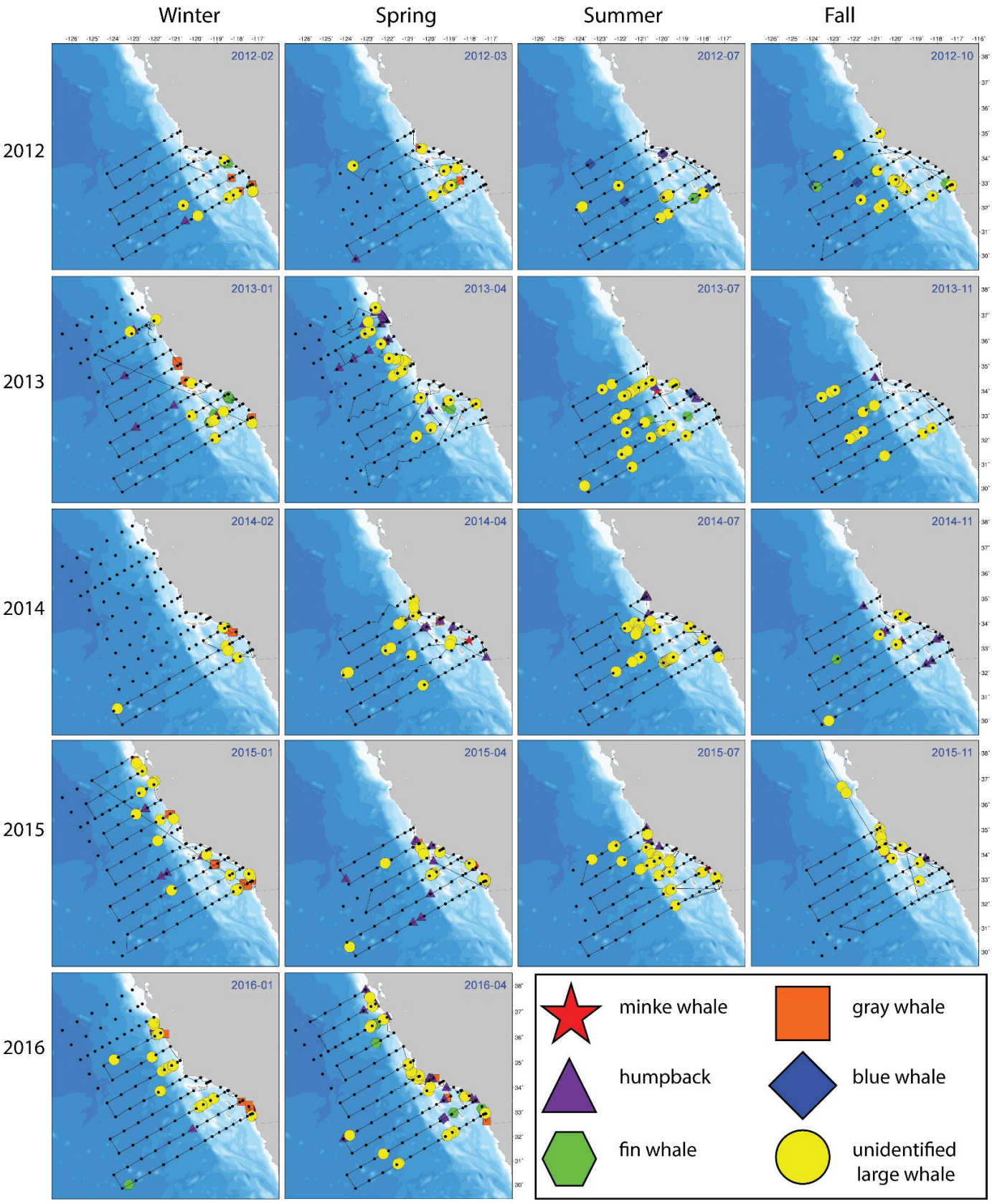

Figure 49. On-effort baleen whale sightings during CalCOFI cruises 2012–16. CalCOFI stations are represented by black dots and the ship's trackline is represented as a solid black line between stations.

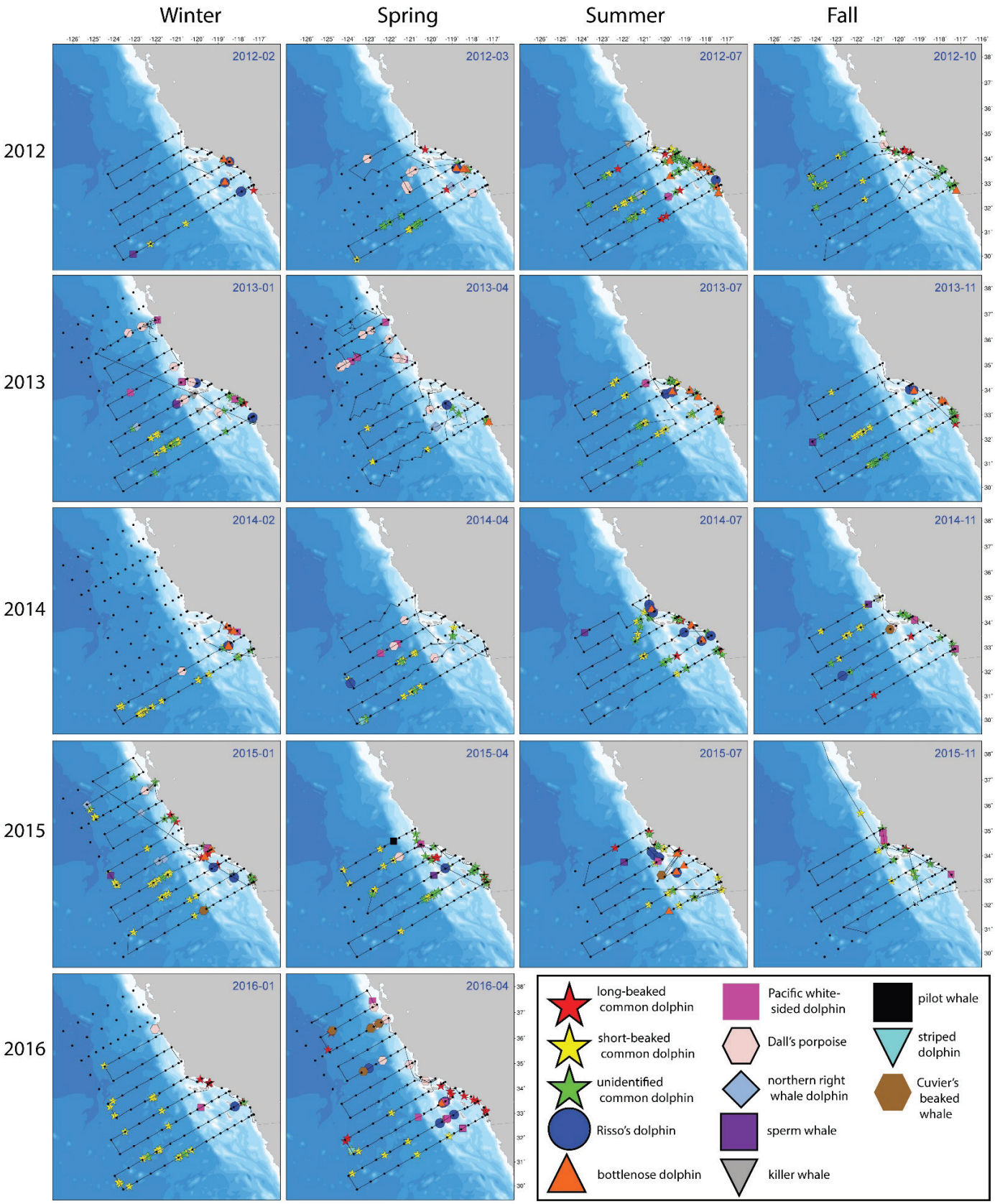

Figure 50. On-effort odontocete sightings during CalCOFI cruises 2012–16. CalCOFI stations are represented by black dots and the ship's trackline is represented as a solid black line between stations.

TABLE 1
List of CCS environmental indices, their current status, trend, implication, and figure reference (e.g., S1 = Supplement Figure S1; http://calcofi.org/ccpublications/state-of-the-california-current-live-supplement.html

Index	Current State	Trend	Implication	Figure
PDO	Positive	Increasing	Warm, low productivity	S1
NPGO	Negative	Increasing	Low to moderate productivity	S1
ENSO (ONI)	Positive	Increasing	El Niño	S1
Upwelling Anomaly	Positive, but delayed	NA	Moderately productive between 36°–42°N	S2
Cumulative Upwelling	Low north of 39°N	NA	Late spring transition north of 39°N	S4
SST Anomaly	Positive	Increasing	Warm surface waters	S3, S5
Wind Anomaly	Anticyclonic	Increasing anticyclonic	Upwelling favorable	S3
Isopycnal Depth, CalCOFI	Deeper than average	Deepening	Increased upper water column temperatures	S6
Oxygen, CalCOFI	Negative anomaly	Decreasing	Change in deep source waters	S6
Nitrate, CalCOFI	Slight positive anomaly	Neutral	Change in stratification	S6
Temperature-Salinity, CalCOFI	Warm and fresh in surface	NA	Change in surface transport	S7
Chlorophyll *a* Profiles, CalCOFI	Negative anomaly	Decreasing	Decreased productivity	S8
Temperature Anomaly, CalCOFI line 80	Positive at 10 m	Increasing	Warm surface layer	S9
Small Pelagic Fish Egg Abundance, CalCOFI	Low for all three species	Decreasing on decadal scales	Associated with reduced spawning stock biomass	S10

southern California, suggesting a strengthening of the California Current. We note that this contrasted with higher than normal salinity off Baja California in 2015. Nitracline depths, compared to the previous 15 years, have been unusually deep over the last two years and stratification in the upper 100 m was unusually strong. Despite these notable perturbations, the effects of the 2015–16 El Niño on hydrographic properties in the CalCOFI domain were not as strong as those observed during the 1997–98 El Niño. These results are summarized as a list of environmental indices in Table 1.

Warm ocean conditions and associated stratification combined with nutrient suppression and silicic acid stress likely favored initiation of the *Pseudo-nitzschia* toxic bloom in fall 2014. The winter/spring phytoplankton bloom of February and early March 2015, with higher nutrient concentrations following the spring transition to upwelling, favored explosive growth of the diatom. Local-scale forcing from coastal upwelling driving richer nutrient conditions and cross-shelf transport provided the ultimate explanation for the development of the *Pseudo-nitzschia* bloom and toxic effects.

The distribution of near-surface temperature and salinity during the 2015–16 El Niño suggests that warm, more saline waters, typically found south of Punta Eugenia, extended to the north during the 2015–16 El Niño. Anomalously warm and saline surface waters off Baja California were associated with very low zooplankton displacement volumes in 2015–16. In contrast, during the 1997–98 El Niño, zooplankton volume was close to the average with abundant copepods, euphausiids, and salps at some stations. Tropical species such as red crab, and the mesopelagic fishes *Vinciguerria lucetia* and *Triphoturus mexicanus* increased in abundance and extended their range northwards in 2015–16, a phenomenon also seen during the 1997–98 El Niño.

Off California, pelagic red crab (*Pleuroncodes planipes*) adults were abundant in the water column and frequently washed up on beaches of southern California in winter and spring 2015–16. They were reported off central California by September–October 2015. In spring 2015, the presence of only adults and the youngest zoea stages, together with their coastal distribution, is suggestive of advective transport from Baja California waters. Glider measurements of integrated transport up to June 2015 did not detect anomalous northward advection. As expected, HF radar indicated northward surface currents along the central California coast in fall and winter 2015–16.

Throughout 2015 and 2016, the zooplankton community on the Oregon shelf was dominated by lipid-poor tropical and subtropical copepods and gelatinous zooplankton. This generally indicates poor feeding conditions for small fishes, which in turn are prey for juvenile salmon. The biomass of southern copepods fluctuated greatly but was generally higher than average throughout 2015 and 2016. The presence of rarely encountered species greatly increased copepod species richness which exceeded the number of species observed during the strong El Niño in 1998. The conditions off Newport, Oregon, appear to have been influenced by intrusion of offshore waters. It is likely that the unusual copepods vagrants of 2015–16 originated from an offshore and southwesterly source, which is an important difference from the southerly origin of vagrants during the 1997–98 El Niño.

Coastal waters cooled off Trinidad Head in northern California, due to winter upwelling events, reinforced by more sustained upwelling in spring and summer. A bloom of toxic *Pseudo-nitzschia* developed, producing high levels of domoic acid. Similar to the Oregon shelf, the copepod assemblage was dominated by a more

diverse, warm water assemblage in 2015. The large cool water associated jellyfish (*Chrysaora fuscescens*) showed reduced abundance off Oregon in 2015, similar to previous warm years (2003, 2005, 2010, 2014).

The very warm conditions were not associated with a large spawning of sardine, but were associated with a northern shift of the sardine spawning area from central California to Oregon. Anchovy larvae were very abundant off Newport, Oregon, in 2014, but not during 2015 or 2016. The ichthyoplankton assemblages off southern California and Oregon were similar to those seen in other anomalously warm or El Niño years. The mesopelagic fish assemblage off southern California exhibited higher abundances of species with southern affinities, and lower abundances of species with northern affinities. The increase in abundance and northward shift of southern species off southern California was similar to what was observed for mesopelagic fish species and red crabs off the Baja Peninsula.

In contrast to the ichthyoplankton, fish, and nekton assemblages in 2015 and 2016 off northern California were different from assemblages present during the 1997–99 El Niño/La Niña and the 2005 warm event. Forage fish such as Pacific herring, northern anchovy, and Pacific sardine were much less abundant in 2015–16 compared to previous years. In contrast, catches of salmon were close to average off northern California. Catches of young-of-the-year rockfishes were high off central California, but low off both northern and southern California. High numbers of warm-water species like red crabs and lizardfish were captured in 2016, but many rare species encountered in summer 2015 were absent in 2016. Similarly to northern California, numbers of adult sardine and anchovy were very low in summer 2016. Multivariate analyses suggest that there may have been a shift in the composition of the forage base since 2013, and this has important implications for predators feeding exclusively on one or another component of the forage base.

Seabirds at Southeast Farallon Island in 2015 exhibited reduced breeding populations, reduced breeding success, lower chick growth rates, and lower fledging weights. Chick diets shifted from a high proportion of rockfish to more anchovies compared with the previous two years. Unusual bird species were observed in the region during the anomalously warm conditions. Common murre reproductive success was lower than average in northern California, similar to observations from central California during 2015, and a complete reproductive failure occurred off central Oregon. Reduced prey availability was likely the cause as chick mortality resulted primarily from starvation, with the added pressure of increasing bald eagle predation in central Oregon. Unlike murres and pelagic cormorants, Brandt's cormorants were more successful in 2015 than previously observed indicating that seabird response to conditions in the CCS is species specific.

After an increase in sea lion pup births at San Miguel Island in 2014, births declined in 2015 and were 16% lower than the long-term average between 1997 and 2015. Pup condition and pup growth for the 2015 cohort was the lowest observed over the time series. The composition of the prey community available to nursing females during 2012, 2014, and 2015 was quite different from previous years when pups were in better condition. The combination of the residual effects of the warm pool of water off the West Coast and the El Niño conditions during the fall and spring of 2014–15 continued to influence the availability of prey to nursing females. Consequently, nursing females were not able to provide enough energy for their pups to grow, pups weaned too early or weaned in poor condition, and large numbers of pups stranded along the California coast.

Both baleen and odontocete whales occurred in lower numbers coincident with anomalous warming off southern California prior to the peak of the 2015–16 El Niño. Baleen whales and short-beaked common dolphins normally occur offshore (e.g., over the continental slope), but in fall 2015 baleen whales (except minke and gray whales) and short-beaked common dolphins extended their distribution inshore.

We note some curious inconsistencies in the recent observations of the California Current System during the anomalous warm conditions. These issues will require more in-depth analyses to resolve than we can present here. Low near-surface salinity off southern California may suggest strengthening of the California Current during the warm anomaly, in contrast to the 1997–98 El Niño when the California Current weakened. Strong stratification off southern California reduced nutrient availability in surface waters and phytoplankton. In contrast, winter preconditioning and upwelling off central California fueled a massive toxic algal bloom. The arrival of weak-swimming red crabs off southern California from the south prior to fall and winter 2015–16 did not appear to be consistent with a lack anomalous northward flow, suggesting either that the crabs are better swimmers than we know, or there were streams of undetected transport from the south. Ichthyoplankton assemblages did not show much difference between warm events off southern California or Oregon, yet there appears to have been a shift in the forage base. This suggests differential survival to recruitment in the recent warm conditions. Finally, seabirds at the Farallones ate more anchovies than rockfishes, yet anchovies are at historically low levels and young-of-the-year rockfishes have been more abundant than normal on the central California coast.

It is clear from the results presented here that the warm anomaly on the ecosystem were complicated, regionally specific, and that we do not fully understand them yet. By highlighting some of the paradoxes in the data collected to date we hope to stimulate further research. Are red crabs in fact good swimmers, or were localized currents transporting these tropical animals northward? Did the warm conditions cause differential survival among fish species, driving a shift in the composition of the forage assemblage? And did the seabirds manage to exploit dense patches of anchovy that represent a spatially restricted refuge of a reduced population? If so, why did their chicks starve? Many questions remain to be answered concerning the ecosystem effects of the marine heat wave and the 2015–16 El Niño.

In closing, we summarize some important differences between our preliminary observations of current conditions and the 1997–98 El Niño event. Warming during the 1997–98 El Niño rapidly deepened over the 1997–98 winter, beginning the previous summer, and ending in the following spring. In contrast, the 2014–16 warming was shallower, began with the North Pacific heat wave in 2014, and did not revert to climatological values until summer of 2016. The recent warm anomaly was both shallower and lasted longer than the 1997–98 El Niño event. Stratification in 2015–16 was primarily driven by the warming of the upper 100 m. The area affected by the marine heat wave and the 2015–16 El Niño was comparable to the 1997–98 El Niño, but lasted longer. Despite unusually deep nutriclines and stratification as strong as the 1997–98 El Niño off southern California, the effects of recent conditions on regional hydrography were not as strong as those observed during the 1997–98 El Niño.

Somewhat surprisingly, zooplankton displacement volumes were much lower off Baja California than during the 1997–98 El Niño, although both periods exhibited increased abundances of red crabs, as well as Panama lightfish (*Vinciguerria lucetia*) and another warm-water associated mesopelagic fish, *Triphoturus mexicanus*. In the northern California Current System off Oregon the species composition of copepods indicated influence of offshore waters, which differs from the more southerly influence detected during the 1997–98 El Niño. The number of copepod species observed off Oregon during the recent warming was higher than during the 1997–98 El Niño. Fish and nekton assemblages were also different in the two periods, perhaps most notably in the very low abundance of forage fishes off Oregon. Finally, there were some indications that the California Current may have strengthened during the 2015–16 warm anomaly, whereas the current weakened during the 1997–98 El Niño. Despite these tantalizing preliminary observations, more analyses are needed before we can make definitive statements about the differences and similarities between the 2015–16 warm anomaly and the 1997–98 El Niño.

ACKNOWLEDGMENTS

This report would have been impossible without the dedicated work of the numerous ship crews and the technician groups that collected the data at sea, often under adverse conditions.

SWFSC and SIO wish to acknowledge the dedication of the NOAA CalCOFI group (comprising fisheries oceanography, ship operations, and the ichthyoplankton lab), and the SIO CalCOFI group and numerous volunteers. Major funding for CalCOFI is provided by NOAA Fisheries. Salaries for S. McClatchie and A. Leising are funded by the NOAA Fisheries and the Environment (FATE) program.

IMECOCAL thank the captain and crew of the R/V *Alpha Helix* of CICESE. Martin de la Cruz provided chlorophyll data and Luis E. Miranda computing assistance.

HF-radar data are available thanks to the initial investment of the state of California in establishing the array in California and to the National Science Foundation for establishing elements of the array in Oregon and California. NOAA-IOOS and participating universities (listed at http://cordc.ucsd.edu/projects/mapping/) provide ongoing funds/support for operation and management.

R. DeLong, J. Harris, H. Huber, J. Laake, A. Orr and many field assistants participated in the data collection and summaries for the sea lion study. Funding was provided by the National Marine Fisheries Service. Research was conducted under NMFS Permit 16087 issued to the Marine Mammal Laboratory, Alaska Fisheries Science Center.

The study of red crabs off southern California is a contribution from the California Current Ecosystem Long-Term Ecological Research site, supported by the US NSF, and from the SIO Pelagic Invertebrate Collection. Inset illustrations within Figure 18 from Boyd, C.M. 1960. *Biol. Bull.* 118:17–30. Reprinted with permission from the Marine Biological Laboratory, Woods Hole, MA.

We are grateful to Paul Fiedler for his internal NOAA review of the manuscript. We also thank three anonymous reviewers who improved the manuscript.

LITERATURE CITED

Anderson, C. R., D. A. Siegel, M. A. Brzezinski, and N. Guillocheau. 2008. Controls on temporal patterns in phytoplankton community structure in the Santa Barbara Channel, California. Journal of Geophysical Research 113: C04038, doi:10.1029/2007JC004321.

Anderson, C. R., M. A. Brzezinski, L. Washburn, and R. Kudela. 2006. Circulation and environmental conditions during a toxigenic *Pseudo-nitzschia australis* bloom in the Santa Barbara Channel, California. Marine Ecology Progress Series 327: 119–133.

Auth, T. D. 2011. Analysis of the spring–fall epipelagic ichthyoplankton community in the northern California Current in 2004–09 and its relation to environmental factors. California Cooperative Oceanic Fisheries Investigations Reports 52: 148–167.

Bakun, A. 1973. Coastal upwelling indices,West Coast of North America, 1946–71, NOAA Tech. Rep., NMFS SSRF-671, 114 pp.

Black, B. A., I. D. Schroeder, W. J. Sydeman, S. J. Bograd, and P. W. Lawson. 2010. Wintertime ocean conditions synchronize rockfish growth and seabird reproduction in the central California Current ecosystem. Canadian Journal of Fisheries and Aquatic Sciences 67: 1149–1158.

Bond, N. A., M. F. Cronin, H. Freeland, and N. Mantua. 2015. Causes and impacts of the 2014 warm anomaly in the NE Pacific, Geophysical Research Letters, 42: 3414–3420, doi:10.1002/2015GL063306.

Boyd, C. M. 1960. The larval stages of *Pleuroncodes planipes* Stimpson (Crustacea, Decapoda, Galatheidae). Biological Bulletin 118: 17–30.

Boyd, C. M. 1962. The biology of a marine decapod crustacean, *Pleuroncodes planipes* Stimpson, 1860. PhD thesis. University of California, San Diego. 123 p.

Boyd, C. M. 1967. The benthic and pelagic habitats of red crab *Pleuroncodes planipes*. Pacific Science 21: 394–403.

Brodeur, R. D., J. P. Fisher, R. L. Emmett, C. A. Morgan, and E. Casillas. 2005. Species composition and community structure of pelagic nekton off Oregon and Washington under variable oceanographic conditions. Marine Ecology Progress Series 298: 41–57.

Campbell, G. S., L.Thomas, K. Whitaker, A. B. Douglas, J. Calambokidis, and J. A. Hildebrand. 2015. Inter-annual and seasonal trends in cetacean distribution, density and abundance off southern California. *Deep Sea Research Part II: Topical Studies in Oceanography*, 112, pp.143–157.

Carter, H. R., U. W. Wilson, R. W. Lowe, M. S. Rodway, D. A. Manuwal, and J. L. Yee. 2001. Population trends of the common murre (*Uria aalge californica*). Pages 33–132 in Biology and conservation of the common murre in California, Oregon, Washington, and British Columbia,Volume 1: Natural history and population trends (D. A. Manuwal, H. R. Carter, T. S. Zimmerman, and D. L. Orthmeyer, Eds.), United States Geological Survey, Information and Technology Report USGS/BRD/ITR-2000-0012, Washington, D.C. Fish and Wildlife Service, Northern Prairie Wildlife Research Center, Dixon, CA.

Chavez, F. P., C. A. Collins, A. Huyer, and D. L. Mackas. 2002. El Niño along the west coast of North America. Progress in Oceanography 54: 1–5.

Di Lorenzo, E., N. Schneider, K. M. Cobb, P. J. S. Franks, K. Chhak, A. J. Miller, J. C. McWilliams, S. J. Bograd, H. Arango, E. Curchitser, T. M. Powell, and P. Rivière. 2008. North Pacific Gyre Oscillation links ocean climate and ecosystem change. Geophysical Research Letters 35, doi:10.1029/2007GL032838.

Di Lorenzo, E., and N. Mantua. 2016. Multi-year persistence of the 2014/15 North Pacific marine heat wave. Nature Climate Change, doi:10.1038/NCLIMATE3082.

Du, X., W. Peterson, J. Fisher, M. Hunter, and J. Peterson. Initiation and development of a toxic and persistent *Pseudo-nitzschia* bloom off the Oregon coast in spring/summer 2015. PLOS One. Submitted June 2015.

Durán, M. J. 2016. Red crabs wash out at La Jolla beaches. The San Diego Union Tribune (http://www.lajollalight.com/news/2016/jun/08/red-crabs/).

Fisher, J. L., W. T. Peterson, and R. R. Rykaczewski. 2015. The impact of El Niño events on the pelagic food chain in the northern California Current. Global Change Biology 21: 4401–4414, doi:10.1111/gcb.13054.

Gómez-Gutierrez, J., and C. Robinson. 2006. Tidal current transport of epibenthic swarms of the euphausiid *Nyctiphanes simplex* in a shallow, subtropical bay on Baja California peninsula, México. Marine Ecology Progress Series 320: 215–231.

Gladics, A. J., R. M. Suryan, R. D. Brodeur, L. M. Segui, and L. Z. Filliger. 2014. Constancy and change in marine predator diets across a shift in oceanographic conditions in the Northern California Current. Marine Biology 161: 837–851.

Gladics, A. J., R. M. Suryan, J. K. Parrish, C. A. Horton, E. A. Daly, and W. T. Peterson. 2015. Environmental drivers and reproductive consequences of variation in the diet of a marine predator. Journal of Marine Systems 146: 72–81.

Gruber, N., and J. L. Sarmiento. 1997. Global patterns of marine nitrogen fixation and denitrification. Global Biogeochemical Cycles 11: 235–266.

Hayward, T. L. 2000. El Niño 1997–98 in the coastal waters of Southern California: A timeline of events. California Cooperative Oceanic Fisheries Investigations Reports 41: 98–116.

Horton, C. A. 2014. Top-down influences of Bald Eagles on Common Murre populations in Oregon. MS thesis, Oregon State University.

Jacox, M. G., E. L. Hazen, K. D. Zaba, D. L. Rudnick, C. A. Edwards, A. M. Moore, and S. J. Bograd. 2016. Impacts of the 2015–16 El Niño on the California Current System: Early assessment and comparison to past events. Geophysical Research Letters 43: 1–9. doi:10.1002/2016GL069716.

Jiménez-Rosenberg, S. P. A., R. J. Saldierna-Martínez, G. Aceves-Medina, and V. M. Cota-Gómez. 2007. Fish larvae in Bahía Sebastián Vizcaíno and the adjacent oceanic region, Baja California, México. Checklist 3: 204–223.

Jiménez-Rosenberg, S. P. A., R. J. Saldierna-Martínez, G. Aceves-Medina, A. Hinojosa-Medina, R. Funes-Rodríguez, M. Hernández-Rivas, and R. Avendaño-Ibarra. 2010. Fish larvae off the northwestern coast of the Baja California Peninsula, Mexico. Checklist 6: 334–349.

Kahru, M., and B. G. Mitchell. 2000. Influence of the 1997–98 El Niño on the surface chlorophyll in the California Current. Geophysical Research Letters 27: 2937–2940.

Kahru, M., R. M. Kudela, M. Manzano-Sarabia, and B. G. Mitchell. 2012. Trends in the surface chlorophyll of the California Current: Merging data from multiple ocean color satellites. Deep-Sea Research II 77: 89–98. http://dx.doi.org/10.1016/j.dsr2.2012.04.007.

Kahru, M., Z. Lee, R. M. Kudela, M. Manzano-Sarabia, and B. G. Mitchell. 2015. Multi-satellite time series of inherent optical properties in the California Current. Deep-Sea Research II 112: 91–106, http://dx.doi.org/10.1016/j.dsr2.2013.07.023.

Lavaniegos, B. E., and M. D. Ohman. 2007. Coherence of long-term variations of zooplankton in two sectors of the California Current System. Progress in Oceanography 75: 42–69

Lea, R., and R. Rosenblatt. 2000. Observations on fishes associated with the 1997–98 El Niño off California. California Cooperative Oceanic Fisheries Investigations Reports 41: 117–129.

Leising, A. W., et al. 2014. State of the California Current 2013–14: El Niño looming. California Cooperative Ocean and Fisheries Investigations Reports 55:31–87.

Leising, A. W., I. D. Schroeder, S. J. Bograd, J. Abell, R. Durazo, G. Gaxiola-Castro, E. P. Bjorkstedt, J. Field, K. Sakuma, R. R. Robertson, R. Goericke, W. T. Peterson, R. D. Brodeur, C. Barceló, T. D. Auth, E. A. Daly, R. M. Suryan, A. J. Gladics, J. M. Porquez, S. McCatchie, E. D. Weber, W. Watson, J. A. Santora, W. J. Sydeman, S. R. Melin, F. P. Chavez, R. T. Golightly, S. R. Schneider, J. Fisher, C. Morgan, R. Bradley, and P. Waryzbok. State of the California Current 2014–15: impacts of the warm-water "blob." California Cooperative Oceanic Fisheries Investigations Reports 56, 31–68. 2015.

Longhurst, A. R. 1967. The pelagic phase of *Pleuroncodes planipes* Stimpson (Crustacea, Galatheidae) in the California Current. California Cooperative Oceanic Fisheries Investigations Reports 11: 142–154.

Lynn, R. J., and J. J. Simpson. 1987. The California Current System: The seasonal variability of its physical characteristics. Journal of Geophysical Research 92: 12947–12966.

Lynn, R. J., and S. J. Bograd. 2002. Dynamic Evolution of the 1997–1999 El Niño-La Niña cycle in the southern California Current system. Progress in Oceanography 54: 59–75.

Marchetti, A., V. L. Trainer, and P. J. Harrison. 2004. Environmental conditions and phytoplankton dynamics associated with *Pseudo-nitzschia* abundance and domoic acid in the Juan de Fuca eddy. Marine Ecology Progress Series 281: 1–12.

McCabe, R. M., B. M. Hickey, R. M. Kudela, K. A. Lefebvre, N. G. Adams, B. D. Bill, F. M. D. Gulland, R. E. Thomson, W. P. Cochlan, and V. L. Trainer, 2016. An unprecedented coastwide algal bloom linked to anomalous ocean conditions. Submitted to Geophysical Research Letters.

McClatchie, S. 2014. Regional fisheries oceanography of the California Current System: the CalCOFI program. Springer. 235pp. ISBN 978-94-007-7222-9.

McClatchie, S., J. Field, A. R. Thompson, T. Gerrodetter, M. Lowry, P. C. Fiedler, W. Watson, K. M. Nieto, and R. D. Vetter. 2016. Food limitation of sea lion pups and the decine of forage off central and southern California. Open Science, 3, p.150628.

Melin, S. R., A. J. Orr, J. D. Harris, J. L. Laake, and R. L. DeLong. 2012. California sea lions: An indicator for integrated ecosystem assessment of the California Current System. California Cooperative Ocean and Fisheries Investigations Reports 53:140–152.

Morgan, C. A., B. R. Beckman, R. D. Brodeur, B. J. Burke, K. C. Jacobson, J. A. Miller, W. T. Peterson, D. M. Van Doornik, L. A. Weitkamp, J. E. Zamon, A. M. Baptista, E. A. Daly, E. M. Phillips, and K. L. Fresh. 2016.

Ocean Survival of Salmonids RME, 1/1/2015–12/31/2015, Annual Report, 1998-014-00. 65pp. Available at: https://pisces.bpa.gov/release/documents/DocumentViewer.aspx?doc=P149018.

Ohman, M., and E. Venrick. 2003. CalCOFI in a changing ocean. Oceanography 16: 76–85.

Perrins, C. M. 1970. The timing of birds' breeding seasons. Ibis 112: 242–255.

Peterson, W. T., J. A. Keister, and L. R. Feinberg. 2002. The effects of the 1997–99 El Niño/La Niña event on hydrography and zooplankton off the central Oregon coast. Progress in Oceanography 54: 381–398.

Ralston, S., J. C. Field, and K. S. Sakuma. 2015. Long-term variation in a central California pelagic forage assemblage. Journal of Marine Systems 146: 26–37.

Reed, T. E., S. Waneless, M. P. Harris, M. Frederiksen, L. E. B. Kruuk, and E. J. A. Cunningham. 2006. Responding to environmental change: plastic responses vary little in a synchronous breeder. Proceedings of the Royal Society of London B 273: 2713–2719.

Reynolds, R. W., T. M. Smith, C. Liu, D. B. Chelton, K. S. Casey, and M. G. Schlax. 2007. Daily high-resolution blended analyses for sea surface temperature. J. Climate 20: 5473–5496.

Ryan, H. F., and M. Noble. Sea level response to ENSO along the central California coast: how the 1997–98 event compares with the historical record. Progress in Oceanography 54: 149–169.

Sakuma, K. M., J. C. Field, B. B. Marinovic, C. N. Carrion, N. J. Mantua, and S. Ralston. In review. Epipelagic micronekton assemblage patterns in the California Current with observations on the influence of "the blob" on pelagic forage in 2015. California Cooperative Oceanic Fisheries Investigations Reports.

Schroeder, I. D., W. J. Sydeman, N. Sarkar, S. A. Thompson, S. J. Bograd, F. B. Schwing. 2009. Winter pre-conditioning of seabird phenology in the California Current. Marine Ecology Progress Series 393: 211–233.

Schroeder, I. D, B. A. Black, W. J. Sydeman, S. J. Bograd, E. L. Hazen, J. A. Santora, and B. K. Wells. 2013. The North Pacific High and wintertime pre-conditioning of California Current productivity. Geophysical Research Letters 40: 541–546.

Schwing, F. B., M. O'Farrell, J. M. Steger, and K. Baltz. 1996. Coastal upwelling indices, West Coast of North America, 1946–95, NOAA Tech. Memo., NOAA-TM-NMFS-SWFSC-231, 144 pp.

Schwing, F. B., T. Murphree, and P. M. Green. 2002. The Northern Oscillation Index (NOI): a new climate index for the northeast Pacific. Progress In Oceanography 53: 115–139.

Simpson, J. 1992. Response of the Southern California current system to the mid-latitude north Pacific coastal warming events of 1982–83 and 1940–41. Fisheries Oceanography 1(1): 57–79.

Sommer, U. 1994. Are marine diatoms favoured by high Si:N ratios? Marine Ecology Progress Series 115: 309–315.

Suchman, C. L., R. D. Brodeur, E. A. Daly, and R. L. Emmett. 2012. Large medusae in surface waters of the Northern California Current: variability in relation to environmental conditions. Hydrobiologia.690: 113–125.

Todd, R. E., D. Rudnick, M. Mazloff, R. Davis, and B. Cornuelle. 2011. Poleward flows in the southern California Current System: glider observation and numerical simulation. Journal of Geophysical Research 116, C02026, doi:10.1029/2010JC006536.

Warzybok, P. M., R. Berger, and R. W. Bradley. 2015. Population size and reproductive performance of seabirds on Southeast Farallon Island. 2015. Unpublished report to the U.S. Fish and Wildlife Service. Point Blue Conservation Science, Petaluma, California. Point Blue Conservation Science Contribution Number 2055.

Wells, B. K., et al. 2013. State of the California Current 2012–13: No Such Thing as an" Average" Year. California Cooperative Ocean and Fisheries Investigations Reports 54:37–71.

Wolter, K., and M. S. Timlin. 2011. El Niño/Southern Oscillation behavior since 1871 as diagnosed in an extended multivariate ENSO index (MEI. ext). International Journal of Climatology 31: 1074–1087.

Zaba, K. D., and D. L. Rudnick. 2016. The 2014–15 warming anomaly in the Southern California Current System observed by underwater gliders. Geophysical Research Letters 43: 1241–1248, doi 10.1002/2015gl067550.